

Scaphoid Fractures – Anatomy, Imaging and Management

by

Arthur Turow

*Thesis
Submitted to Flinders University
for the degree of*

Masters of Surgery

Faculty of Medicine, Nursing and Health Sciences

June 2020

Supervisors

Prof Gregory I Bain

Professor of Upper Limb and
Research in the Department of
Orthopaedic Surgery, Flinders
University

Prof Ruurd L Jaarsma

Clinical and Academic Director of
Orthopaedics and Trauma Surgery
for the Southern Adelaide Local
Health Network

Contents

Contents.....	3
Dedication.....	7
Thesis Summary.....	8
Thesis Declaration.....	10
Acknowledgements.....	11
List of studies.....	12
Study I: The dorsal non-articulating area of the scaphoid.....	12
Study II: Book chapter - Scaphoid Plating.....	12
Study III: Technique description: Dorsal plating of unstable scaphoid fractures and non-unions...	13
Study IV: A New Radiographic View of the Scaphotrapezotrapezoid Joint.....	13
Study V: Scaphoid Fracture Mapping – a 3D Computed Tomography Analysis.....	14
Research Outcomes.....	15
Prizes.....	15
Publications.....	15
Conference presentations.....	15
Other.....	17
Abbreviations.....	18
Chapter One – Background.....	19
Introduction.....	19
Anatomy.....	20
Proximal Pole.....	22
Waist.....	23
Distal Pole.....	25
Vascular Anatomy.....	26
Biomechanics.....	28
Epidemiology.....	30
Diagnosis.....	31
Clinical assessment.....	31
Plain radiography.....	33
Computed Tomography.....	36
Magnetic resonance Imaging.....	39

Other modalities	40
Treatment	41
Non-Operative	41
Surgical fixation.....	43
Assessment of fracture union	49
Clinical outcomes	51
Distal pole fractures.....	51
Waist fractures.....	52
Proximal pole fractures.....	54
Articular surfaces of the scaphoid	57
Chapter Two – Dorsal Bare Area of the Scaphoid.....	61
Non-articulating areas of the scaphoid.....	61
Study I - The dorsal non-articulating area of the scaphoid – A cadaveric study.....	64
Abstract.....	65
Introduction	66
Materials & Methods.....	68
Results.....	70
Discussion.....	71
Conclusion.....	73
Acknowledgments.....	74
Figures.....	75
Chapter Three – Scaphoid fracture Plating.....	78
Plating in orthopaedics	78
The headless compression screw	79
Prognostic factors of fixation	81
Case Example	86
Importance of the Problem.....	86
Main Question	88
Current Opinion	88
Finding the Evidence	88
Quality of Evidence	89
Findings	90
Recommendations	95
Conclusion.....	96

Author's Preferred Technique	97
Pearls and Pitfalls	97
Figures	98
Chapter Four – Dorsal scaphoid plating.....	103
Study III – Technique description: Dorsal plating of unstable scaphoid fractures and non-unions	103
Abstract.....	103
Introduction	104
Surgical options.....	104
Biomechanics	105
Anatomy.....	107
Indications.....	107
Contraindications.....	109
Technique.....	110
Complications.....	112
Rehabilitation.....	113
Figures.....	114
Chapter Five – Imaging the STTJ	121
STTJ Imaging.....	121
STTJ Osteoarthritis	122
STTJ Osteoarthritis in Scaphoid fractures	124
Study IV - A New Radiographic View of the Scaphotrapeziotrapezoid Joint	128
Abstract.....	129
Introduction	130
Materials & Methods	132
Results.....	134
Discussion.....	134
Conclusion.....	136
Acknowledgments.....	136
Figures.....	137
Chapter Six – CT analysis of the scaphoid fracture.....	143
Fracture mapping.....	143
Scaphoid fracture classifications.....	145
Study V - Scaphoid Fracture Mapping – a 3D Computed Tomography Analysis	150
Abstract.....	151

Introduction	152
Material and methods	153
Results	157
Discussion.....	162
Figures.....	167
Plate design.....	183
Conclusion.....	186
Future Directions	187
References	188

Dedication

To my parents Alexander and Nelia. You provided me with the foundations that allowed me to achieve my full potential, to study medicine and to pursue orthopaedic surgery. Спасибо вам от всего сердца.

To my beautiful wife Melissa and my two gorgeous children Mila and Oliver. Your unconditional love, support and understanding gave me strength to undertake this higher degree. I just would not have been able to do it without you.

Thesis Summary

Scaphoid fractures are common and account for 60% of all carpal fractures. The diagnosis can be challenging and management is time sensitive. Extensive knowledge about morphology, ligamentous attachments and vascularity of the scaphoid exists; however, some details, such as carpal kinematics and size of articular or non-articular areas remain elusive. Equally, scaphoid fracture fixation has seen a revolutionary transformation in the past three decades. Nonetheless, despite best practice treatment, poor outcomes persist in up to 10% of patients.

This work studies cadaveric wrists to gain further insights into the anatomy and imaging of the scaphoid. The dorsal non-articulating area was examined first. The area was on average 188 mm² in size and resembled that of a lazy-S. We also demonstrated that it had a predictable orientation in relation to the radius when viewed face-on. An increased understanding about the dorsal bare area was utilised to develop dorsal plating, a novel technique taking the tension side of the scaphoid into consideration. Our preliminary findings demonstrated that, during hardware insertion, avoiding the distal scaphoid articulation could be challenging. Consequently, cadaveric specimens underwent serial X-rays to examine the scaphotrapeziotrapezoid joint. The complex shape of the scaphotrapeziotrapezoid joint was best visualised at 48° supination from a fully pronated wrist with a proximally directed X-ray beam angle of 22°. A significant finding was that this dedicated, scaphotrapeziotrapezoid view could be achieved with the wrist in neutral position. Elimination of thumb or wrist movement can allow for more efficient intra-operative imaging and reduce discomfort in the outpatient setting where patients are frequently imaged to investigate pain.

Plain radiography of the scaphotrapeziotrapezoid joint highlighted the challenges of imaging the complex shape of the scaphoid with two-dimensional techniques. A three-dimensional investigation into the morphology of acute scaphoid fractures followed. Scaphoid fractures presenting to Flinders Medical Centre and the Southern Adelaide Health Network over a ten-year period were examined. Acute fractures of less than six weeks with an available CT were studied and their fracture patterns

mapped in 3D. In 75 CT scans, four main fracture patterns were identified: proximal pole, oblique waist, transverse waist and distal pole. We demonstrated that certain fractures were associated with displacement and unique dorsal and volar comminution patterns.

In summary, our understanding about the scaphoid continues to evolve. This understanding can assist in selecting the right treatment for the right patient. With modern imaging techniques, scaphoid fractures can be assessed in more detail. Consequently, knowledge about fracture morphology can provide insights into fracture stability and prognosticate likely failure or success of a particular treatment method.

Thesis Declaration

I, Arthur Turow, certify that this thesis:

1. does not incorporate without acknowledgment any material previously submitted for a degree or diploma in any university; and
2. to the best of my knowledge and belief, does not contain any material previously published or written by another person except where due reference is made in the text.

Acknowledgements

I would like to thank Professor Gregory Bain and Professor Ruurd Jaarsma for their supervision, leadership, support and patience during the preparation of this work. I would like to acknowledge Kym Peter Mason for his critical review of the thesis. I would also like to acknowledge the Department of Radiology at Flinders Medical Centre and my co-authors from the individual studies. The Department of Radiology provided radiology staff, dedicated imaging facilities and allowed access to past CTs. Joideep Phadnis has provided a tremendous amount of mentoring, editorial work and clinical guidance for the cadaveric studies. Anne Eva Bulstra has put substantial effort into CT fracture mapping paper and her determination allowed for the study to progress beyond just its foundations. Finally, thank for the support I received from the Flinders Medical Centre Research team, especially Kimberley Bryant, and the Flinders University Office of Graduate Research staff.

List of studies

Study I: The dorsal non-articulating area of the scaphoid

Aim: To examine the dorsal non-articulating area of the scaphoid and identify surgically relevant anatomy

Methods: Ten embalmed adult cadaveric upper limbs were assessed. The dorsal non-articulating area was measured and described in relation to its dorsal blood supply and ligamentous attachments.

Conclusion: The mean size of the dorsal non-articulating area was 188 mm², with a mean angle subtended between the radial shaft axis and the bare area of 97°. This study adds to existing research of the scaphoid in that it more clearly describes the dorsal non-articulating area, in particular its surface area, shape and orientation.

Study II: Book chapter - Scaphoid Plating

Aim: To review literature review about the concept of scaphoid fracture plating

Background: Since it became available in the 1980, the single head-less compression screw has been the mainstay of surgical fixation of the scaphoid. Other fixation options are staples, wires and mini plates. The concept of plating has been introduced in the middle of last century with compression plates by Ender and Vespasiani. Several variations of compression and angular-stable locking plates have been developed.

Conclusion: Plating of the scaphoid is an evolving concept and its techniques are undergoing development. Early clinical outcome data on scaphoid plating has been promising; however, more research is needed to define the indications of scaphoid plating.

Study III: Technique description: Dorsal plating of unstable scaphoid fractures and non-unions

Aim: To describe a novel fixation technique of unstable fracture and scaphoid non-unions.

Technique: Indications for scaphoid plating are evolving. Acute, displaced scaphoid fractures or fractures with delayed union or non-union are suitable for plating. Pre-existing articular degeneration, proximal pole fractures or volar bone loss are not suitable for plate fixation. Using the dorsal approach to the scaphoid, the fracture is prepared and bone graft impacted. A pre-contoured, titanium, locking mini-plate is placed on the dorsal bare area of the scaphoid. The fracture is reduced and compressed using a reduction clamp. At least three screws are placed into each fracture fragment and interlocked into the plate. Post-operative rehabilitation consists of immediate mobilisation, a removable wrist splint that is weaned over two weeks, serial X-Rays and a computed tomography scan at three months.

Conclusion: The dorsal plate is placed on the biomechanically favourable tension side of the scaphoid bone for dynamic compression. Dorsal scaphoid plating provides a more stable construct than the traditional Herbert screw and mitigates the need for vascular or corticocancellous bone grafting in most cases.

Study IV: A New Radiographic View of the Scaphotrapeziotrapezoid

Joint

Aim: To achieve ideal scaphotrapeziotrapezoid joint (STTJ) visualisation using serial radiographs while maintaining the wrist in neutral position.

Methods: Computed tomography 3-D reconstructions of three uninjured wrists were initially used to determine an approximate X-ray beam angle. Serial radiographs of twelve cadaveric wrists were

taken. Forearm rotation and beam tilt were then adjusted until an unobscured view of the STTJ was achieved.

Conclusion: The STTJ was best visualised in semi-pronation (48° from a fully pronated wrist) and with a caudal beam angle of 22°. This can aid in imaging the STTJ in the ambulatory setting as well as in the operating room.

Study V: Scaphoid Fracture Mapping – a 3D Computed Tomography

Analysis

Aim: Scaphoid fractures have traditionally been described using plain radiography. The aim of this study was to characterise acute scaphoid fracture morphology using three-dimensional computed tomography (CT).

Methods: Seventy-five CT scans of scaphoid fractures less than six weeks from time of injury were included in this retrospective, multicentre study. CTs were segmented and converted into 3D models. Following virtual fracture reduction, fractures were mapped onto a 3D scaphoid model.

Conclusion: Most fractures were comminuted (52%) or displaced (64%). 73% of displaced fractures had concomitant comminution. Waist fractures had higher rates of comminution and displacement when compared to proximal or distal pole fractures. Comminution was located along the dorsal ridge and the volar scaphoid waist. Treatment of waist fractures should include careful examination of these anatomical areas. Inspection of the 3D anatomy of the fracture plane, concurrent comminution and direction of displacement can be a valuable tool in scaphoid fracture management.

Research Outcomes

Prizes

Dodridge Prize - Best Paper Presentation at 2018 Hand Surgery Society Annual Meeting, Preliminary Study - Scaphoid Fracture 3D CT Analysis; 10th October 2018, Adelaide Convention Centre

Publications

Bain, G.I., Turow, A. and Phadnis, J., 2015. Dorsal plating of unstable scaphoid fractures and nonunions. *Techniques in hand & upper extremity surgery*, 19(3), pp.95-100;

<https://www.ncbi.nlm.nih.gov/pubmed/26053203>

Turow, A., Phadnis, J. and Bain, G.I., 2019. A new radiographic view of the scaphotrapeziotrapezoid joint—a cadaveric study. *Skeletal radiology*, pp.1-6;

<https://www.ncbi.nlm.nih.gov/pubmed/31104145>

Turow, A. & Bain I.G. *Chapter 30 – Scaphoid Plating in Scaphoid Fractures, Evidence-Based Management*; 1st ed, 2017

Conference presentations

Podium presentation at 79th AOA Annual Scientific Meeting, Canberra, ACT, 6th October 2019; *Three-Dimensional Computed Tomography Analysis of Acute Scaphoid Fracture Patterns*, Arthur Turow and Anne Eva Bulstra; Miriam Oldhoff; Batur Hayat; Job Doornberg; John White; Ruurd Jaarsma; Gregory Bain

Podium presentation at the 2019 SA Hand Surgery Society Annual Meeting, Adelaide, SA, 30th September 2019; *3D Mapping of Scaphoid Fractures and Comminution*, Arthur Turow and Anne Eva Bulstra; Miriam Oldhoff; Batur Hayat; Job Doornberg; John White; Ruurd Jaarsma; Gregory Bain

Podium presentation by Anne Eva Bulstra at the 14th International Federation of Societies for Surgery of the Hand, Germany, Berlin; *Scaphoid Fracture Classification – A three-dimensional Computed Tomography Analysis*, Arthur Turow and Anne Eva Bulstra; Miriam Oldhoff; Batur Hayat; Job Doornberg; John White; Ruurd Jaarsma; Gregory Bain

Podium presentation by Anne Eva Bulstra at the Australian Orthopaedic Association SA/NT branch Annual Scientific Meeting, Sportsmed, *Scaphoid Fracture Classification – A three-dimensional Computed Tomography Analysis*, Arthur Turow and Anne Eva Bulstra; Miriam Oldhoff; Batur Hayat; Job Doornberg; John White; Ruurd Jaarsma; Gregory Bain

Podium presentation at 2018 SA Hand Surgery Society Annual Meeting, Adelaide, SA 10th October 2018; *Preliminary results – Scaphoid Fracture 3D CT Analysis*, Arthur Turow and Anne Eva Bulstra; Miriam Oldhoff; Batur Hayat; Job Doornberg; John White; Ruurd Jaarsma; Gregory Bain

Podium presentation at the 75th AOA Annual Scientific Meeting, Brisbane, QLD, 13th October 2015; *Cadaveric study of the scaphoid bare area*, Arthur Turow; Gregory I. Bain; Joideep Phadnis

Podium presentation at the 75th AOA Annual Scientific Meeting, Brisbane, QLD, 13th October 2015;

Dorsal plating of unstable scaphoid fractures and non-unions, Arthur Turow; Gregory I. Bain; Joideep

Phadnis

Podium presentation at the Australian Orthopaedic Association SA/NT branch Annual Scientific

Meeting, The Queen Elizabeth Hospital, Adelaide, SA, 10th April 2015; *Dorsal plating of unstable*

scaphoid fractures and non-unions, Arthur Turow; Gregory I. Bain; Joideep Phadnis

Other

Preparation of the 2015 AAOS Annual Meeting ICL 266 presented by Prof Gregory I Bain, Las Vegas,

NV, USA, 24-28th March 2015, *Scaphoid Fractures and Nonunions: What's Hot, What's Not*; Gregory I.

Bain, Arthur Turow

Abbreviations

ASB	–	Anatomical snuff box
CAS	–	Capitate articular surface
CT	–	Computed Tomography
DAS	–	Distal articular surface
DIC	–	Dorsal intercarpal ligament
DISI	–	Dorsal intercalated segmental instability
DRUJ	–	Distal radioulnar joint
dSLL	–	Dorsal scapholunate ligament
LAS	–	Lunate articular surface
MPR	–	Multiplanar reconstruction
MRI	–	Magnetic Resonance Imaging
OA	–	Osteoarthritis
PA	–	Postero-anterior
PACS	–	Picture archiving and communication system
PAS	–	Proximal articular surface
pSLL	–	palmar scapholunate ligament
RSC	–	Radioscaphocapitate
SLAC	–	Scapholunate advanced collapse
SLIL	–	Scapholunate interosseous ligament
SNAC	–	Scaphoid non-union advanced collapse
STTJ	–	Scaphotrapeziotrapezoid joint
STTL	–	Scaphotrapeziotrapezoidal ligament
TT	–	Trapezio-trapezoid
XR	–	X-ray

Chapter One – Background

Introduction

Before the discovery of radiography by Roentgen in 1895, only injuries around the wrist that resulted in gross deformity were recognised to be worthy of treatment (Taleisnik, 1988). Even as X-rays became more available, surgeons gave the scaphoid and other carpal bones little attention. Sir John Charnley is famously known for stating that “one does never operate on a bone that one can swallow”. It seemed then, that the scaphoid, when fractured, was either ignored or was easily treatable. Barton, in his 1982 review of scaphoid fractures wrote: “When I was appointed a consultant in 1971, I had no questions about fractures of the scaphoid” (Barton, 1992). Much has changed since then. Doing a simple title search on Medline, reveals no less than 985 journal articles published about the scaphoid in the last ten years - an average of two articles per week. Early observations about scaphoid fractures were made by Destot at the beginning of last century (Destot, 1925). He identified that scaphoid fractures were the most frequently fractured carpal bone. Fractures were common in men than women due to exposure to higher risk activities. Destot also knew that the majority of fractures involved the waist and there was a proportion of fractures with concomitant carpal and radial fractures or dislocations. He recognised that diagnosis may be difficult as injuries to the radius and lunate may mask a scaphoid fracture. Destot’s remarks on prognosis were those of reservation, noting that bony union was uncommon and that most fractured healed with pseudo-arthritis.

Destot’s last observation has had wide-reaching implications in the medical field. Medical school teaches that scaphoid fractures are not to be missed and one should always be highly suspicious of radial sided wrist pain. Some resultant over-treatment of wrist injuries as suspected scaphoid fractures does occur; however, current treatment of scaphoid fractures is frequently accompanied by delayed diagnosis, inappropriate treatment and patient-related systemic or local factors (Nguyen

et al., 2008, Mallee et al., 2014). These challenges have resulted in most emergency and orthopaedic departments adopting a protocol for radial-sided wrist pain as well for displaced and un-displaced scaphoid fractures. Despite the plethora of scaphoid research, some areas remain untouched. This thesis is aimed at exploring scaphoid anatomy, novel treatment options and investigating if some of the previously published imaging techniques could be improved.

Anatomy

The scaphoid arises from two chondrification zones, a process that completes by the 7th week of gestation. Failure of fusion of those two zones, leads to an additional bone interposed between the scaphoid and the neck of the capitate, known as the os centrale (Slutsky and Slade, 2011).

Ossification of the carpus starts in the first two months of life in a circular fashion (Aggrawal, 2014), with the pisiform ossifying last (Figure 1.1).

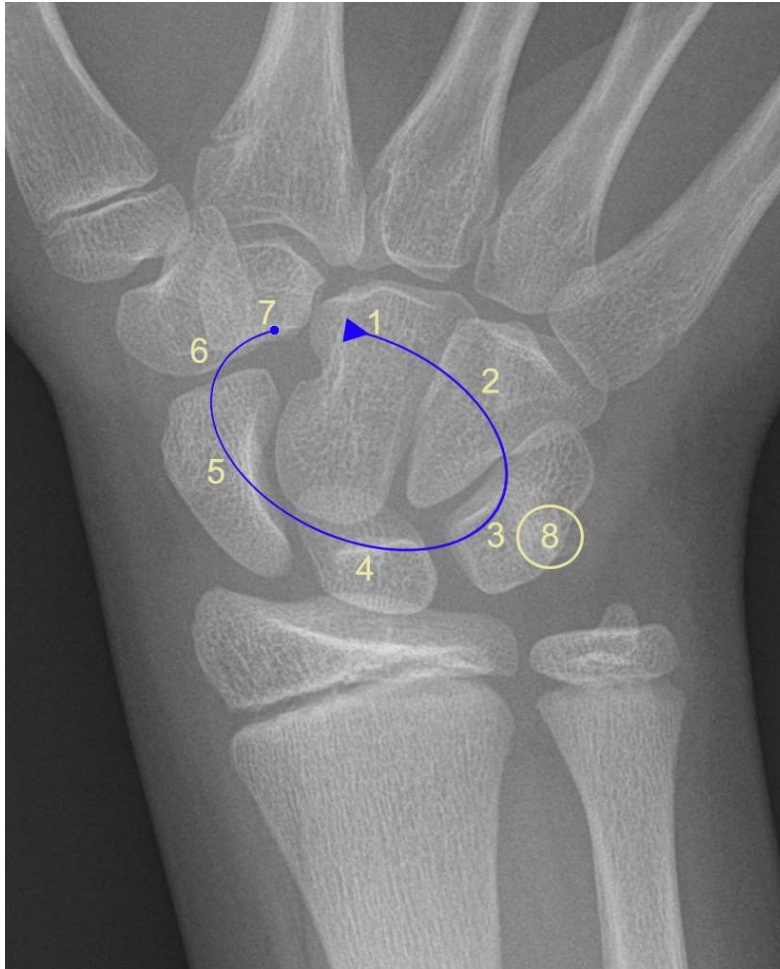


Figure 1.1: Ossification of the carpus: (1) Capitate - 2m; (2) Hamate - 3m; (3) Triquetrum – 3y; (4) Lunate – 4y; (5) Scaphoid – 4-5y; (6) Trapezium – 4-5y; (7) Trapezoid – 4-5y; (8) Pisiform – 9-12y

The majority of the scaphoid is covered in hyaline cartilage. Only 20% is non-articular and serves as attachment for ligaments, governing its biomechanics. In a neutral wrist, the scaphoid lies 65° to the sagittal, longitudinal axis of the radius. The scaphoid can have a variable shape. Past morphological work has focussed on identifying various scaphoid types based on the dorsal ridge appearance (Ceri et al., 2004, Fogg, 2004). For example, Fogg (Fogg, 2004) has examined 100 cadaveric scaphoids and divided these into two types, depending on whether the dorsal bare area had a single or multiple crests. He related these morphological differences back to ligamentous variations. Both scaphoid types had distinct scaphotrapeziotrapezoid, scaphocapitate and dorsal intercarpal ligament arrangements. These differences suggested discrete kinematics of the two scaphoid types, which

had previously also been observed by other authors (Moojen et al., 2002, Moritomo et al., 2000b): type one scaphoids are rotating and type two scaphoids are extending/flexing.

Proximal Pole

Most authors regard the proximal third of the scaphoid as the proximal pole (Bohler et al., 1954, Cooney et al., 1998, Slutsky and Slade, 2011). The scaphoid fossa of the radius articulates with the proximal pole. This fossa has a 22° ulnar inclination and 11° of volar tilt. The proximal pole finds attachment to the lunate via the scapholunate interosseous ligament (SLIL). The SLIL separates the radiocarpal joint from the midcarpal joint (Slutsky and Slade, 2011). The SLIL consists of three parts: volar, proximal and dorsal (Figure 1.2) (Apergis and SpringerLink, 2013). The SLIL is a strong ligament, able to withstand up to 300N of force, mostly attributed from its dorsal component. The volar part can resist up to 150N and the proximal part only 25-50N (Berger et al., 1999). The dorsal and volar ligaments are made up of collagen fascicles, while the proximal SLIL is made up of fibrocartilage with almost no collagen (Berger et al., 1999). The proximal part protrudes into the radiocarpal joint, similar to a knee meniscus, and can resist axial compression and shear stress. In contrast, the dorsal and volar parts prevent rotation and translation. The scapholunate joint allows for 20° of motion. Injury to the SLIL alters the wrist kinematics and results in scaphoid flexion and pronation as well as lunate extension (Short et al., 1995).

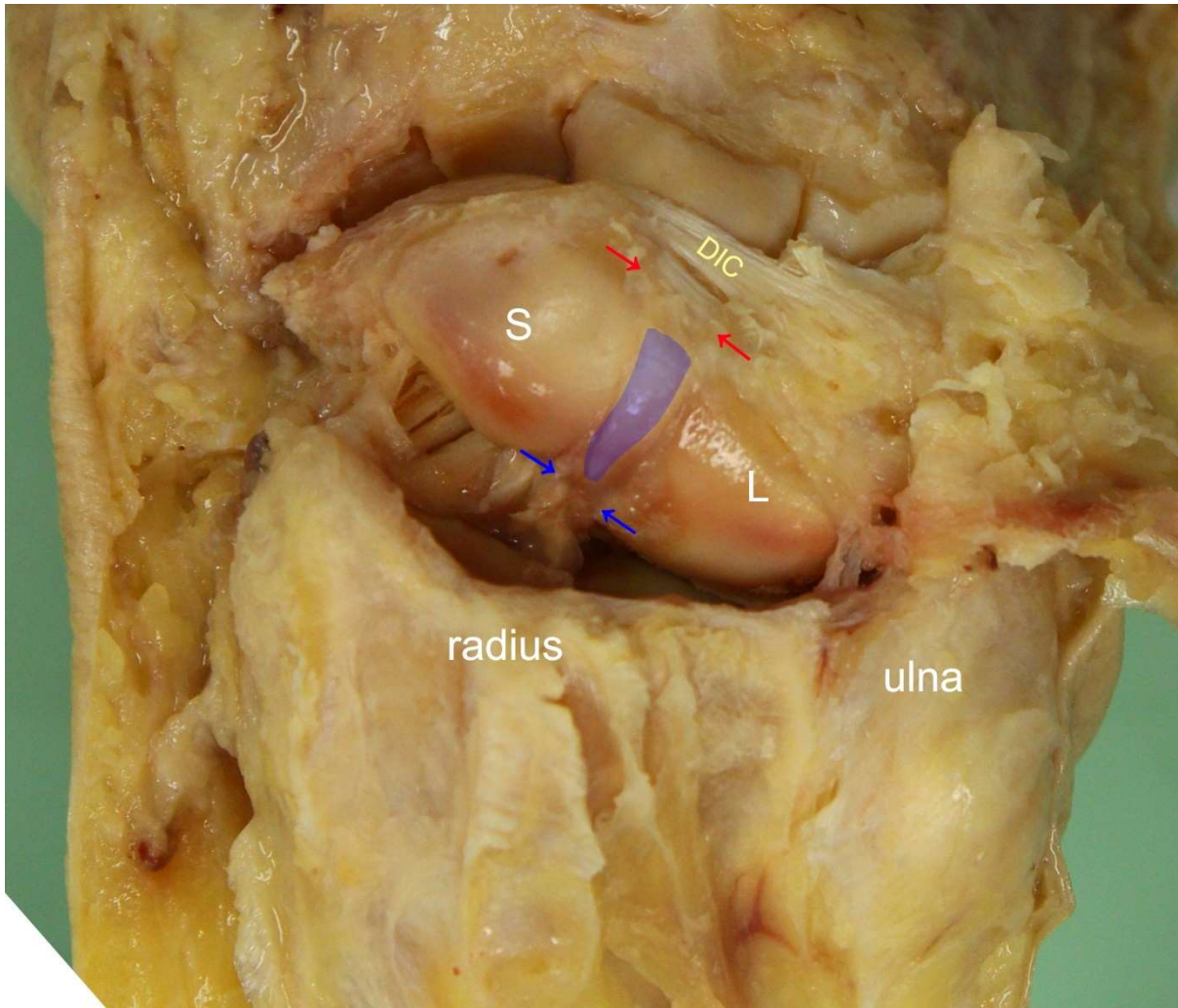


Figure 1.2: Cadaveric dissection of a right wrist from study I. The anatomy of the SLIL anatomy is shown. The dorsal part (*red arrows*) is bordered distally by the dorsal intercarpal ligament (DIC), more specifically the lunotriquetral component of the DIC. The proximal part is the *shaded blue* area. Finally, the volar component (*blue arrows*) of the SLIL is continuous with the volar capsule. S: scaphoid, L: lunate.

Waist

The middle third of the scaphoid, or the scaphoid waist, serves as the site of ligament attachment and most of the vascular supply. The majority of the non-articulating area of the scaphoid is found at the waist (Lanz, 2004). One dorsal and two volar ligaments attach to the waist.

The radioscapocapitate (RSC) ligament is the most radial of the volar radiocarpal ligaments, originating from the palmar aspect of the radial styloid. It finds attachment to the waist and the proximal part of the distal pole. The attachment to the capitate has seen some debate. Some authors have found that only a small portion of the RSC ligament terminates at the capitate. The remainder of RSC ligament fibres interdigitate with ulnocapitate and triquetrocipitate ligaments, forming the arcuate ligament (Berger, 1997, Taleisnik, 1976). Other authors have questioned this and demonstrated that the bulk of the RSC ligament to be attached to the capitate (Buijze et al., 2011b, Buijze et al., 2011a). The RSC ligament lies in the concavity of the scaphoid and acts as fulcrum around which the scaphoid rotates (Su-Bum et al., 2012, Slutsky and Slade, 2011). The second ligament to attach to the volar scaphoid is the palmar scaphotriquetral ligament. The palmar scaphotriquetral ligament has a fan-like attachment to the scaphoid and a more distinct attachment to the triquetrum. It is separated from the capitate by a synovial fold and is thought to act as a suspensory ligament for the capitate, especially in wrist dorsiflexion (Sennwald et al., 1994). The scaphotriquetral ligament and its relationship to the capitate has also been questioned (Buijze et al., 2011a).

Dorsal ligaments attach to the dorsal bare area, a zone with varying arrangements of sulci and ridges (Ceri et al., 2004). The dorsal intercarpal (DIC) ligament is a weak capsular ligament that acts as a dorsal buttress to the head of the capitate, reciprocal to the volar scaphotriquetral ligament (Slutsky and Slade, 2011). Several studies have identified several types of the DIC ligament, based on its attachment to the scaphotrapezotrapezoid joint (Smith, 1993). The DIC originates from the triquetrum, courses over the capitate and attaches to scaphoid, trapezium and trapezoid. It usually interdigitates with the dorsal radiocarpal ligament at its ulnar origin, preventing ulnar drift of the carpus (Slutsky and Slade, 2011). The proximal portion of the DIC ligament has been described as the dorsal scaphotriquetral ligament. It is thicker than the rest of the DIC ligament and attaches to the dorsal scaphoid, the scaphoid apex (Berger, 1997). Moritomo and colleagues have hypothesised that scaphoid fracture instability and, consequently, non-union is closely related to the attachment of the

dorsal scaphotriquetral ligament at the scaphoid apex (Moritomo et al., 2008). Furthermore, as highlighted above, it has been hypothesised that variable attachment to the dorsal scaphoid might reflect varying scaphoid kinematics and different scaphoid types (Fogg, 2004).

Distal Pole

The distal pole extends to the scaphotrapeziotrapezoid joint and articulates at its ulnar border, a concave facet, with the capitate. This facet has been shown to exhibit two types: elongated and shallow or round and deep (Fogg, 2004). This variation has been shown to correlate with capitate and lunate morphology. A deep scaphoid facet is associated with a type two lunate and either a round or V-shaped capitate. In contrast, a shallow and elongated scaphoid facet usually occurs with a flat capitate and a type one lunate (Yazaki et al., 2008).

The distal pole is stabilised by the scaphotrapezial and the scaphocapitate ligaments. The scaphocapitate ligament crosses the midcarpal joint, just distal to the radioscapholunate ligament. It is the thickest of all ligaments attaching to the scaphoid and has the largest area of attachment (Apergis and SpringerLink, 2013). The scaphocapitate ligament, together with the radiocapitate ligament, forms the radial arm of the arcuate ligament. Failure of the scaphocapitate ligament can lead to midcarpal instability (Heras-Palou, 2009).

The Scaphotrapeziotrapezoid joint

The scaphotrapeziotrapezoid joint (STTJ) is a multi-facet articulation, formed by the distal, triangular shaped articular surface of the scaphoid, the trapezium and the trapezoid. The trapezoid articulates with the adjacent trapezium and capitate. The distal scaphoid has been described to have a ridge traversing the articular surface in an oblique fashion (Compson et al., 1994, Moritomo et al., 2000b, Taleisnik, 1985), although this has been contested by some authors (Berger, 1997, Nuttall et al.,

1998). One anatomical study has found a clearly visible ridge to be present in 56% of examined specimens (Moritomo et al., 2000b). Another study demonstrated that such a ridge, if present, is cartilaginous only and provides no constraints to the STTJ (Fogg, 2004).

Previous kinematic work has generally demonstrated that the trapezium and trapezoid move in unison relative to the scaphoid (Kauer, 1986, Moritomo et al., 2000b). A recent in-vivo analysis has demonstrated small relative motion between the trapezium and trapezoid, in particular in wrist ulnar deviation (Sonnenblum et al., 2004); however, the overall values of displacement were small. Both bones move with only a single arc of motion. The ulnar-flexion and radial-extension motion path is parallel to the trapezoid-trapezium articular surface. An articular ridge on the distal scaphoid may represent that path of motion (Fogg, 2004, Sonnenblum et al., 2004).

The STTJ is stabilised, like most other carpal joints, by volar ligaments (Berger, 2001, Kijima and Viegas, 2009, Moritomo et al., 2000b). The capitate-trapezium ligament, stretches from the trapezium, bypassing the trapezoid, and attaches to the capitate. It acts as a volar labrum, deepening the socket of the STTJ. The main stabiliser, however, is the V-shaped scapho-trapezium ligament, closely related to the flexor carpi radialis tendon. It is twice as strong as the scapholunate ligament and prevents rotary subluxation of the scaphoid (Apergis and SpringerLink, 2013, Boabighi et al., 1993).

Vascular Anatomy

The vascular supply of the scaphoid comes from the radial artery (Figure 1.3). The vessels enter the scaphoid through non-articular volar and dorsal surfaces, which are also the sites of ligamentous attachments. The dorsal blood supply accounts for 70-80% of vascularity, supplying the waist and the proximal pole (Gelberman and Menon, 1980). The dorsal scaphoid branch arises in 70% of cases directly from the radial artery. In 23% of cases this artery originates from the intercarpal artery, a

vessel that forms the dorsal intercarpal arch at the level of the midcarpal joint. In a small subset of cases, namely 7%, the dorsal blood supply is shared between the radial artery and the intercarpal artery (Apergis and SpringerLink, 2013). The palmar blood supply accounts for 20-30% of vascularity, supplying the distal pole of the scaphoid. The palmar blood supply is shared between the superficial palmar artery, a direct branch of radial artery, and several smaller vessels entering the scaphoid through the tubercle. These smaller vessels usually arise from the superficial palmar branch of the radial artery (Freedman et al., 2001).

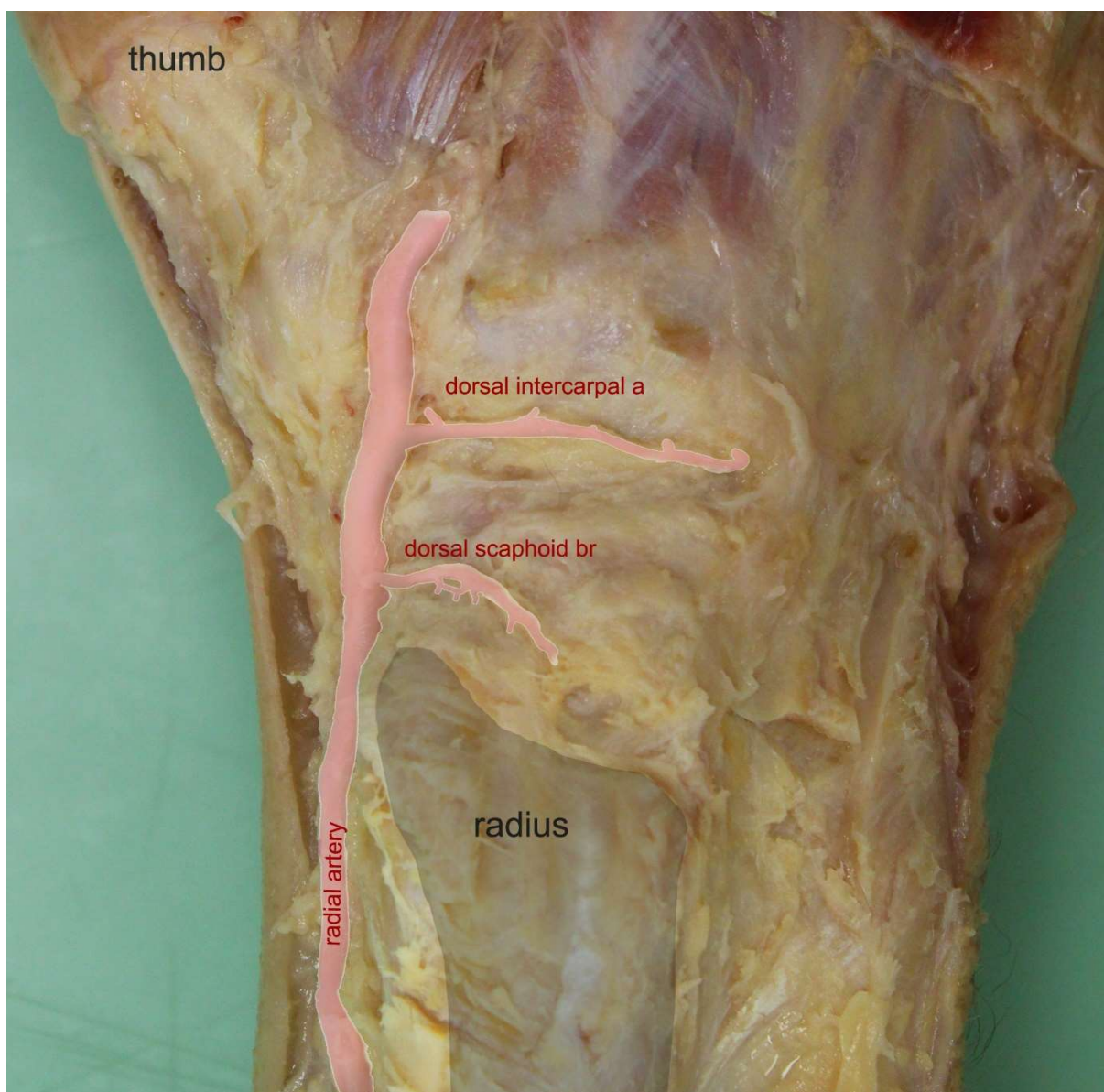


Figure 1.3: Cadaveric dissection of right wrist from study I. The dorsal blood supply of the scaphoid is shown. The scaphoid is still covered by the capsule and overlying dorsal ligaments. The dorsal scaphoid branch of the radial artery is shown branching just distal to the radial styloid. The dorsal

intercarpal artery branches from the radial artery more distal and in this specimen is not supplying the dorsal scaphoid

Biomechanics

The biomechanics of the carpus are governed by its 21 articulations and their ligamentous and bony make up. Out of the 19 forearm muscles that move the carpus, only the flexor carpi ulnaris (FCU) attaches to the carpus. FCU is commonly mistaken to attach to the pisiform and the hook of hamate (Botte, 2003); in fact, it only attaches to the pisiform and forces on the carpus are transferred by separate ligaments, namely the pisohamate and pisometacarpal ligaments (Sinnatamby and Last, 2003).

Carpal and scaphoid kinematics are complex. Several theories have been offered in the past (Figure 1.4). The row theory separates carpal bones into the proximal row (triquetrum, lunate) and distal row (trapezium, trapezoid, capitate, hamate) with the scaphoid acting as the link between them (Johnston, 1907). The column theory separates the carpus into the central (lunate, capitate, hamate), lateral (scaphoid, trapezium, trapezoid) and medial (triquetrum, pisiform) columns (Navarro, 1921). Several studies have found that a spectrum of row and column mechanics exists (Craigien and Stanley, 1995, Garcia-Elias et al., 1995).

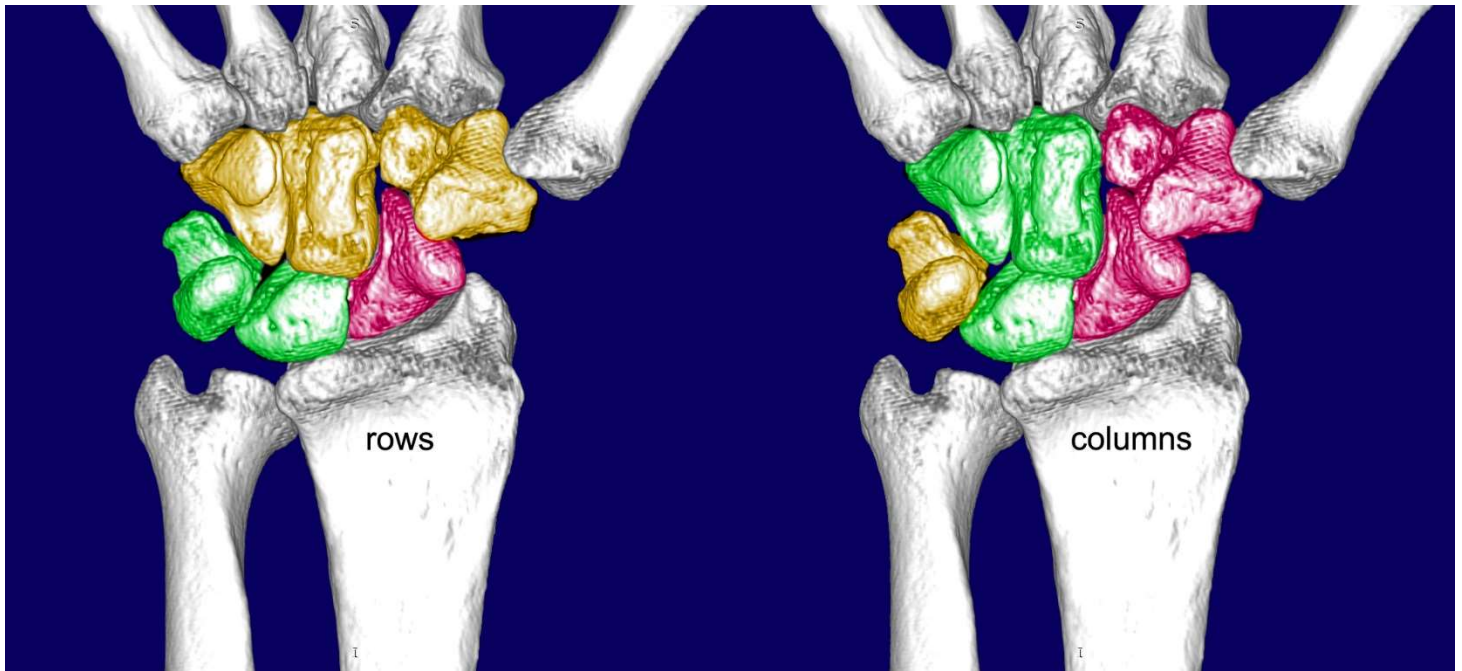


Figure 1.4: Carpal kinematic theories – rows with scaphoid acting as bridge vs columns.

Irrespective of theory, scaphoid kinematics are closely linked to lunate and capitate morphology.

Morphological differences of the capitate have been discussed above. Two types of lunate can be identified on the plain radiograph by measuring the distance between the capitate and the triquetrum (Galley et al., 2007, Viegas et al., 1990). A distance of less than 2mm corresponds to a Viegas type 1 lunate and distance of more than 4mm is a Viegas type 2 lunate. A type 2 lunate has an additional facet articulating with the hamate and, consequently, is restricted in rotation and translation compared to its type 1 counterpart.

Fogg has observed two patterns of dorsal ridge morphology which is accompanied by separate ligamentous attachments (Fogg, 2004). He hypothesised that this influenced scaphoid kinematics. A rotating scaphoid had a narrow scaphotrapezium ligament attachment to the scaphoid with DIC and RSC ligaments not attaching to the scaphoid at all. With a narrow pivot point distally, this scaphoid type would rotate around the DIC and RSC, acting as suspensory cables. Translation would be facilitated by a flat capitate type and a type 1 lunate. In contrast, an extending/flexing scaphoid had a broad scaphotrapezium ligament attachment to the scaphoid with both DIC and RSC attaching to the

scaphoid waist. Consequently, rotatory movement would be limited and restrict the scaphoid to flexion and extension only. This scaphoid type is associated with a double-facet type 2 lunate.

Epidemiology

The scaphoid fracture is the most commonly fractured bone of the carpus. Scaphoid fractures account for 59-82 % of all carpal fractures (Figure 1.5) (Green and Wolfe, 2011). They are commonly associated with extension and radial deviation of the wrist (Weber and Chao, 1978). Most injuries occur as a result of a low-energy event, such as fall onto the outstretched hand (35%) or during sports (59%). High energy trauma is less common and includes a fall from height, motor vehicle accidents or extreme sports (Green and Wolfe, 2011). Scaphoid fractures are commonly seen in the young and healthy and rarely occur in the children or the elderly, where distal radius fractures are more frequently seen. Epidemiological studies demonstrate that scaphoid fractures are more common in males up to the age of 50-60, at which point age-specific incidence is similar (Wolf et al., 2009, Larsen et al., 1992, Hove, 1999, Duckworth et al., 2012, Adler and Shaftan, 1962). Incidence in the general population ranges between 12-43 per 100000 (Hove, 1999, Garala et al., 2016, Duckworth et al., 2012). Incidence in populations at risk, i.e. young males participating in physical activities, is higher at 121 per 100000 (Wolf et al., 2009).

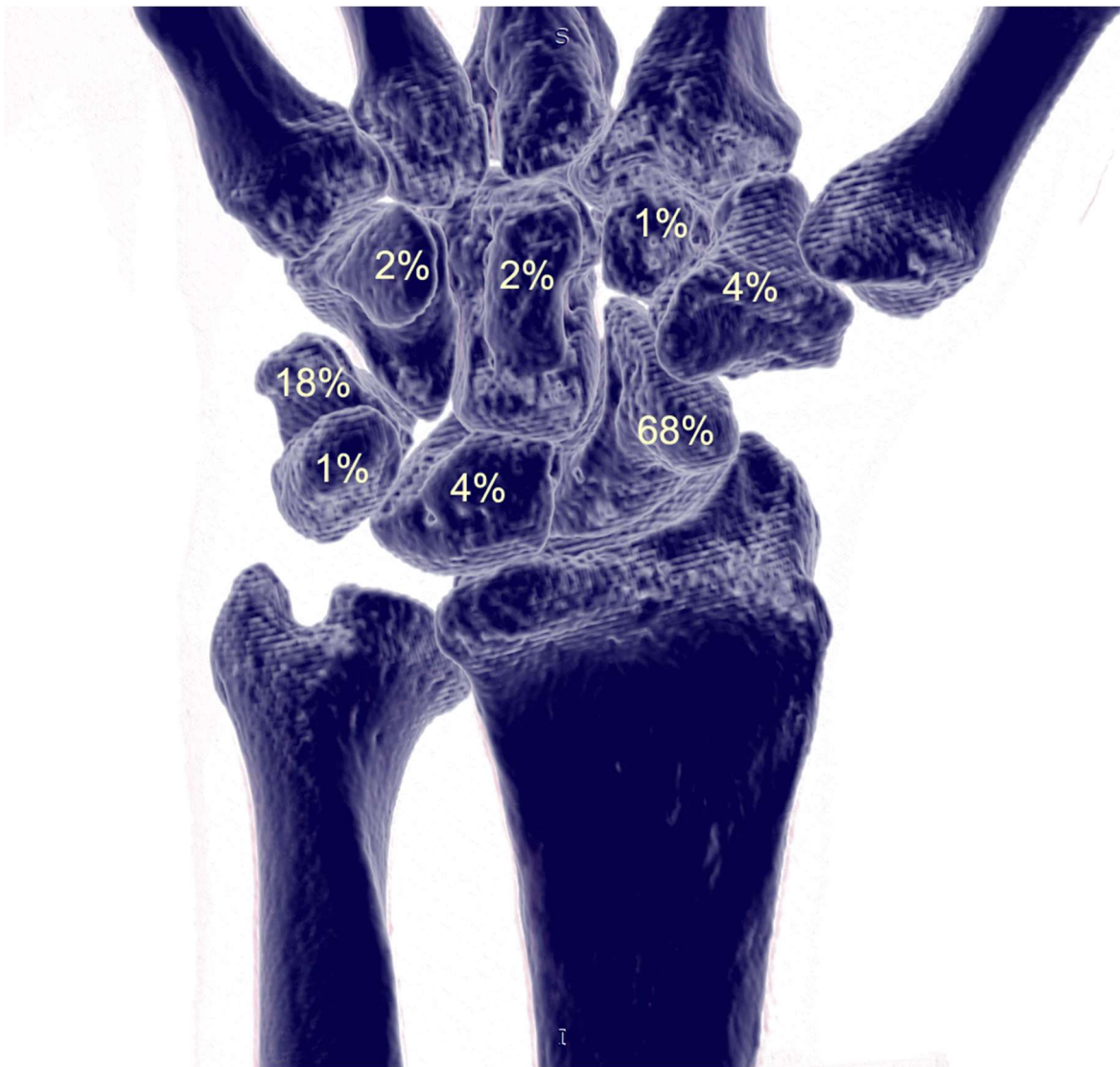


Figure 1.5: Incidence of carpal fractures (volar view of a wrist), adapted from the incidence data reported by Green and colleagues (Green and Wolfe, 2011)

Diagnosis

Clinical assessment

Diagnosing scaphoid fractures or ligamentous injuries around the scaphoid can be challenging. Many symptoms are subtle, some have settled when being seen in the outpatient department or can be mistaken for other wrist pathology, such as distal radius fractures, sprains or tendon injuries. Missed

scaphoid fractures carry a risk of delayed diagnosis, mistreatment and ultimately of non-union. This can result in persistent pain, altered wrist dynamics and finally degeneration of the carpus.

Initial assessment involves recent or past trauma, pain history, functional requirements and relevant medical history. On clinical examination the radial wrist is palpated systematically, identifying areas of most tenderness (Figure 1.6). Furthermore, scaphoid specific tests are performed: (1) anatomical snuff box (ASB) tenderness, (2) tenderness on axial loading of the thumb and (3) scaphoid tubercle tenderness.

In isolation each test has 100% sensitivity by low specificity (Parvizi et al., 1998). Parvizi and colleagues studied 215 patients with as suspected scaphoid fracture. The authors showed, that when all three tests were used in combination for acute fracture presentations, specificity increased to 74%. Similarly, Bergh and colleagues combined those three tests into a clinical scaphoid score, where ASB was given three points, tubercle tenderness 2 points and axial compression of the thumb one point (Bergh et al., 2014). A score of four or more showed a sensitivity of 77%. A score of less than four was found to have a negative predictive value of 96%, making scaphoid fracture unlikely. A recent meta-analysis confirmed the benefit of combining scaphoid examinations. The authors demonstrated that only using ASB for diagnosing scaphoid fractures, up to 13% of scaphoid fractures could be missed (Mallee et al., 2014); however, they noted that past studies had suffered from heterogeneity and that further research would be needed to optimise scaphoid fracture diagnosis by using a standardised examination and imaging protocol.

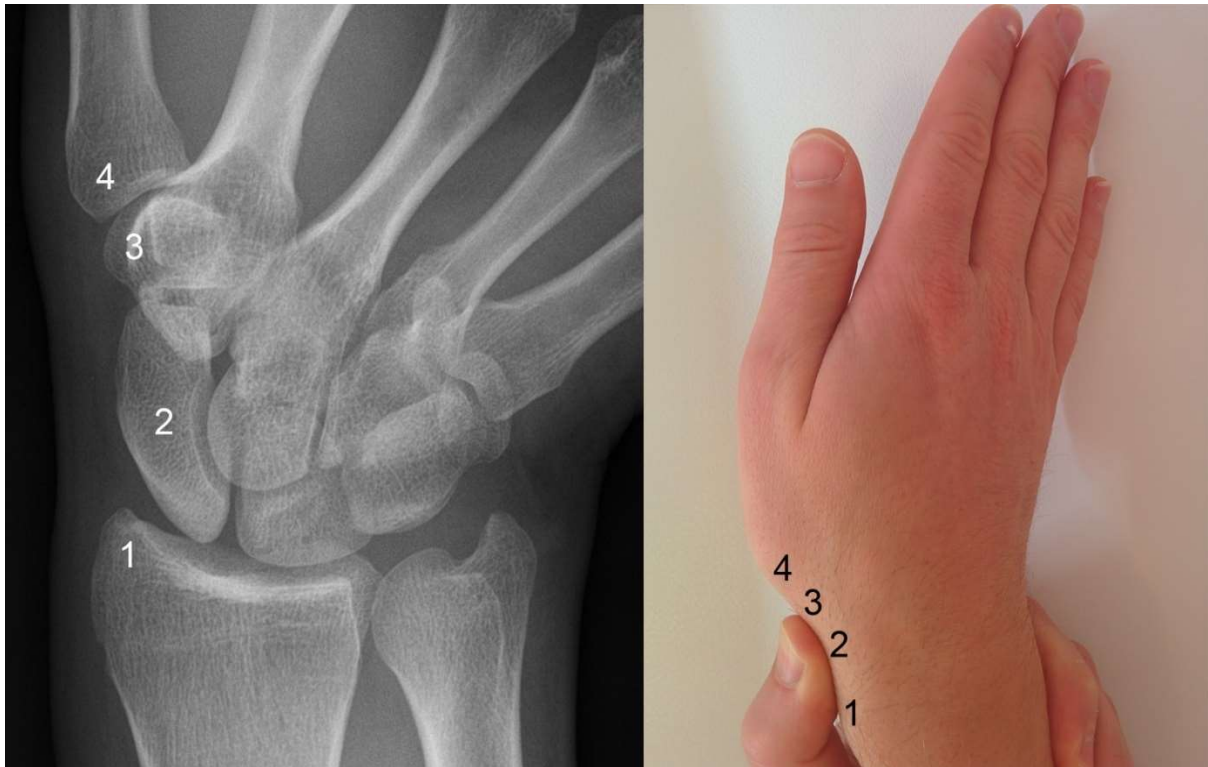


Figure 1.6: Palpation of the radial wrist when examining the scaphoid. 1: Radial styloid, 2: Scaphoid, 3: Trapezium, 4: Thumb metacarpal

Plain radiography

Plain radiographs are the standard initial imaging modality of suspected scaphoid fractures; however, there is considerable lack of uniformity in which images are obtained (Shenoy et al., 2007). Four views for a suspected fracture are recommended: (1) Posterior-anterior (PA), (2) lateral, (3) 30° uptilt and (4) PA with ulnar deviation (Figure 1.7) (Newberg et al., 2000). Initial radiographs are known to miss up to 25% of scaphoid fractures (Dorsay et al., 2001, Fusetti et al., 2005, Kukla et al., 1997). Consequently, the anxiety to miss a scaphoid fracture, usually leads to immobilisation of most patients presenting with radial wrist pain. It has been shown that for every patient with a confirmed scaphoid fracture, more than five patients are overtreated (Jenkins et al., 2008). Additional X-ray

markers for scaphoid fracture have been investigated. In 1975, Terry and Ramin described the “scaphoid fat stripe” (they termed it the “navicular” fat stripe) (Terry and Ramin, 1975). It is a small linear collection of fat between the radial collateral ligament and the tendon sheaths of the 1st extensor compartment. The scaphoid fat stripe was thought to become more pronounced with trauma (Figure 1.8). The clinical relevance of the scaphoid fat stripe was investigated by Annamalai and Raby (Annamalai and Raby, 2003). The authors found that it was a poor predictor for an occult scaphoid fracture, finding a fat stripe only in 50% of 50 magnetic resonance imaging (MRI) confirmed scaphoid fractures.

In cases with clinical signs and symptoms of a scaphoid fracture, where the radiological diagnosis is uncertain, repeat examination and imaging at two weeks is routinely performed. The sensitivity and specificity of clinical signs at two weeks has not been investigated, but is thought to be unreliable when compared to the acute assessment (Parvizi et al., 1998). Repeat radiography is postulated to increase radiolucency at the fracture site due to fracture resorption. Studies investigating this have demonstrated poor interobserver reliability of 18-53% (Low and Raby, 2005, Tiel-van Buul et al., 1992). Mallee and colleagues investigated if waiting up to six weeks would improve diagnostic accuracy (Mallee et al., 2016). The authors found that the six-week radiographs were good at excluding scaphoid fractures (negative predictive value 79-94%), however, they were poor at recognising fractures (positive predictive value 14-26%).



Figure 1.7: Pain radiography for scaphoid fractures: Postero-anterior, postero-anterior with ulnar deviation, lateral and 30° with uptilt



Figure 1.8: – Scaphoid fat stripe in an acute scaphoid fracture

Computed Tomography

As opposed to plain radiography, computed tomography (CT) provides high resolution, cross-sectional imaging of the scaphoid. Fractures on CT are identified by sharp lucent lines within the trabecular bone, a break in the cortical continuity, a step in the cortex that does not follow the outline of the bone in adjacent slices and comminuted fracture fragments (Davies et al., 2011).

Trabecular fractures with a preserved cortical line can be difficult to distinguish from normal, dorsal nutrient vessels. Nevertheless, CT has been shown to be valuable in cases with initially normal

radiographs (Hindman et al., 1989). It can be used to assess fracture displacement, comminution, associated bony injuries and union or non-union of fractures. CT has been shown to have high sensitivity (99%) and specificity (84%) for diagnosing acute fractures. However, sensitivity (73%) and specificity (80%) values for scaphoid fracture union assessment are somewhat lower (Hannemann et al., 2013). CT has been proposed to be used routinely with positive bone scan results (Waizenegger et al., 1994). The combination of radiography and CT has been proposed as routine, initial investigations for suspected scaphoid fractures (Lozano-Calderón et al., 2006). Lozano-Calderón and colleagues found the combined CT/radiography specificity to be lower than for plain CT alone. The authors proposed a higher false positive rate to be beneficial in avoiding inadequate treatment of potentially missed fractures.

Scanning along the longitudinal axis of the scaphoid to better delineate fracture morphology has been first proposed by Saunders in 1988 (Sanders, 1988). The corresponding reconstructions of the scaphoid have been shown to reliably determine fracture morphology (Sanders, 1988, Bain, 1999) and can accurately diagnose fracture union or non-union (Hannemann et al., 2013). Most studies describing scanning along the longitudinal axis of the scaphoid, require an overhead arm position while prone with the wrist in radial deviation and neutral flexion. The scan is then centred along the 1st metacarpal as a surrogate of the scaphoid axis.

Multiplanar reconstruction

The routine CT ordered for treatment follow-up or surgical planning of a scaphoid fracture usually occurs in the prone position with the hand overhead in the “superman” position (Davies et al., 2011). The wrist is placed in the centre of the gantry and scanning is then performed along the axis of the forearm. Scans that focus on any components of the wrist commence proximal to the distal radioulnar joint (DRUJ). In contrast, CT scans of the hand start distal to the DRUJ. Modern CT scanners provide fine high-resolution images at 0.625mm thickness. These source images are then reformatted to the coronal and sagittal planes. CT protocols vary from institution to institution, but

the longitudinal axis of the radius is routinely used for those reconstruction (Davies et al., 2011). Consequently, the majority CT scans assessed by the treating clinician are centred on the wrist (Figure 1.9). Scanning along the longitudinal axis of the scaphoid can assist in fracture plane assessment, especially when there is volar collapse of the scaphoid with a resultant humpback deformity (Bain, 1999, Sanders, 1988). However, with modern picture archiving and communication systems (PACS) multiplanar reconstruction can be performed in real time from the source fine slice images without relying on the position of the patients limb on the gantry (Haak et al., 2016) (Figure 1.9 & 1.10).



Figure 1.9: CT multiplanar reconstructions of the neutral wrist; fine slice axial source images (0.625mm; yellow plane) were used to create sagittal (blue plane) and coronal reconstructions (pink plane)



Figure 1.10: CT multiplanar reconstructions using the longitudinal scaphoid axis as reference (0.625mm; yellow plane)

Magnetic resonance Imaging

Magnetic resonance imaging has been shown to have excellent sensitivity (100%) and specificity (95-100%) (Breitenseher et al., 1997, Hunter et al., 1997). A recent meta-analysis compared bone scintigraphy, CT and MRI in identifying occult scaphoid fractures (Yin et al., 2010). The authors found MRI to be more sensitive than CT (96% vs 93%). Both CT and MRI were equally as specific at 99%. When compared to bone scintigraphy, MRI was found to have the same sensitivity and an excellent diagnostic value for excluding scaphoid fractures. However, bone scintigraphy was less specific (89%) at diagnosing scaphoid fractures. MRI has been shown to be more cost effective than serial radiography and clinical examination (Brooks et al., 2005, Yin et al., 2015, Karl et al., 2015). This has also been confirmed in a small Australian cost-effectiveness study investigating early MRI in a rural hospital setting (Kelson et al., 2016). Prolonged, unnecessary immobilisation can be avoided if a scaphoid fracture is ruled out early with a negative MRI scan.

An early MRI following injury can be a valuable investigation in the management of the occult scaphoid fracture. Brydie and colleagues, for example, examined 195 patients with a suspected

scaphoid fracture (Brydie and Raby, 2003). After initially normal radiographs, MRI scans were performed within 14 days of injury. Only 19% of patients had a confirmed scaphoid fracture; however, the authors reported that 92% of patients had their management altered as a result of the MRI scan. Furthermore, 61% of patients had no injuries at all and were able to be discharged immediately following the MRI. Similarly, Mack and colleagues followed a similar investigative path, with MRI scans performed on average 6.6 days after initial injury (Mack et al., 2003). The authors were able to shorten the time of immobilisation in 40% of cases and 33% were discharge with a normal MRI study. MRI can be a powerful tool in streamlining care for patients presenting with suspected scaphoid fractures, shortening treatment duration and cutting down on time to diagnosis (Wijetunga et al., 2019). However, as Brydie and colleagues found, appropriate case selection is crucial. Performing an MRI scan without initial radiographs, can be indicative of incomplete patient assessment and can result in low value MRI scans (Brydie and Raby, 2003).

Other modalities

Bone Scintigraphy

Bone scintigraphy can be used as a second-line imaging modality in patients with persistent suspicion of a scaphoid fracture after negative plain radiographs (Slutsky and Slade, 2011). The fractured scaphoid usually appears as focal areas of hyperaemia and active bony remodelling. Areas of decreased uptake, suggestive of avascular bone, are rarely seen (Munk et al., 1997). Its advantage is its high sensitivity (94-100%) in acute scaphoid assessment. However, specificity is variable (60-95%) (Stordahl et al., 1984, Vrettos et al., 1996) due to concomitant conditions mimicking a scaphoid fracture, such as bone bruises, carpal instability, soft tissue damage or synovitis and joint degeneration. Furthermore, the predictive value of bone scintigraphy is time dependant. Scans should be delayed by 48hrs following an acute injury to avoid diffuse hyperaemia as a consequence of traumatic synovitis, making interpretation difficult (Slutsky and Slade, 2011, Munk et al., 1997).

Rhemrev and colleagues compared bone scintigraphy with CT and found bone scintigraphy to have a 95% sensitivity and 94% specificity (Rhemrev et al., 2010). Bone scanning had a 68% positive predictive value and a 99% negative predictive value.

A negative bone scan rules out a scaphoid fracture, which is why it can be a valuable imaging modality. A positive scan usually warrants further axial imaging, such as an MRI or CT in order to guide further treatment (Munk et al., 1997).

Sonography

Ultrasound is an uncommon modality to investigate or diagnose scaphoid fractures. Surrogate markers of scaphoid fracture, such as an effusion in the wrist joint or in the STTJ have been studied previously and showed promising results (Fusetti et al., 2005, Hodgkinson et al., 1993); however, this appears to be highly operator dependent. Furthermore, sonography is only able to image the dorsal scaphoid and would require further investigations to guide treatment.

Treatment

Non-Operative

Splinting, using a backslab or a full cast, remains the mainstay of treatment of scaphoid fractures.

Cast immobilisation has been shown to produce excellent union rates (Clay et al., 1991, Böhler et al., 2003). Böhler and colleagues evaluated 557 scaphoid fractures and found that after an average of 59 days of cast immobilisation 97% of scaphoid fractures united. Other studies have reported non-union rates with cast immobilisation of 10-12% (Dias et al., 1989, Clay et al., 1991). Dias and colleagues performed a randomised controlled trial investigating the utility of cast immobilisation as opposed to early surgical fixation (Dias et al., 2005). The authors found an even higher anticipated non-union rate of 22% for fractures treated non-operatively. However, their study was relatively small compared to other large-scale studies and conversion from cast immobilisation to surgical

fixation was instigated at 12 weeks post injury where fractures were deemed to be delayed rather than non-united. The authors recommended an aggressive conservative treatment algorithm which included fracture re-assessment by radiography and CT at six weeks post injury. Cases with fracture gap widening or significant progression failure at that time point would then be converted to surgical fixation. The authors anticipated that this should result in union rates of 95%.

Several cast immobilisation criteria have been investigated in the past. The inclusion of the thumb in what is now commonly known as the scaphoid cast became popular in the 1950s (Barton, 1992).

Multiple studies have investigated the utility of thumb inclusion. Erhart and colleagues, for example, have demonstrated that, despite cast immobilisation, simulated thumb grasping can produce 0.0038 ± 0.051 Nm of torque and up to 4N of force on an osteotomised scaphoid model in an in vitro study (Erhart et al., 2016). In contrast, none of the clinical studies were able to demonstrate that the scaphoid cast produces better outcomes than the traditional below elbow cast (Clay et al., 1991, Yanni et al., 1991). In vivo motion studies have confirmed that scaphoid movement in thumb spica or standard casts are very small and are not influenced by cast choice (Kawanishi et al., 2017). Similarly, Moritomo and colleagues demonstrated that interfragmentary movement in scaphoid fractures is much smaller than the movement of each fragment. The authors found interfragmentary motion to be 33% of global wrist motion in the flexion-extension arc and only 1% of global wrist motion in the ulno-radial wrist deviation arc (Moritomo et al., 2008). Cast material for scaphoid fractures has not been investigated in great detail. Some inferred conclusions can be drawn, however, from evidence in the paediatric fracture management. More modern, synthetic casting materials have been shown to result in less complications and lower loss of reduction rates than the traditional plaster of Paris (Inglis et al., 2013). The most important part in the control of wrist motion during scaphoid immobilisation is limiting extension and ulnar deviation. Slight flexion of the wrist can produce better fracture apposition (Berlin, 1929) and wrist extension may lead to increased fracture instability (Yanni et al., 1991). The neutral wrist usually results in locking of the scaphoid between the trapezium and the radius. This locking effect between distal and proximal struts can be

diminished when the wrist is mobilised into ulnar deviation (Kawanishi et al., 2017).

Delayed treatment

Treatment delay can have adverse effects on union rates and union times. There is increased risk of non-union with delayed fracture diagnosis and consequent, late treatment commencement. Non-union rates of delayed scaphoid fracture immobilisation have been reported in the order of 40-88.1% (Wong and von Schroeder, 2011, Langhoff and Andersen, 1988). However, Langhoff and Andersen found that delays of up to four weeks showed no effect on fracture non-union rates (Langhoff and Andersen, 1988). Time to union is also increased when treatment is delayed. Mack and colleagues demonstrated that subacute scaphoid fractures took almost twice as long to unite than acute fractures (19 weeks vs 10 weeks) (Mack et al., 1998). Similar findings have also been reported by Bannerman who identified 16 scaphoid fracture 30 to 180 days old to unite after an average time of casting of five months (Bannerman, 1946). Despite poor outcomes of subacute scaphoid fractures, there is evidence to suggest that a period of immobilisation can still be beneficial for subacute fractures. Grewal and colleagues evaluated outcomes for subacute scaphoid fractures, presenting six weeks to six months after injury (Grewal et al., 2015). The authors examined 28 scaphoid fractures in patients with no risk factors for non-union, i.e. diabetes, fracture comminution or humpback deformity of the scaphoid. They found that casting of 11-14 weeks resulted in a union rate of 82%. The authors concluded that a trial period of up to three months of immobilisation for subacute scaphoid fractures should be considered.

Surgical fixation

Non-displaced fractures

Controversy exists with regard to management of acute, non-displaced scaphoid fractures.

Management includes cast immobilisation or percutaneous screw fixation. The union rate for acute,

non-displaced fractures treated with cast immobilisation ranges between 88% to 95% (Cooney et al., 1980). Dias and colleagues recommended acute, non-displaced fractures to be managed non-operatively (Dias et al., 2005). The authors randomised 88 patients with acute scaphoid fractures into a casting treatment path and a surgical arm. They found that patients managed with surgical fixation, had better range of motion, grip strength and patient reported outcome measures at eight weeks post-operatively. Grip strength remained significantly better at three months when compared to the non-operative cohort; however, outcomes measures normalised between the two treatment groups at six months and this remained at the final one-year follow-up. The authors concluded that, given the favourable results of cast immobilisation and the lack of any identifiable patient outcome measures differences compared with surgically managed patients at six months, non-displaced fractures should be managed with cast immobilisation in order to prevent overtreatment.

Surgical fixation of the acute non-displaced scaphoid fracture has been proposed by several authors (Bond et al., 2001, McQueen et al., 2008). Percutaneous screw fixation of non-displaced fractures can avoid complications associated with cast immobilisation, such as prolonged immobilisation, joint stiffness, skin breakdown, more frequent outpatient reviews as well as delayed return to work (Kawamura and Chung, 2008). In addition, despite being more challenging than open techniques, the percutaneous approach offers the advantages of preserving carpal ligaments, minimising vascular injury and scarring. This can decrease the impact on range of motion post-operatively (Kawamura and Chung, 2008). Bond and colleagues performed a prospective randomised controlled trial comparing percutaneous screw fixation in eleven patients with cast immobilisation in 18 patients (Bond et al., 2001). The authors found a faster time to union time in the surgical group (7 weeks) versus the cast immobilisation group (12 weeks). Patients that were immobilised in a cast took almost twice as long to return to work (15 weeks) compared with the surgical group (8 weeks). Several cost-effectiveness analyses have demonstrated that treatment of non-displaced fractures with minimal invasive techniques to be overall superior to non-operative treatment in plaster.

Patients spent less time with their wrist immobilised and were able to return to work quicker (Davis et al., 2006, Papaloizos et al., 2004).

There is no clear consensus on the best management of acute, non-displaced scaphoid fractures. Prolonged cast immobilisation is becoming less well tolerated with patients wanting to return to work and sports. Early surgical fixation can be considered in young, high demand patients. Poly-trauma patients with an undisplaced scaphoid fracture already undergoing surgery or where a scaphoid fracture would delay or hinder rehabilitation should also be considered for early fixation. The decision for surgery of non-displaced scaphoid fractures should be in discussion with the patient, taking their expectations for short-term and long-term outcomes into consideration.

Unstable fractures

Surgical fixation is recommended for displaced, open and proximal pole fractures. Scaphoid fractures that are considered unstable should also undergo operative intervention (Tait et al., 2016). Fractures associated with carpal instability, such as perilunate dislocations, are unstable. Furthermore, the unstable scaphoid fracture is one that shows $\geq 1\text{mm}$ displacement, a lateral intra-scaphoid angle of $\geq 35^\circ$, a scapho-lunate angle of $\geq 60^\circ$, comminution or bone loss (Suh and Grewal, 2018). Fractures that are undisplaced on presentation, but progressively displace during cast immobilisation should be considered unstable and warrant surgical fixation.

Numerous techniques for open reduction and internal fixation have been described. The headless compression screw, placed along the longitudinal axis of the scaphoid, has become the most common fixation method (Suh and Grewal, 2018). The benefit of the headless compression screw is that it can be recessed below the articular cartilage and that it can be inserted through either the volar or dorsal approach. The volar approach preserves the dominant, dorsal blood supply of the scaphoid and allows good visualisation of the distal pole and the scaphoid waist. Longer screws can be placed through the volar approach (Meermans and Verstreken, 2012), by utilising the scaphoid

tubercle for additional screw purchase. Its disadvantages are a relatively limited exposure of the proximal pole and disruption of the radial carpal ligaments, namely the RSC and the radiolunate ligaments. Repair of those ligaments and a consequent period of immobilisation are further downsides of the volar approach. The dorsal approach allows for superior exposure of the proximal pole and easier screw placement as the longitudinal axis of the scaphoid is directly visualised (Kawamura and Chung, 2008). Cadaveric studies have demonstrated that the dorsal approach allows for a more central screw placement, especially in proximal pole fractures (Chan and McAdams, 2004). The tenuous, dorsal blood supply can be disrupted during the dorsal approach; however, there is currently no evidence to suggest that the dorsal approach to the scaphoid increases the rates of avascular necrosis following fixation.

Neither of the two approaches are superior to one another, rather the choice of surgical approach is dependent on surgical preferences of the treating surgeon and on the scaphoid fracture configuration, associated comminution, bone loss or ligamentous injury. For example, a distal radius fracture requiring volar, locked plate fixation with an associated scaphoid waist fracture would be best managed using the volar approach. The modified volar Henry approach can be extended distally, following the flexor carpi radialis tendon. Division of the RSC and the radiolunate ligaments would expose the volar scaphoid waist and the scaphoid tubercle. This would allow for simultaneous fixation of the scaphoid waist fracture and the distal radius fracture.

In contrast, a greater arc perilunate dislocation with a displaced scaphoid waist fracture would be best managed with a dorsal approach (Figure 1.11). This would allow reduction of the scaphoid waist fracture, using the dorsal ridge and the proximal articular surface as guides for restoration of length and rotation. Associated ligamentous injuries could also be assessed with a dorsal exposure. An injury to the lunotriquetral ligament and incongruity of the lunotriquetral articulation, for example, could be directly evaluated and stabilised accordingly.



Figure 1.11: Acute, dorsal trans-scaploid perilunate dislocation

Scaphoid non-union

Non-union is the arrest of fracture healing beyond six months. It is demonstrated on serial radiographs. Failure of trabecular bridging across a fracture site or a persistent fracture line are signs of failure of union. Progressive evidence of failure to unite, such as sclerotic fracture margins, cyst formation, collapse of fracture fragments or worsening deformity can accompany scaphoid non-union. Scaphoid collapse in non-union is frequently associated with loss of the volar cortical scaphoid length. This leads to an increased lateral intra-scaploid angle of $\geq 35^\circ$, resulting in the humpback deformity of the scaphoid (Sanders, 1988). Union that is achieved between three and six months is considered delayed union (Kawamura and Chung, 2008). Non-union can be attributed to delayed presentation or diagnosis, inadequate immobilisation at initial diagnosis, fracture instability, associated injury to carpal ligaments and disruption to the blood supply either from injury or from iatrogenic causes (Steinmann et al., 2002). Untreated scaphoid non-union can progress to carpal collapse and avascular necrosis of the proximal fracture fragment. It leads to a predictable pattern of

degenerative radiocarpal osteoarthritis (Watson and Ballet, 1984). Narrowing of the radio-scaphoid articulation is followed by, arthrosis of the proximal fragment at its radial articulation. The ulnar aspect of the capitate head erodes last. Scaphoid non-union is usually associated with dorsal intercalated segmental instability (DISI). In DISI, the proximal scaphoid fragment extends with the lunate. The distal fragment is anchored by scaphocapitate and scaphotrapezotrapezoidal ligaments (STTL), leading to relative flexion of the distal fragment. The goals of scaphoid non-union treatment are to achieve fracture healing and to restore carpal alignment. Carpal alignment is crucial in preserving kinematics of the carpus and to prevent osteoarthritis (Ruby et al., 1985, Kawamura and Chung, 2008).

Surgical techniques for the treatment of scaphoid non-union include the use of non-vascularised or vascularised bone grafts together with supplementary internal fixation. Non-vascularised bone grafts are aimed to fill the non-union site and to restore scaphoid length in the sagittal and frontal planes (Slutsky and Slade, 2011). The Russe bone grafting technique involves debridement of the non-union site from the volar approach, creation of a rectangular window and filling of the defect with corticocancellous bone graft from the iliac crest. An alternative technique is the precision bone grafting technique (Waitayawinyu et al., 2007). The volar scaphoid is cored out using a tube saw. A dowel-shaped graft is harvested from the ilium with a slightly larger tube saw than the one used on the scaphoid. This graft is inserted into the non-union site, providing a volar cortical strut and cancellous bone across the fracture fragments. The graft can then be secured with either Kirschner wires or with a headless compression screw. Supplementary screw fixation across the corticocancellous graft has been shown to provide better stability and to result in higher union rates of up to 94% when compared with wire fixation of the graft (77% union) (Merrell et al., 2002). Vascularised bone grafts are hypothesised to supply the non-union site with growth factors, aid in re-vascularisation of avascular bone and, consequently, provide a more reliable union following grafting (Chang et al., 2006). Several donor sites of vascular pedicles have been described (Tambe et

al., 2006). These include the pronator quadratus pedicle bone graft, grafts based on the index finger metacarpal or thumb metacarpal and pedicles from the ulnar carpal artery. Free vascularised bone grafts from the femoral supracondylar region or the ilium have also been described. However, the dorsal radial vascularised bone graft supplied by the 1,2 intercompartmental supraretrinacular artery has been the most researched grafting technique (Zaidenberg et al., 1991). Union rates for non-vascularised bone grafting have been reported to range between 70%-90% (Chang et al., 2006). In cases with concomitant avascular necrosis of the proximal fragment, non-vascularised bone grafting appears to be less effective with a union rate of 47% (Merrell et al., 2002). Vascular bone grafting is surgically demanding and good outcomes are not universal. Despite smaller studies reporting excellent outcomes (Zaidenberg et al., 1991), some authors warn that good outcomes are based on careful patient and fracture configuration selection as well as on meticulous surgical technique (Chang et al., 2006).

In cases where scaphoid non-union has led to degenerative arthritis involving most of the wrist, salvage procedures can be considered depending on the symptoms, activity limitations and functional demand of the patient. This could include scaphoid excision, limited carpal fusion, proximal row carpectomy, wrist arthrodesis or total wrist arthroplasty.

Assessment of fracture union

Wrist mobilisation following treatment of a fractured scaphoid is based on clinical signs and radiographic features on serial radiographs. Clinical assessment involves comparable examination techniques to diagnosis of acute scaphoid fractures. The negative predictive value for a combined assessment of anatomic snuff box tenderness, pain on axial compression of the thumb, tenderness over the scaphoid tubercle and thumb range of motion has been reported to be 100% (Parvizi et al., 1998). Reliance on only one of the above tests should be avoided, as their diagnostic value decreases when used in isolation. Range of motion assessment following cast immobilisation can be limited due to associated wrist and thumb stiffness, especially when a thumb-spica cast was used.

Radiological assessment involves plain radiography with the addition of more advanced modalities, such as CT or MRI, when plain radiography is inconclusive. Rigid scaphoid fixation of unstable fractures relies on absolute stability principles of fracture management. This results in interfragmentary compression with absence of micromotion under physiological loading. In contrast, in relative stability, such as intramedullary nailing of long bones or bridge plating of comminuted fractures, callus formation is stimulated by controlled fracture micromotion (Kojima and Pires, 2017). Similarly, in non-displaced, stable scaphoid fractures, fragment interdigitation can mimic an absolute stability construct. As 80% of the scaphoid is articular and bathed in synovial fluid, fracture haematoma and its associated growth factors are washed away and, hence, callus formation is discouraged. Based on these principles, plain radiography assessment of scaphoid fracture union has focussed on trabecular bridging, rather than callus formation (Hackney and Dodds, 2011).

Interpretation of trabecular bridging can be challenging to assess. Serial radiographs are likely subject to slight rotational variation and, consequently, trabeculae can appear to be bridged, when in fact they are not. Dias and colleagues have assessed inter-observer reliability of union assessment based on plain radiography (Dias et al., 1988). The authors demonstrated that there was poor agreement on trabecular bone bridging across the fracture line at twelve weeks after injury. Consequently, assessment of trabecular bridging can be unreliable and inaccurate. This can either delay wrist mobilisation and overestimate the time needed for cast treatment (Leslie and Dickson, 1981) or compromise successful fracture healing due to premature return to full activities.

MRI has been proposed to assess fracture union (Kulkarni et al., 1999, Imaeda et al., 1992). As acute fractures undergo healing, high intensity signal can be observed of the distal fragment on T2-weighted MRI. When union is achieved, both T1-weighted and T2-weighted imaging normalise and are iso-intense. In cases of non-union or where union is unlikely, both T1- and T2-weighted images remain hypo-intense. Kulkarni and colleagues (Kulkarni et al., 1999) postulated that non-union can be predicted with MRI at six weeks following injury. The authors observed re-vascularisation of both

fracture fragments by a double fracture line on MRI, the re-vascularisation front. Absence of this front was associated with eventual non-union of a fracture. The main disadvantage of MRI is that it tends to demonstrate abnormal signal until normal marrow crosses the fracture site (McNally et al., 2000). Furthermore, metal artefacts following fracture fixation make interpretation of union challenging. This can potentially result in persistence of mobility limitations or prolonged immobilisation while awaiting MRI findings to return to normal. Consequently, MRI is usually reserved for fracture diagnosis rather than union determination.

In contrast, CT scans are more readily used to assess fracture union. CT scans can be reformatted in multiple planes and provide definition of the trabecular architecture as the scaphoid undergoes union. Reformatting of scans in the coronal and sagittal planes using the longitudinal axis of the scaphoid as reference rather than the transverse plane of the wrist or forearm facilitates a more accurate assessment of union (Sanders, 1988). Trabecular bridging is assessed on CT in all reformatted planes and the percentage of bridging assessed. There is some debate about what percentage is regarded as union. Singh and colleagues, for example, investigated partial scaphoid union in 66 non-operatively managed scaphoid fractures (Singh et al., 2005). The authors were able to demonstrate that partial union with trabecular bridging of more than 25% resulted in full union at final follow-up of 23-40 weeks. Most authors, however, define union as more than 50% of trabecular bone bridging on CT (Hackney and Dodds, 2011, Suh and Grewal, 2018).

Clinical outcomes

Distal pole fractures

The majority of distal pole fractures are avulsion fractures of the scaphoid tubercle. Intra-articular distal pole fractures are less common and usually result from impaction of the trapezium and trapezoid bone against the distal articular surface of the scaphoid (Clementson et al., 2017). Distal

pole fractures are usually treated with cast immobilisation for six weeks. Given the good vascular supply of the distal pole, fractures are known to heal well with minimal complications (Mody et al., 1993). In addition, the strong surrounding STTJ ligaments, namely the capitate-trapezium and the V-shaped scapho-trapezium ligaments, impart stability to the fractured distal pole and minimise motion during fracture healing. Complications of distal pole fractures are rare. Oron and colleagues (Oron et al., 2013) identified eight distal pole non-unions (4%) in their study of 193 scaphoid non-union cases. The authors found that delayed or inadequate treatment to had been the major cause for non-union of the distal pole. In addition, all of their non-union cases were intra-articular fractures and had DISI deformity, suggesting concurrent ligamentous injury or high energy trauma associated with the index fracture mechanism. Clementson and colleagues followed up 41 distal pole fractures after a median of ten years post injury (Clementson et al., 2017). A CT was performed to assess fracture union and any degenerative changes of the STTJ. The authors found no self-reported impairment on patient outcome scores and were only able to identify one non-union in a tubercle avulsion case. Seven patients (17%) had STTJ arthritis. None of the patients had any residual symptoms. Grip and pinch strength were preserved in all patients. Overall, complications of distal pole fractures are rare.

Waist fractures

Outcomes of non-displaced waist fractures are generally good, irrespective of treatment chosen. Cast immobilisation for non-displaced waist fractures has been assessed by several CT-based studies (Clementson et al., 2015, Grewal et al., 2013, Geoghegan et al., 2009). Observed union rates after 4-10 weeks of a short arm thumb spica cast were 90-100%. Grewal and colleagues expanded their CT-driven outcome study to investigate risks factors for non-union (Grewal et al., 2013). They identified inter-fragmentary translation of 1mm to increase non-union risk by 27%. This almost doubled (53%) when translation of more than 1.5mm was observed. Humpback deformity was also associated with higher rates of non-union. Fracture line sclerosis did not affect non-union rates; however, sclerotic

fractures took significantly longer to unite (166 days) when compared to fractures with no sclerosis (67 days). Surgical fixation of non-displaced fractures has been reported to result in union rates of 82-100% (Clementson et al., 2015, Bond et al., 2001, McQueen et al., 2008). Clementson and colleagues showed surgical fixation to result in inferior union rates (82%) when compared to cast immobilisation (90%) (Clementson et al., 2015). In contrast, both Bond and colleagues (Bond et al., 2001) as well as McQueen and colleagues (McQueen et al., 2008) demonstrated percutaneous screw fixation to result in 100% union based on serial radiographs. Both studies reported earlier union rates with screw fixation and quicker return to work.

Non-operative treatment of unstable scaphoid fractures is known to result in poor outcomes. Cooney and colleagues examined 13 patients with acute, displaced scaphoid fractures immobilised in a cast (Cooney et al., 1980). Six patients failed to unite (46%). Three of the seven fractures that united showed signs of malunion and associated carpal instability. Malunion led to post-traumatic arthritis, chronic pain and decreased range of motion. Outcome studies for surgical management of unstable scaphoid fractures usually show favourable results. Union rates have been reported to be 83-100% (Herbert and Fisher, 1984, Matson et al., 2017, Rettig et al., 2001). Compared to non-displaced fractures, unstable scaphoid fractures take longer to unite. Time to union ranges between 2.8-4.2 months (Herbert and Fisher, 1984, Matson et al., 2017). The standard of care for unstable fractures involves open reduction of articular surfaces, bone grafting of comminution or impaction and internal fixation with a headless compression screw. Percutaneous fixation is uncommon; however, some evidence suggests that this might be a viable option for the unstable scaphoid fracture. Matson and colleagues (Matson et al., 2017) reported on closed reduction and percutaneous screw fixation in 14 patients. Thirteen scaphoids united (93%) after an average of 11.5 weeks. Similarly, Chen and colleagues (Chen et al., 2005) reported 100% union with percutaneous fixation of unstable scaphoid waist fractures. Some of the problems of percutaneous management include complications of screw insertion, such as painful hardware, superficial infection, cutaneous

nerve irritation, hardware failure and post-operative reflex sympathetic dystrophy (Matson et al., 2017). Furthermore, closed reduction of displaced fractures might not always be possible. In fact, closed reduction has been shown to have a failure rate of up to 50% (Matson et al., 2017). Overall complications of surgical management of waist fracture vary between 0% and 29% (Tait et al., 2016). Bushnell and colleagues investigated complication rates following percutaneous screw fixation (Bushnell et al., 2007). Minor complications were found to occur in 8%. Major complications, such as hardware failure, periprosthetic failure or non-union, were much more common at 21%.

Proximal pole fractures

The proximal pole is subject to poor blood supply due to retrograde blood flow. This leaves the scaphoid at risk of non-union and avascular necrosis (Gelberman and Menon, 1980). Non-union rates have traditionally been reported to be higher than any other scaphoid type, ranging from 20-40% (Gellman et al., 1989). A meta-analysis by Eastley and colleagues (Eastley et al., 2013) demonstrated that 34% of acute proximal pole scaphoid fractures progressed to non-union. Furthermore, cast immobilisation may need to be continued for up to nine months before union is achieved, resulting in unacceptably high morbidity from non-operative treatment (Puopolo and Rettig, 2003). Consequently, the majority of authors recommend surgical fixation of proximal pole fractures (Rettig and Raskin, 1999). Displacement and chronicity are associated with poor outcomes of proximal pole fracture. Gholson and colleagues developed an algorithm for non-union risk based on a retrospective analysis of 351 scaphoid fractures in children and adolescents managed with cast immobilisation (Gholson et al., 2011). Acute proximal pole fractures united in 95% of cases if no displacement was present. With displacement, union significantly decreased to 28%. Fractures older than six weeks united in 50% of cases when non-displaced and only in 2% when displaced.

Even with surgical fixation, non-union of the proximal pole fracture remains a common concern. Brogan and colleagues performed a retrospective review spanning nearly two decades (Brogan et al., 2015). They identified union in only 43% of their 23 patients at 14 weeks following surgical fixation.

Predictors of poor outcome were fracture displacement and high energy injury mechanisms. Delay in surgery did not influence union rate. Other studies demonstrate more favourable outcomes. Rettig and Raskin (Rettig and Raskin, 1999) achieved 100% union after headless compression screw fixation. Union was confirmed by CT, 10 weeks after fixation. A meta-analysis mirrored Rettig's and Raskin's findings (Suh and Grewal, 2018). Out of 155 patients examined, cast immobilisation resulted in a union rate of 77% after 16 weeks. Operative treatment demonstrated a better union rate of 95% and a shorter time to union of 9 weeks.

Post-operative complications of proximal pole fracture fixation are similar to those encountered in waist fracture fixation. Aside from non-union, hardware failure and wound infections have been reported (Vinnars et al., 2008). The most pertinent complication of proximal fixation, however, is fracture and fragmentation of the proximal fragment at the screw head (Rancy et al., 2016). The proximal fragment is smaller in size than in waist fractures and can be sclerotic, especially when treated as part of a delayed presentation. Antegrade screw insertion can lead to stress risers and subsequent peri-implant fracturing.

The proximal pole of the scaphoid is frequently poorly defined by clinical studies (Eastley et al., 2013). Some authors refer to the proximal pole as the proximal third (Rettig and Raskin, 1999), whereas others as the proximal 25% (Gellman et al., 1989). Despite the lack of uniformity, one particular subtype of proximal pole fractures, the proximal fifth fracture (Figure 1.12), frequently represents a treatment challenge. These very proximal fractures are commonly displaced due to the strong ligamentous attachment to the lunate and the imparted extension moment. Furthermore, they are often too small to be amenable for screw fixation and are fixed with wires instead. These far-proximal fractures are known to have the worst clinical outcomes out of all proximal pole fractures. The reported non-union rate for those fractures is approaching nearly 100% (Tait et al., 2016).



Figure 1.12: Example of a proximal fifth pole fracture. Note the pure articular configuration of the fracture with a substantial articular gap between the dorsal non-articular ridge and the proximal fracture fragment

Articular surfaces of the scaphoid

More than 80% of the surface anatomy of the scaphoid is articular. There are four articular areas of the scaphoid (Figure 1.13).

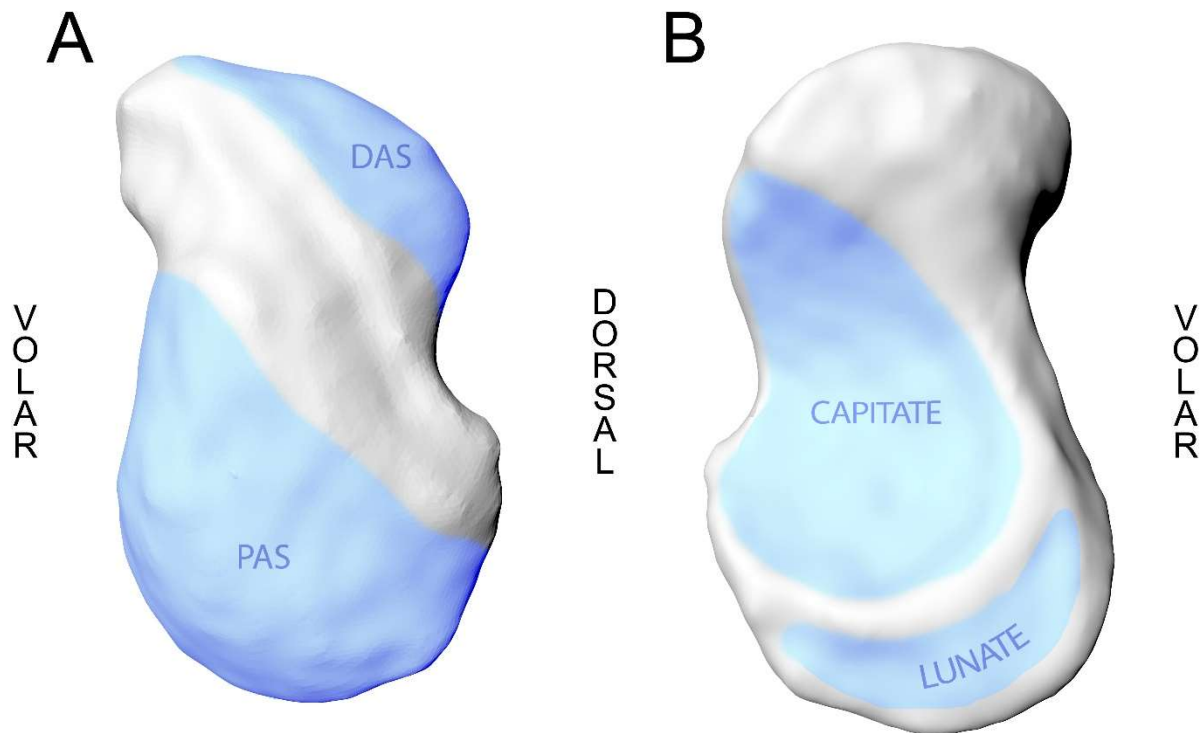


Figure 1.12: Articular surfaces of the scaphoid viewed from the radial (A) and the ulnar (B) aspects of the scaphoid; PAS: Proximal articular surface, DAS: distal articular surface

The proximal articular surface (PAS) is convex and fits into the convex distal radial articular surface.

The distal radius inclines at an average of 23° to the longitudinal axis of the radius (Solgaard, 1984).

The inclination of the distal radius is matched by the PAS of the scaphoid, resulting in an oblique position of the scaphoid within the carpus. Axial load against the distal radius is shared with the adjoining lunate and its corresponding radial facet. Kinematics of the scaphoid are highly complex and motion can be altered by underlying variations of ligamentous support (Patterson et al., 2003).

Most of the load through the radiocarpal joint, namely 60%, is transmitted through the proximal

articular surface. The remaining load is transferred via the radio-lunate joint. The contact area between the scaphoid and radius has been reported to represent only a minor proportion (20.6%) of the total available surface area, regardless of wrist position (Viegas et al., 1999). The contact area of the PAS with the radial styloid is 47% larger than the lunate with its radial fossa. As the wrist undergoes ulnar deviation, the scaphoid becomes more horizontally oriented and, consequently the contact area increases. The volar tilt of the distal radial articular surface and the ligamentous suspension of the scaphoid, result in shifting of the loading area as the wrist is mobilised from flexion to extension. In flexion, contact between PAS and radius are dorsal. This shifts to a central position in the neutral wrist and localises to the volar radius as the wrist extends (Patterson et al., 2003).

The second articular facet of the proximal pole lies on the ulnar aspect, the lunate articular surface (LAS). The LAS faces ulnar and slightly palmar. It is convex and crescent-shaped. Despite Fogg demonstrating little variation of the LAS among different scaphoid types (Fogg, 2004), the articulation does appear to show some variability. Berger and colleagues, for example, reported that the articulation has no convexity and is, instead, flat (Berger and Garcia-Elias, 1991). Moreover, as the articulation between the scaphoid and the capitate varies in extent and location in relation to the waist, the LAS can vary in size (Compson et al., 1994). The LAS is matched by a corresponding articulation on the lunate (Fogg, 2004). The SLIL defines the boundaries of the LAS. Proximally, a small ridge elevates above the LAS for attachment of the SLIL. This is mirrored on the dorsal side. The palmar scaphoid has a shallow fossa for attachment of the palmar SLIL. As part of the scapholunate articulation, the LAS plays an important role in wrist stability and kinematics and together with the SLIL acts an anchor point to the proximal carpal row (Slutsky and Slade, 2011). The shape of the lunate is known to restrict midcarpal range of motion to flexion and extension. A double-facet lunate, or a type 2 lunate, presents articulations to both the capitate and the hamate and consequently limits full circumduction at that joint. Despite being bridged by the strong SLIL, the

LAS facilitates a significant amount of motion. As the wrist is mobilised from full flexion to full extension, the scaphoid can rotate up to 80.3° (Berger and Garcia-Elias, 1991). In contrast, the lunate is less mobile at 58.6° of rotation. The difference in absolute rotation of the scaphoid and the lunate, results in the remainder of the rotation occurring at the scapholunate joint (24-34°).

The ulnar aspect of the scaphoid has a second distal facet, the capitate articular surface (CAS). The CAS is the most concave part of the scaphoid. It supports part of the capitate head. The capitate morphology is variable, resulting in differently shaped CAS. Yazaki and colleagues reported on capitate morphology (Yazaki et al., 2008). They identified three capitate types. The flat type was identified most frequently (65%). It was characterised by a transversely oriented articulation between the capitate and the lunate. The resultant CAS was oriented perpendicular to the capitolunate joint and was elongated in the proximal to distal direction. The spherical capitate type was present in 21% of cases. The spherical type had a continuous articulation with the scaphoid and the lunate. The CAS was continuous with the lunate articulation, forming a smooth arc. Finally, the V-shaped type was least common at 14%. The capitate had an identifiable ridge between the lunate and the CAS, acting like a keel. The appearance of the CAS in the V-shaped type capitate was somewhere in between the previous two types. It was elongated more than in the spherical type, continued in the proximal to distal directed, but was less elongated than in the flat type. The flat type was associated with a type one lunate; that is a lunate with single capitate articular facet. The V-shaped type was more commonly seen in the type two lunate. Type two lunates have a radial facet for the capitate and an ulnar facet for the hamate. Despite this morphological link between the scaphoid, capitate and the lunate, biomechanical studies have failed to demonstrate differences in load distribution across the CAS in type one and type two lunates (Nakamura et al., 1997).

Biomechanical studies investigating the CAS in isolation are lacking. Cadaveric and trauma studies have suggested, however, that the dorsal CAS undergoes progressively more dorsal loading as the wrist reaches full extension (Mazur et al., 1997, Stein and Siegel, 1969). Force transmission across

the midcarpal joint is shared between the scaphoid, lunate and triquetrum. The scaphoid transfers the majority of load (51%). The contribution of axial load transfer across the CAS is 28% (Patterson et al., 2003).

The distal pole of the scaphoid contributes to the multi-facet distal articular surface (DAS). The DAS is convex and articulates with the trapezium radial and trapezoid ulnar, forming the STTJ. Kauer reported that the DAS consists of two distinct facets, divided by a ridge, which lies at the junction between the trapezium and trapezoid (Kauer, 1986). He hypothesised that this ridge corresponded to the range of motion path and assisted in static alignment. The mechanism of arc of motion constraint of the ridge has been confirmed by other studies; however, it has been shown that this ridge can be absent in up to 19% of scaphoids and in a further 25% can only be identified by palpation (Moritomo et al., 2000b). Moritomo and colleagues examined the morphology of the DAS in 165 cadavers. The authors were able to classify the shape of the DAS into three types. Type A was most common (58%) and was wide on the dorsoulnar side. The radiopalmar aspect had a tapered appearance. The type B DAS (38%) was widest dorsoulnar and had a rounded radiopalmar surface. Finally, the type C articulation was least common (10%) and was narrow at the dorsoulnar aspect. The radiopalmar appearance was rounded, similar to the type B DAS (Moritomo et al., 2000b). The DAS is one of the four areas of contact during axial loading of the midcarpal joint. It distributes 23% of axial load (Patterson et al., 2003). The DAS experiences a substantial arc of motion as the wrist mobilises. Despite being separated by a distinct articulation, the trapezium and trapezoid rotate as a single unit around the DAS. This rotation is largest with ulnar deviation (44° - 51°) compared with wrist extension (17° - 18°) or flexion (15° - 21°) (Sonnenblum et al., 2004). The axis of rotation is oblique to the sagittal plane of the wrist, with the arc oriented in a ulno-flexion to radio-extension direction. This is irrespective of whether the wrist is undergoing flexion/extension or radial/ulnar deviation (Moritomo et al., 2000a).

Chapter Two – Dorsal Bare Area of the Scaphoid

Non-articulating areas of the scaphoid

The non-articular areas of the scaphoid represent 20% of the entire surface of the scaphoid and provide attachment to ligaments linking the proximal and distal rows of the carpus. Three distinct areas have been described: the tubercle, the volar waist as well the dorsal ridge and sulcus. The tubercle is part of the distal pole. As the distal pole is largely articular, any part of the distal pole that is non-articular is regarded as the tubercle. It is continuous with the dorsal ridge and clear boundaries are difficult to determine. Nonetheless, Compson and colleagues described the tubercle as pyramidal in shape with three sides. The proximal extent lies on the palmar side. Distally it is confined by the trapezium part of the DAS and the radial end of the dorsal ridge. The third side lies ulnar and may contain a groove for the flexor carpi radialis (Compson et al., 1994). The flexor retinaculum of the flexor carpi radialis as well as the transverse carpal ligament have been reported to attach to the tubercle (Fogg, 2004). The palmar scaphotrapeziotrapezoid ligament complex also receives attachment to the tubercle. It consists of two limbs, the radial band attaches to the trapezium and the ulnar band to the trapezoid (Moritomo et al., 2000b). Tubercle fractures are thought to be the result of avulsion of part of the scaphotrapeziotrapezoid ligament (Drewniany et al., 1985). Several small arterial branches enter the tubercle from its volar surface. These vessels commonly arise directly from the radial artery and supply the distal pole of the scaphoid. In some instances, the arteries arise from the superficial palmar branch of the radial artery (Freedman et al., 2001, Gelberman and Menon, 1980).

The narrowest part of the scaphoid is the waist. The waist defines the boundary between the proximal and the distal pole (Compson et al., 1994). Depending on wrist position, radiographs demonstrate the waist in different profiles, corresponding to separate areas of the scaphoid. A true

appreciation of the scaphoid waist can be obtained by examining the 3D morphology, such as during surgical exposure, morphological inspection in cadaveric studies or by utilising CT axial imaging with three-dimensional reconstruction. Consequently, studies examining scaphoid pathology show poor agreement on nomenclature relating to the scaphoid waist. For example, a meta-analysis examining the union rates after proximal pole fractures found that the majority of studies (82%), did not define the proximal pole. The remaining 18% of studies used anatomical landmarks for identification of the proximal pole; however, there was disagreement whether the proximal pole accounted for 25% or for a third of the scaphoid (Eastley et al., 2013). The volar waist finds attachment to the scaphocapitate, the RSC and the palmar scaphotriquetral ligaments. The scaphocapitate ligament is the largest of the volar scaphoid ligaments with a thickness of 2.2mm and a width of 6.7mm (Buijze et al., 2011a). Its attachment occupies the largest area of the waist. The scaphocapitate ligament has been shown to have a yield strength of 100N (Apergis and SpringerLink, 2013). Proximal to the scaphocapitate, lies the RSC, the most radial of the palmar radiocarpal ligaments. It has variable attachment to the scaphoid (Fogg, 2004) and some authors consider it a continuation of the palmar wrist capsule (Apergis and SpringerLink, 2013, Buijze et al., 2011a). Assessment of the RSC on magnetic resonance arthrogram has demonstrated only a small fibrous band attaching the RSC to the waist of the scaphoid (Theumann et al., 2003). Similar to the RSC, the palmar scaphotriquetral ligament is embedded within the volar wrist capsule. It lies deep to the RSC. Its fan-shaped fibres attaching to the scaphoid waist are thin and interdigitate with those of the RSC (Sennwald et al., 1994).

The dorsal non-articulating area extends obliquely across the scaphoid, separating the DAS and PAS. It has been described to have a proximal ridge and a distal sulcus (Compson et al., 1994). The most ulnar aspect of the ridge is defined as the scaphoid apex (Moritomo et al., 2008). The dorsal sulcus projects more radial and is confluent with the tubercle. The dorsal area is highly variable and its morphology has been linked to carpal kinematics (Ceri et al., 2004, Fogg, 2004). The dorsal wrist

capsule, the DIC and the radioscapoid ligament attach to the dorsal non-articular area of the scaphoid. The DIC is attached to the triquetrum and continues radially in two portions. The distal band fans out and attaches to the trapezium and trapezoid. The proximal, thicker portion attaches to the dorsal scaphoid. There is substantial variability in the DIC and its attachment to the scaphoid (Apergis and SpringerLink, 2013, Fogg, 2004, Viegas et al., 1999). The radioscapoid ligament originates from the radial styloid and attached to the dorsal ridge (Fogg, 2004). It is described as the radial collateral ligament by some authors (Fisk, 1970) and is likely a variant of the RSC. There are several foramina, providing arterial supply to 80% of the scaphoid in a retrograde manner. The branch to the dorsal ridge of the scaphoid is given off by the radial artery in the majority of scaphoids. The dorsal intercarpal artery, forming the dorsal intercarpal arterial arch, can give off the dorsal branch in 23% of cases (Gelberman and Menon, 1980). The peculiar intraosseous blood supply of the scaphoid is mirrored by its osseous morphology. Dorsal vascular foramina are more frequently encountered at the distal pole and can be absent at the proximal ridge in up to 18% of scaphoids (Ceri et al., 2004).

The non-articular areas of the scaphoid are crucial in wrist kinematics and scaphoid fracture healing. Recent studies have reported on utilising the volar non-articulating area for fracture fixation (Leixnering et al., 2011). Variation of the dorsal non-articulating area has been described (Ceri et al., 2004), but data on the exact size and shape of the dorsal non-articulating area has been lacking.

Study I - The dorsal non-articulating area of the scaphoid – A cadaveric study *

Arthur Turow^{1,2} MBBS; Joideep Phadnis^{2,3} MBChB; Gregory I. Bain^{1,2} MBBS, FRACS, PhD

¹Flinders University of South Australia, Adelaide, Australia

² Department of Orthopaedic Surgery, Flinders Medical Centre, Adelaide, Australia

³ Brighton & Sussex University Hospitals, Brighton, United Kingdom

Abstract

Background: Scaphoid osteology and ligamentous anatomy has been studied extensively in the past; however, to date, no previous research examined the dimensions of the dorsal non-articulating area.

Methods: This study assesses the area in relation to its dorsal blood supply and ligamentous attachments in ten embalmed cadaveric wrists.

Results: The mean size of the dorsal non-articulating area was 188 mm². The area was 17% larger for males (206mm²) than for females (170mm²) and this was statistically significant (p=0.04). The mean angle subtended between the radial shaft and the axis of the non-articulating area was 97° (84-117°). The mean angle between axis of the scaphoid and the dorsal non-articulating area was 12° (8-15°). The mean distance between Lister's tubercle and the dorsal branch of the radial artery was 33.9mm (27.9-40.4). It was significantly longer in males (36.2mm males; 30.9mm females; p=0.04). The mean distance from the radial styloid to the dorsal branch of the radial artery was 13.3mm (7.4-17.4mm) with no statistically significant gender differences (12.7mm males; 14.2mm females; p=0.68).

Conclusion: This study adds to existing literature of the scaphoid in that it more clearly describes the dorsal non-articulating area. The results of this study could be used to develop and expand on existing surgical techniques to treat scaphoid fractures and non-union as well as scapholunate instability.

Introduction

The scaphoid has a complex three-dimensional geometry and it has been extensively studied and imaged (Ceri et al., 2004, Fogg, 2004, Schmidt and Lanz, 2004, Gelberman and Menon, 1980, Slutsky and Slade, 2011). More than 80% of the surface area of the scaphoid is articular cartilage with small non-articular areas on the volar and dorsal aspects (Schmidt and Lanz, 2004). Much of the non-articular surface has ligament attachments, which are important for carpal stability and kinematics. This includes the dorsal scapho-lunate ligament, DIC and the STTL.

The scaphoid receives its major blood supply from the scaphoid branch of radial artery via the dorsal ridge. The proximal pole and 70-80% of the internal vascularity of the scaphoid are supplied by these dorsal vessels. The distal pole and the remaining 20-30% of the internal vascularity are supplied by volar vessels (Gelberman and Menon, 1980).

Much of the morphological research has focussed on the articular morphology (Fogg, 2004, Ceri et al., 2004, Compson et al., 1994) and to some extent on osteology of the dorsal non-articulating area (Compson et al., 1994). Ceri et al. (Ceri et al., 2004) examined 200 scaphoids and reported on four distinct variations of the dorsal scaphoid. Other authors (Compson et al., 1994) also identified variability of the dorsal scaphoid and proposed the scaphoid be considered as a body and a tubercle. Fogg (Fogg, 2004) identified differences in the dorsal scaphoid ridge and in the DIC and STTL attachments to the dorsal scaphoid. He hypothesised that this resulted distinct scaphoid kinematic patterns.

A sound understanding of scaphoid anatomy is required for the management of scaphoid fractures (Bain et al., 2015, Dodds et al., 2014, Leixnering et al., 2011), non-union and scapholunate instability. Recent advances in surgical techniques in plating of the scaphoid (Bain et al., 2015), but also scapholunate reconstruction, put particular emphasis on the dorsal non-articular area of the scaphoid. Despite extensive research of the scaphoid morphology, osteology and kinematics, the

exact shape and the surface area of the dorsal aspect have received little attention, and no published data on these parameters exists to date.

The aim of this study is to examine the dorsal non-articulating area of the scaphoid and identify surgically relevant information. This, improved anatomic understanding, could then be used for surgical fixation of scaphoid pathology.

Materials & Methods

Specimens

Ten embalmed adult cadaveric upper limbs were supplied by the Department for Anatomy & Histology at Flinders University, South Australia. Ethics approval was granted from the Southern Adelaide Clinical Human Research Ethics Committee (Approval SAC HREC EC00188). Wrists were secured in pronation and the same investigator (A.T.) performed all dissections. After excision of superficial structures, the joint capsule and ligaments were exposed. The radial artery was preserved on the dorsum of the hand and wrist, and the dorsal scaphoid branch of the radial artery identified. The origin of the dorsal scaphoid branch of the radial artery was identified. The distance from Lister's tubercle and the radial styloid was measured. A capsulotomy was then performed, exposing the dorsal scaphoid. The capsule, DIC and accompanying vessels were elevated, taking care not to disrupt the dorsal scapholunate ligament. Any observed congenital or osseous anomalies were excluded.

Photography

Photographs were taken for analysis (Canon EOS 650D; 18-55mm lens). The camera was positioned perpendicular and 45cm from the dorsal non-articulating area of the scaphoid. A measuring tape was placed alongside each specimen as a scale. The best two out of six images were taken to allow depiction of the entire dorsum of the scaphoid and to minimise any obliquity or parallax errors.

Two hypodermic needles were placed into the scapholunate joint, one proximal and one distal, to mark the most ulnar border of the scaphoid. Lister's tubercle, the tip of the radial styloid and the origin of the dorsal scaphoid branch of the radial artery were identified.

Assessment

For each wrist, photographs were imported into Photoshop CS5™ and analysed. To correct for specimen alignment discrepancies, the axis of the radial shaft and the radiocarpal joint were identified and aligned with a radius template. The dorsal non-articulating area was traced on each image. A grid overlay was placed over the non-articulating area. The size of each square on the grid

was matched to scale provided by the measuring tape and calibrated at 1mm^2 . The size of the non-articulating area was determined by counting the number of 1mm^2 squares within the traced area. Squares on the periphery were only included if more than half of the square was filled (Figure 2.1). Non-articulating area assessments were repeated by a second investigator and any discrepancies were re-assessed.

Three axes were used for spatial analysis: (A) the axis of the dorsal non-articulating area was determined by placing a length line along the longest axis of the dorsal non-articulating area, ensuring that equal amounts of non-articulating area were lying of each side of that line; (B) the longitudinal axis of the scaphoid was determined with the same method; and (C) the longitudinal axis of the radius. The orientation of the dorsal non-articulating area was measured in relation to the scaphoid axis (A & B) and to the radius (A & C).

The length of each dorsal non-articulating area was measured along the axis of the dorsal non-articulating area (A). At the ulnar and radial margins of the traced area, widths were measured. In order to account for variations at those margins, measurements were performed at 10% and 90% of the area lengths.

All grids were placed on a template to allow comparison and to gain an understanding of the mean surface shape (Figure 2.2).

Statistical analysis

Differences in the dorsal non-articulating area and the origin of the dorsal scaphoid branch of the radial artery in relation to Lister's tubercle and radial styloid were analysed using two-sample t-test.

A result was considered statistically significant when the p-value was less than 0.05.

Results

No wrists needed to be excluded for pre-existing pathology. Optimal exposure of the non-articulating area of all wrists was obtained with the wrists in a flexed and pronated position.

Surface area

Ten wrists were studied, five males and five females with a mean age of 80.6 years (range: 57-95; Table 2.1). The mean size of the dorsal non-articulating area was 188 mm²; this was 17% larger for males than for females (206 vs 170; p=0.04). The dorsal non-articulating areas varied widely amongst specimens. The mean length was 263mm. Males had significantly longer (p=0.0001) and radially broader non-articular areas (p=0.02). When taken together, the areas had similar widths at their ulnar and radial aspects (p=0.87). There was a proximal extension of the non-articulating area at the scaphoid waist, but this was variable (Figure 2.1).

Further measurements

The mean angle subtended between the radial shaft and the axis of the non-articulating area was 97° (84-117°). The mean angle between axis of the scaphoid and the dorsal non-articulating area was 12° (8-15°). The mean distance between Lister's tubercle and the dorsal branch of the radial artery was 33.9mm (27.9-40.4). It was significantly longer in males (36.2 vs 30.9; p=0.04). The mean distance from the radial styloid to the dorsal branch of the radial artery was 13.3mm (7.4-17.4) and this was similar amongst genders (p=0.68).

Discussion

In our study, the dorsal non-articulating area had a broad variation between wrists. Males had a 17% larger dorsal non-articulating area than females. Similar gender differences were identified in relation to the length and the radial width of the area measurements. The shape of the area resembled that of a lazy-S as it curved from the broad ulnar scapholunate ligament insertion to the distal scaphoid pole. The first arm of the S-shape appeared to follow the contour of the distal scaphoid. This could potentially serve as natural barrier to radioscapoid impingement in extremes of wrist extension. There were no distinct tapering points through its course distally between the radial and trapeziotrapezoidal articular surfaces. Optimal exposure of the non-articulating area of all wrists was obtained with the wrists in a flexed and pronated position.

The scaphoid receives its vascular supply predominately from dorsal branches of the radial artery (Gelberman and Menon, 1980). A scaphoid branch was identified in eight wrists and this was on average 13.3mm from the radial styloid and 34.0mm from Lister's tubercle. While distances of the dorsal scaphoid branch to the Lister's tubercle were longer for males; radial styloid measurements did not demonstrate any length relationship to arterial branches. Previous research on morphometry and microarchitecture by Bindra and colleagues (Slutsky and Slade, 2011) confirms the propensity for males to have larger wrists and, consequently, scaphoids.

The main weakness of this study is the relatively small sample size. This prevented detailed statistical analysis on our findings to be performed and exposes this study to sampling bias. Furthermore, the dorsal non-articulating area of the scaphoid is a complex surface with each scaphoid demonstrating variable ridges and sulci. We acknowledge potential bias, when examining this 3-dimensional surface with 2-dimensional image processing, as previously reported (Ceri et al., 2004, Fogg, 2004). Finally, we used embalmed cadaveric specimens for assessment. This predisposed results to measurement errors due to some underlying tissue distortion from the embalming process.

This study adds to the understanding of the dorsal non-articulating area. It expands on existing anatomical knowledge of the scaphoid. It could be utilised in a variety of applications. Cross-sectional imaging could utilise the size and orientation of the dorsal non-articulating area in reporting of acute injuries or degenerative conditions. Scaphoid kinematics are complex and knowledge about the dorsal non-articulating area could be used to broaden our knowledge of ligamentous attachment and, consequently, movement characteristics of the scaphoid. Finally, this information may be used to alter or develop surgical techniques suitable for the treatment of scaphoid fractures, scapholunate instability and non-union.

Future expansions of the dorsal scaphoid non-articulating area research could include larger studies that incorporate un-embalmed as well as dry-bone specimens. In addition, improvement in advanced imaging modalities, such as magnetic resonance imaging, could allow examination of the dorsal non-articulating area in-vivo as well as in large numbers, eliminating the need to use cadaveric specimens.

Conclusion

No previous research on the dorsal non-articulating area measurements has been published to date.

This study adds to existing research of the scaphoid in that it more clearly describes the dorsal non-articulating area, in particular its surface area, shape and orientation. The results of this study can be used to develop novel surgical techniques, namely scaphoid plating. Further to that, knowledge about the dorsal non-articulating area can aid in the development of scaphoid specific plates.

Acknowledgments

The authors thank the Department for Anatomy & Histology at Flinders University of South Australia for providing the cadavers, in particular Prof. Rainer Haberberger and Gregory Souter for their continued support of this study.

Figures

Table 2.1: Wrist dissection details of the ten examined wrists; distances expressed in mm; surface area in mm² and angles in degrees; RA – radial artery; inter-axis angle – angle subtended between axis dorsal non-articulating area and axis of scaphoid

Wrist Number	Gender	Age	Mean Area (mm ²)	Dorsal scaphoid branch RA		Orientation	Inter-axis angle
				Lister's tubercle	Radial styloid		
1	F	83	167.5	-	-	100	11
2	M	95	232.0	40.4	14.4	107	9
3	F	90	179.0	30.9	15.6	89	15
4	F	88	137.5	27.9	10.5	87	10
5	M	67	227.0	39.6	17.4	102	12
6	F	91	185.5	32.4	16.5	92	15
7	M	79	178.0	32.0	7.4	114	9
8	M	75	176.0	33.3	11.1	88	15
9	M	57	215.0	35.9	13.2	89	12
10	F	81	181.0	33.3	15.9	106	13

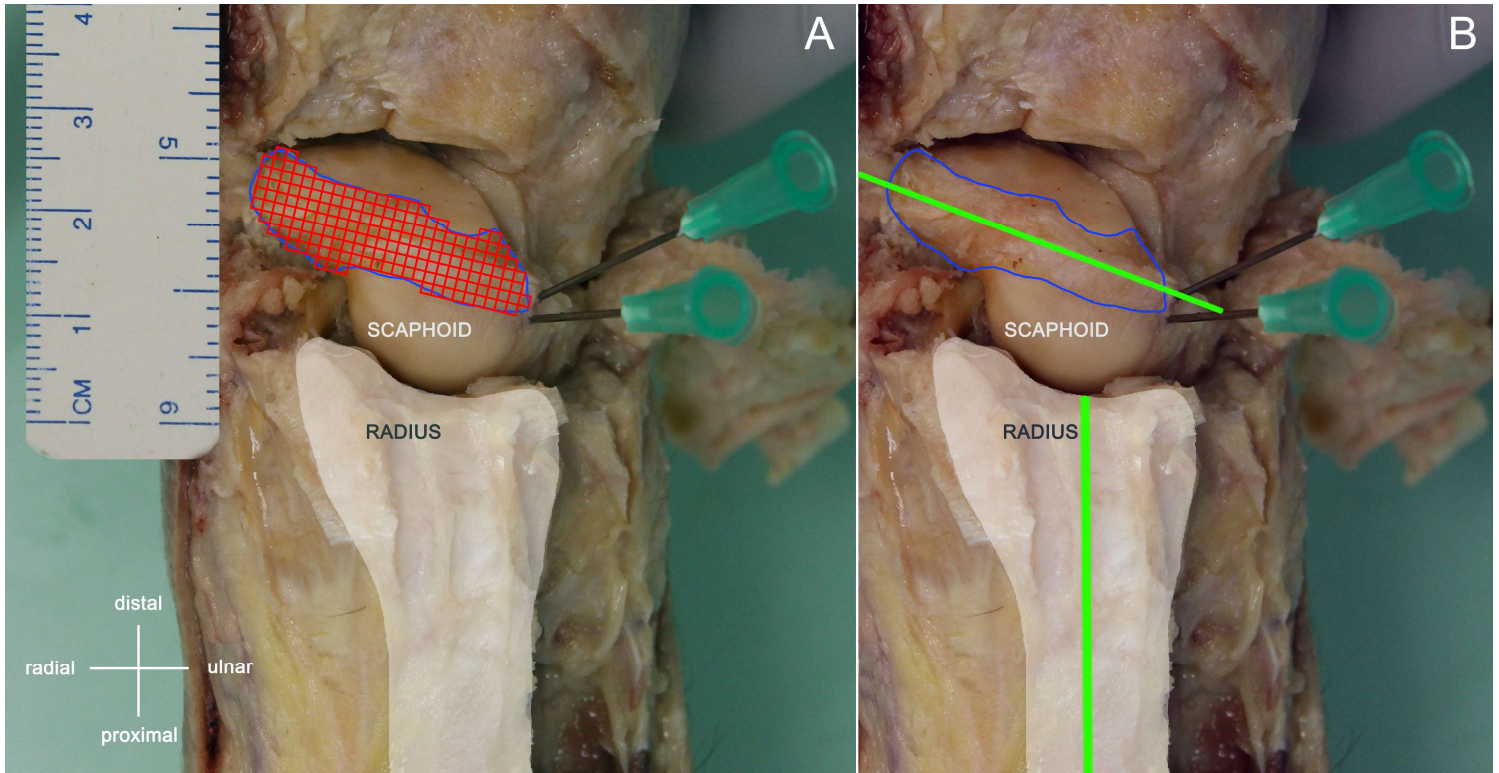


Figure 2.1: (A) Analysis of the non-articulating area of the scaphoid: trace of the dorsal non-articulating area (blue line) with a grid overlay (red). Two hypodermic needles are placed in the scapholunate joint for reference. (B) radial shaft axis and non-articulating area of the scaphoid axis

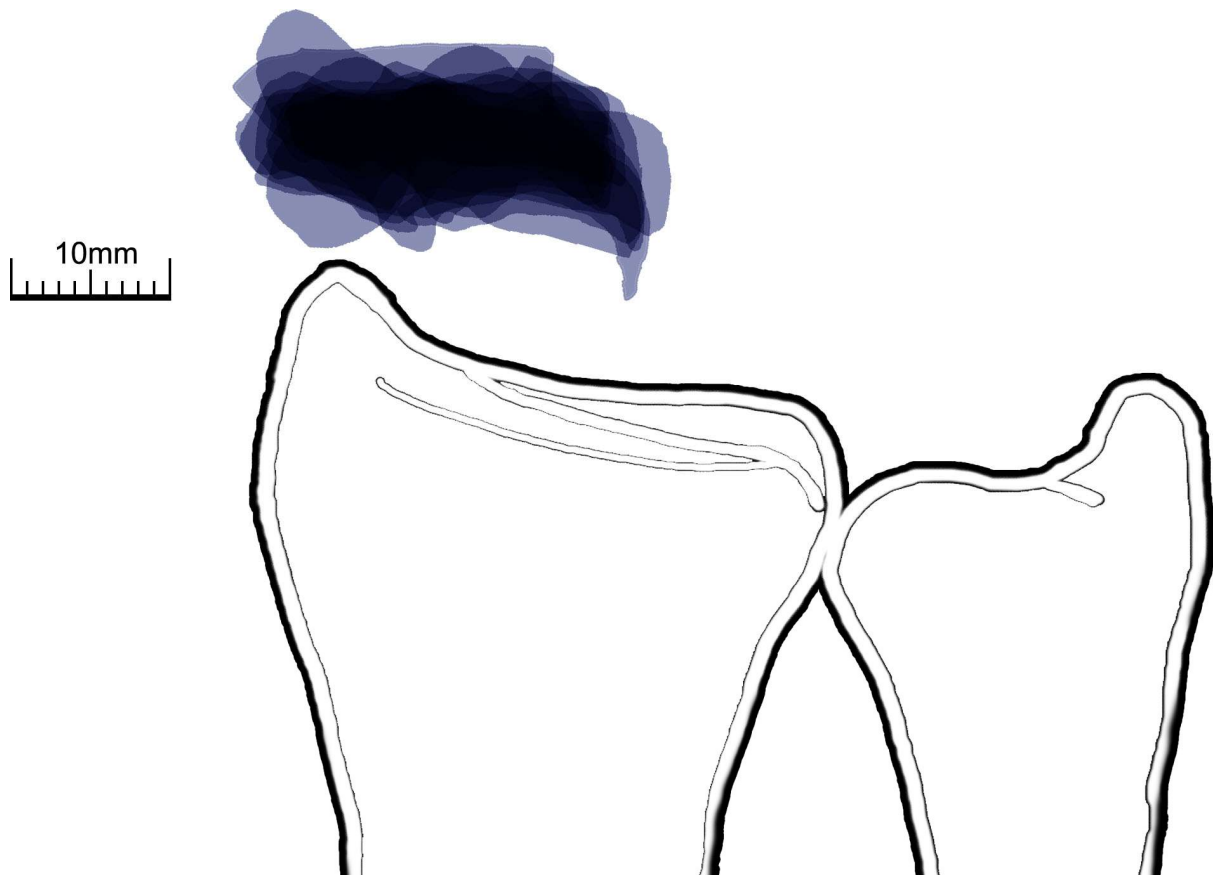


Figure 2.2: Combined shape of all ten dorsal surface areas; darker areas correspond with more overlap between samples

Chapter Three – Scaphoid fracture Plating

Plating in orthopaedics

Fracture management relies on stability, a concept that is crucial for successful outcomes. Stability can be imparted to fractures by external splints or casts, intramedullary devices, external fixators or by internal plates. The stability of a fracture determines its strain, which in turn controls how a fracture heals (Egol et al., 2004). Fracture strain is the ratio of change in the fracture gap divided by the absolute fracture gap. Strain of less than 2% results in absolute stability and a fracture heals without any callus. A relative stability construct is achieved, when fracture strain is 2-10%, facilitating callus formation. Strain of more than 10% exceeds tissue compliance and leads to fracture non-union (Egol et al., 2004). Plates for the management of fractures have been used since the end of the 19th century (Lane, 1895). Early plate designs suffered from corrosion or insufficient strength (Uthoff et al., 2006). Continued development over the following five decades introduced tapered ends, altered metal choice and introduced stronger plate designs. The recognition that fractures required interfragmentary compression to reduce fracture strain allowed Danis to develop a compression plate using a tightening side screw (Danis, 1949). This revolutionised all future plate development and is the basis for orthopaedic implants available today. Danis' compression side screw was eventually abandoned in favour of oval screw holes, allowing interfragmentary compression during screw tightening (Bagby and Janes, 1958). Despite the advances in plate design, some fracture types continued to be challenging to treat. These included intra-articular fractures, extra-articular fractures with a short metaphyseal segment and fractures involving osteoporotic or pathological bone (Haidukewych and Ricci, 2008). Furthermore, bone loss underneath compression plates was observed. It was proposed that stress shielding resulted in endosteal bone resorption (Uthoff et al., 2006). To remedy above shortcoming of conventional plates, the first locking plates were introduced in 1987 (Fernández et al., 2001). Locking plates introduced the concept of biological osteosynthesis, whereby interfragmentary compression is abandoned for the benefit of preserved

periosteal blood supply (Gerber et al., 1990). Locking plates prevent screw and bone motion by controlling axial screw orientation. This creates a single-beam construct, whereby the plate, screws and bone function as a unit. The single beam construct has been shown to be four times stronger than load-sharing constructs (Gautier et al., 2000). Fracture reduction and fragment interference determines whether a plate will be load-bearing or load-sharing (Egol et al., 2004). Compression plates or conventional plates acting as neutralisation plates following inter-fragmentary reduction and compression are load-sharing. They achieve rigid fixation by minimising gap formation and accomplish a low-strain construct. Locking plates are load-bearing, creating a different biological environment for bone union compared with compression plates.

The headless compression screw

The development of fixation techniques for upper limb fractures build on the success of plate design and the expanding knowledge about construct stability and the stress/strain relationship driving fracture healing. Fixation of upper limb fractures lagged behind those of the lower limb as surgeons put emphasis on restoration of gait and the capacity to work. In 1895, Lane wrote in his paper on fracture treatment “We may conclude that in fractures of the long bones of the upper extremity it is not of such vital importance to reconstitute the damaged skeleton in its original form as it in the case of the leg” (Lane, 1895). Nonetheless, the development of orthopaedic implants advanced and expanded to smaller bones, including the scaphoid. Implants used for scaphoid fixation initially included smooth Kirschner wires and the AO-type compression screw. Kirschner wires allowed for fracture stabilisation but lacked compression. Introducing more and thicker wires across a fracture allowed for more rigid constructs. Studies examining K-wire scaphoid fixation demonstrated promising results with a union rate of 97% (Stark et al., 1987). The AO-type cannulated compression screw was able to achieve significant inter-fragmentary compression, yielding short fracture healing times (Trumble et al., 1996). The AO-type screw had a traditional screw head, which had to be considered when choosing screw trajectory and in the long-term management of implant

prominence (Herbert and Fisher, 1984). The original scaphoid, headless compression screw, known as the Herbert screw, was introduced in 1984 and revolutionised the management of scaphoid fractures (Herbert and Fisher, 1984). The thread of the leading end of the Herbert screw has a wider pitch than the thread of the trailing end. As the screw is advanced past the fracture into the distal fragment, the wider pitch cuts into bone at a more rapid rate than the trailing narrow screw thread. With this variable pitch the screw allows for inter-fragmentary compression. The original screw was not cannulated and required a special guiding jig for screw insertion. The screw demonstrated excellent union rates compared with smooth wire fixation, but often resulted in peripheral screw placement when compared to AO-type cannulated compression screw (Trumble et al., 1996).

Building on the success of the original Herbert screw, second generation implants were cannulated and focussed on increasing compressive strength and versatility (Fowler and Ilyas, 2010). Screws could be inserted over an accurately placed guide wire without a guiding jig. The Acutrak screw (Acumed, Beaverton OR, USA) abandons the smooth shank of the Herbert screw and is fully threaded. It has a variable thread pitch along its entire length, resulting in gradual compression during its insertion. The Herbert-Whipple (Zimmer Inc.) screw increased the diameter of the shaft improving the cantilever support of the scaphoid during flexion and extension. The drawback of this change was a shallower thread, decreasing cancellous bone purchase, which could compromise rotational resistance (Slutsky and Slade, 2011). The AO headless compression screw (Synthes) and the TwinFix (Stryker, Kalamazoo MI, USA) maintained the narrow shank, improved on the thread design and introduced different size screws for increased versatility. Finally, the Integra Kompressor (Integra, Plainsboro NJ, USA) introduced modularity by decoupling fracture fixation and compression using a uniformly threaded screw with an interlocking wide-pitch attachment.

Prognostic factors of fixation

Scaphoid fracture morphology, time of presentation and patient injury circumstances such as presence of poly-trauma and functional requirements make prognosticating outcomes of scaphoid fractures challenging. Most literature reporting on scaphoid non-union consists of small case series, comparing one treatment method to another. Outcomes from these series usually demonstrate favourable union outcomes and prognostic factors are derived from a small sub-set of patients with poor outcomes.

One well established, patient specific factor adversely affecting scaphoid union is tobacco smoking. Little and colleagues examined 64 scaphoid fracture fixations with a median follow-up of 42 weeks (Little et al., 2006). Non-union rate was 26%. Out of the 17 patients with non-union, 76% were smokers. Another series reported even worse results for smokers (Dinah and Vickers, 2007). Smoking was associated with a 60% non-union rate compared with 28% in non-smokers.

Further to that, osteosynthesis and implant choice has been identified to influence treatment outcomes. Reported union rates vary greatly, though, depending on what fracture types are examined. In scaphoid non-union, for example, screw fixation has been shown to yield union rates of 94-100% (Tsuyuguchi et al., 1995, Trumble and Vo, 2001). In contrast, Kirschner wire fixation demonstrates greater variability with union rates of 56-100% (Barton, 1997, Chen et al., 1999). A meta-analysis has shown screw fixation to be superior to smooth wire fixation in established, unstable proximal pole non-union using non-vascularised bone grafting methods (Merrell et al., 2002). Screw fixation had a union rate of 88% compared with 47% in wire use. Another meta-analysis of 1602 patients confirmed that osteosynthesis resulted in better union than non-operative treatment (90% and 79%, respectively; (Pinder et al., 2015)); however, the study failed to demonstrate an inferiority of wire fixation. Union rates were 88% in scaphoid fractures fixed with a screw and 91% for those fixed using Kirschner wires. Interestingly, better union rates in the wire group were most pronounced when used together with vascularised bone graft (94% wires, 87%

screws). The advantage of using smooth wires disappeared when fractures were fixed with non-vascularised bone graft (88% wires, 90% screws). The authors hypothesised that screw insertion across a vascularised bone graft may disrupt its internal vascularity and, hence, worsen outcomes. Shifting the focus to screw fixation, several implant related factors can affect treatment success. A fully threaded screw can increase interfragmentary compression (Patel et al., 2019). Fully threaded constructs may not be best suited for all fracture types, though, as compression varies with distance between the trailing edge of the screw and the fracture location (Dodds et al., 2006, Patel et al., 2019). Biomechanical testing has demonstrated that a screw diameter of more than 1.5mm significantly increases construct stiffness and improves load-to-failure (Beutel et al., 2016). Construct stiffness can also be increased by placing the screw centrally into the middle third of both the proximal and distal poles on antero-posterior and lateral radiographs (McCallister et al., 2003). Compared with eccentrically placed screws, centrally placed screws have 43% greater stiffness, can resist more than twice the load at 2mm displacement (113%) and result in 39% greater load to failure. Centrally placed screws maximise use of the available cancellous bone in both fracture fragments and allow for longer screws to be contained within the scaphoid. A longer screw can distribute forces along the entire scaphoid and decrease forces acting on the scaphoid during wrist mobility (Slutsky and Slade, 2011). This was confirmed by a biomechanical assessment of the effect of screw length on interfragmentary displacement in a cadaveric model (Dodds et al., 2006). Longer screws were found to have greater rotational stability than shorter screws. Despite biomechanical advantages of certain screw designs and greater stiffness of long, centrally inserted screws, outcome data is lacking.

The duration of post-operative cast immobilisation has been investigated as a potential factor influencing outcome. Union rates have been shown to not improve when wrists are immobilised beyond six weeks (Inoue et al., 1997). Further to that, any cast immobilisation following surgery is unlikely to result in better union rates. Merrell and colleagues pooled results from studies using

post-operative immobilisation and those allowing free range of motion (Merrell et al., 2002). In 519 patients, union rates were the same (74%), irrespective of immobilisation.

Another consideration is previous scaphoid, adjacent ligamentous or carpal surgery. This could potentially distort anatomy, compromise vascular supply or alter ligamentous support. Furthermore, unsuccessful scaphoid surgery with either implant failure or non-union requiring re-operation has declared its bone stock and vascular bed as challenging to manage and could result in poor union outcomes. There are currently no studies available that address this issue directly. Pooled meta-data identified 61 patients with previous surgery (Merrell et al., 2002). There was a trend for better outcome with the use of vascular bone grafts; however, data was lacking and results were underpowered reflected by a large range of union rates (0-100%).

Graft source, choice and type are further variables that could predict union outcome. Earlier studies have traditionally used iliac bone for grafting. More recently, there is a tendency of choosing the distal radius as the donor site (Pinder et al., 2015). A prospective, randomised controlled trial compared 50 patients treated for scaphoid non-union using non-vascularised bone graft from the radius to an equivalent group of 50 patients in whom iliac crest bone graft was used (Garg et al., 2013). There was no difference in union rate (87%) or functional scores after a minimum of three years follow-up. The only difference was donor site morbidity for patients treated with iliac crest bone graft. The authors concluded that there was no advantage in using iliac bone graft to justify greater donor site morbidity in surgical fixation of scaphoid non-unions. In a systematic review, Sayegh and Strauch evaluated graft choice, i.e. cancellous-only or corticocancellous bone (Sayegh and Strauch, 2014). Union rates were higher for cancellous-only (95%) than for corticocancellous (92%) grafts, but this did not reach statistical significance. More importantly, cancellous-only grafts united significantly quicker (11 weeks) compared to corticocancellous grafts (16 weeks). In contrast, corticocancellous grafts improved native scaphoid anatomy to a greater extent than cancellous-only grafts, restoring scapholunate and radiolunate angles. Bone graft types used in scaphoid surgery

include non-vascularised and vascularised bone grafts. Vascularised bone grafts have gained popularity in recent years with the perceived benefit of providing live osteocytes to and stimulating angiogenesis at the fracture site. This is hypothesised to result in direct healing rather than creeping substitution (Klifton et al., 2018). There is currently no data available to quantify post-operative blood flow of vascularised bone grafts following surgery. Equally, no data is available for osteocyte quantity and amount of available growth factors in vascularised compared to non-vascularised bone grafts. Nonetheless, vascularised bone grafts have been shown to yield unions rates of 86-100% (Lim et al., 2013, Malizos et al., 2007). Vascular bone grafts are frequently considered in proximal pole fractures with avascular necrosis. In that setting, vascular bone grafts have been shown to result in good outcomes, but the superiority over non-vascularised bone grafts remains to be established. Merrell and colleagues found superior union rates (88%) compared to non-vascular bone graft types (47%) (Merrell et al., 2002). In contrast, Pinder and colleagues failed to demonstrate any significant union rate differences: 92% for vascular bone grafts and 88% for non-vascularised bone grafts (Pinder et al., 2015).

Study II – Book chapter, scaphoid plating

Arthur Turow¹ MBBS; Gregory I. Bain^{1,2} MBBS, FRACS, PhD

¹ Flinders University, Adelaide, South Australia, Australia

² Department of Orthopaedic Surgery, Flinders Medical Centre, Adelaide, Australia

Case Example

PANEL 1: Case Example

A 30-year-old male fell onto his outstretched hand after tripping over and presented to his local practitioner and was treated for a soft-tissue injury. His pain settled with conservative treatment. A recurrent fall seven months later exacerbated his pain and prompted a presentation to the orthopaedic outpatient department where X-rays of his wrist were taken (Figure 1). X-rays showed a non-united scaphoid waist fracture. Given the delayed presentation, the patient underwent open reduction and internal fixation with a dorsal plate (Figure 2).

Importance of the Problem

Overview

A single headless compression screw has been the mainstay of scaphoid fracture treatment, since it became available in the 1980s (Herbert and Fisher, 1984). A single screw provides only limited stability, and is especially poor with rotation. There are alternatives to screw fixation, which include using multiple screws, staples, plates and potentially external fixateurs (Bain et al., 2015).

Two screws (Garcia et al., 2014) can be used to reduced interfragmentary rotation. Increased fixation can also be achieved with an anti-rotation wire (Adolfsson et al., 2001, Soubeyrand et al., 2010, Bond et al., 2001) instead. Accomplishing rotational stability and accurate screw positioning with two screws across a usually narrow scaphoid waist can be very challenging, though.

The scaphoid staple is an alternative to screw fixation. Since its introduction in 1980, only a few authors have reported on clinical outcomes, with described union rates of 92% for non-unions (Dunn et al., 2016).

Non-union remains a significant complication of scaphoid fractures. Scaphoid waist fractures have a reported non-union rate of 5-15% (Prosser and Isbister, 2003, Langhoff and Andersen, 1988), irrespective of treatment. Internal fixation was previously reserved for unstable fracture patterns, but can also include high-demand patients with simple, transverse fractures.

Plating rationale

The concept of plating of the scaphoid has been first introduced in the middle of last century with compression plates by Ender and Vespasiani (Saffar and SpringerLink (Online service), 1990) (Figure 3.3). These beaked plates were designed to allow for compression across the scaphoid and prevented escape of the bone graft from the fracture site, something that other fixation methods at that time were not able to provide. These hooked plates saw some use in the late 80s and early 90s, but their use rapidly declined with the clinical introduction of the Herbert screw in 1984 (Herbert and Fisher, 1984).

Scaphoid plating has been re-introduced recently with both volar (Figure 3.4) and dorsal techniques. The need for plating has arisen from concerns regarding mechanical stability of a single screw across scaphoid fractures with an unstable fracture pattern (Bain et al., 2015, Ghoneim, 2011, Leixnering et al., 2011) and the assumption that a plate would provide a more stable construct than a compression screw. Plate fixation of the scaphoid has been pursued with the theoretical benefit of a multiple divergent screw fixation that lends stability in multiple vectors. The potential advantages of stable plate fixation are likely to be greater in unstable fractures, where greater stability is required to obtain stability, such as fractures that are oblique, with comminution or non-unions with bone loss.

Main Question

What are the indications and techniques for plate fixation of acute scaphoid fractures and scaphoid non-unions?

Current Opinion

Scaphoid plating is evolving and should be reserved for cases where stability is paramount. This could include high-energy injuries with associated scaphoid fracture, non-union where previous treatment has failed or in high demand patients that require early return to activities.

Finding the Evidence

Pubmed (Medline): (scaphoid bone[MeSH Terms] OR scaphoid fracture) AND

plate*[Title/Abstract]) OR plating* [Title/Abstract]) AND (Humans[Mesh] AND (English[lang] OR

French[lang] OR German[lang]) NOT fusion[Title/Abstract]) AND (Humans[Mesh] AND (English[lang]

OR French[lang] OR German[lang])))) NOT four-corner[Title/Abstract]) NOT

humerus[Title/Abstract]) NOT radius[Title/Abstract]) NOT ulna*[Title/Abstract]) AND

(Humans[Mesh] AND (English[lang] OR French[lang] OR German[lang])))) NOT

arthrodesis[Title/Abstract]) NOT knee[Title/Abstract] Sort by: Relevance Filters: Humans; English;

French; German

Quality of Evidence

Level I:

Systematic Reviews/Meta-analyses: 0

Randomized trials: 0

Level II:

Randomized trials with methodological limitations: 0

Level III:

Retrospective comparative studies: 0

Level IV:

Case series: 9

Findings

Biomechanics

When placed perpendicular to the fracture line, the Herbert screw is able to achieve inter-fragmentary compression. It is capable of resisting bending forces, but is unable to withstand cyclical multi-axis loading or rotation (Wheeler and McLoughlin, 1998, Luria et al., 2010, Rankin et al., 1991, Shaw, 1987, Toby et al., 1997). Previous biomechanical work has focused predominantly on pull-apart and compression strengths as well as bending resistance (Hart et al., 2016, Newport et al., 1996, Toby et al., 1997). Torsional resistance has been evaluated amongst different screw designs in scaphoid models (Newport et al., 1996, Wheeler and McLoughlin, 1998), but the lack of in-vivo studies leaves a large gap between such models and the complex kinematics (Fogg, 2004) and torsional forces a scaphoid experiences.

A recent in-vitro study (Jurkowitsch et al., 2016) compared rotational stability of a single compression screw to two screws and to an angular stable plate. The authors found superior rotational stability for two screws and for the locking plate construct ($P < 0.05$). There were no statistically significant differences between two screws and the plate.

More than 80% of the surface area of the scaphoid is articular surface with small non-articular areas on the volar and dorsal aspects (Schmidt and Lanz, 2004). Consequently, plate placement depends on those bare areas. Dorsal placement of the plate has been hypothesized to be biomechanically superior to a volar position, as a dorsal plate occupies the tension side of the scaphoid. Thereby, a dorsal plate is thought to act as a tension band plate during wrist mobilization, achieving dynamic compression (Bain et al., 2015, Müller et al., 1992). In fact, some research indicates that kinematics of various scaphoids differ substantially depending on their dorsal ligamentous arrangement. Fogg (Fogg, 2004) examined 100 scaphoids and divided them based on their dorsal morphology. In type I scaphoids, the DIC does not attach to the dorsal bare area and the STTL complex has a V-shaped configuration. In contrast, type II scaphoids receive a DIC slip and the STT ligament has an inverted-V attachment (Figure

3.5). Fogg (Fogg, 2004) hypothesized type I scaphoids to be rotating and type II scaphoids to undergo flexion and extension through wrist palmar- and dorsiflexion.

Indications

Scaphoid plating has been used in a variety of circumstances. Broadly, plating is indicated where greater stability is sought. This may be the case in unstable fracture patterns, following high-energy injury with associated carpal dislocations or in cases of non-union. High-demand patients might also be a potential cohort where early return to activity is critical.

In the acute setting, a plate can be used for unstable fracture patterns (Herbert type B). An angle stable plate can buttress bone graft, prevent fracture collapse and provide rotational stability. Consequently, a scaphoid plate can be used to bridge comminution and to neutralize shear forces across an oblique scaphoid fracture. The ideal indication for a dorsal plate is a comminuted scaphoid fracture.

Scaphoid non-union is challenging to treat and requires a rigid fixation for a longer period of time than acute fractures. Biomechanically, plating provides greater stability than screw fixation (Jurkowitsch et al., 2016). The plate can also be used as a buttress for bone graft to avoid graft escape. Graft options include cancellous, corticocancellous or vascularized (Dodds et al., 2014) bone grafts. Cancellous autologous bone graft can be obtained from the ipsilateral distal radius (Bain et al., 2015) or iliac crest (Leixnering et al., 2011). Corticocancellous grafts have been advocated by some authors (Merrell et al., 2002, Ghoneim, 2011) to restore volar cortical loss.

Contraindications

Plating of the scaphoid invites a new set of challenges. The scaphoid is a small bone, with a large articular surface. Therefore, there are some situations where plating will be difficult or contraindicated.

Scaphoid fractures of the proximal or distal pole usually prevent adequate fragmentary screw purchase and, consequently, are not suitable to plate fixation. Volar cortical loss and severe humpback deformity require osseous reconstruction and significant implant support. A volar plate with bone graft is one option.

A dorsal plate may still be considered with concurrent cancellous bone grafting. Some studies have shown union rates of up to 96% in non-united scaphoid fractures with associated humpback deformity that were treated with cancellous bone grafting (Finsen et al., 2006, Kirkham and Millar, 2012, Park et al., 2013, Slade et al., 2003).

Scaphoid fractures with advanced carpal arthritis are better managed with a salvage procedure. Patients with mild radiocarpal arthritis can still be considered for internal fixation, when a radial styloidectomy is performed in conjunction with the scaphoid fixation.

Surgical Technique

Volar

An incision overlying the flexor carpi radialis (FCR) is commenced 2cm proximal to the scaphoid tubercle and carried towards the base of the thumb. The superficial palmar branch of the radial artery may be ligated if required. The FCR sheath is incised and the tendon retracted ulnar to expose the wrist capsule. Pronator quadratus is exposed through a longitudinal incision of the floor of the FCR sheath. Radial artery and volar carpal branch to the distal pronator quadratus are identified and protected. Incision of the radioscapocapitate ligament exposes the volar scaphoid.

The fracture is prepared by debriding the fibrous tissue and sclerotic bone. Preservation of the dorsal fibrous non-union tissue can aid in preventing extrusion of bone graft from the dorsal scaphoid. K-wires in each fracture fragment are used as joysticks to facilitate manipulation and reduction. In some instances, a scaphocapitate K-wire can aid in provisional fixation during bone grafting. The fracture site and bone defects are packed with cancellous bone graft from the iliac crest or the distal radius.

A titanium, pre-contoured volar scaphoid 1.5mm mini-plate (Medartis AG, Austrasse, Basel, Switzerland) is placed on the volar bare area. In some instances, it might be required to re-contour the plate or to remove some of the screw holes to avoid impingement. The plate acts a bridging plate and buttresses any bone graft. At least three screws are then placed into each fracture fragment. Screws are aimed away from the fracture plane and positioned in a divergent configuration to increase angular fixation. Fluoroscopy is then used to ensure that the plate and screws do not impinge in any wrist position and that they do not protrude dorsally.

Dorsal

A longitudinal incision is made halfway between the radial and ulnar styloid. The extensor retinaculum is released over the 2nd compartment, and the extensor tendons retracted. The joint capsule is incised longitudinally and the dorsal bare area of the scaphoid exposed. For plate fixation the soft tissue attachment over the dorsal ridge needs to be released, unfortunately this includes the dorsal vessels. For this reason, the main indication is complex wrist injuries with scaphoid comminution. The scapholunate ligament should not be disturbed.

The fracture site is debrided and reduced, with either K-wire joysticks or point to point reduction clamps. Cancellous bone from the distal radius can be harvested and impacted into the fracture site. The humpback deformity can represent a challenge for dorsal plating. In acute fractures volar cortical loss is usually minimal and the deformity can be corrected with anatomical fracture reduction and cancellous bone grafting. Non-union with volar cortical loss requires bone grafting and stable internal fixation.

A titanium, trapezoidal eight to ten-hole locking 1.5mm mini-plate (Medartis AG, Austrasse, Basel, Switzerland) is contoured to conform to the dorsal shape of the scaphoid. Similar to volar plating, one of the proximal and/or distal screw holes may need to be cut from the plate to prevent plate impingement. For fractures that extend into the distal waist, plate position over the increasing convex

scaphoid requires careful evaluation. Plate in-setting may be required to avoid impingement into the scaphotrapeziotrapezoid joint and to ensure adequate fracture spanning.

Principles of screw placement are similar to volar plating. Following fracture compression, at least three screws are placed into each fracture fragment. Screws are aimed away from the fracture site to maximize angular fixation and rigidity. Once fixation is complete, the wrist is closely examined clinically and under fluoroscopy to ensure that the plate and screws do not impinge in any wrist position. This includes identifying if (a) the plate impinges on the dorsal radius in wrist extension, (b) the screws violate the articulations including the STTJ and mid-carpal joints and (c) if screws protrude excessively through the volar cortex.

Clinical Data

The majority of the available outcome data on scaphoid plating is on the Ender plate (Braun et al., 1993, Stankovic and Burchhardt, 1993, Geisl and Puhlinger, 1986, Ender, 1977, Mirrer et al., 2016, Bohler and Ender, 1986). Union rates are reported between 89% (Geisl and Puhlinger, 1986) and 99% (Bohler and Ender, 1986). The Ender plate has been used for both the volar and dorsal approach. Huene and Huene (Huene and Huene, 1991), for example, report on 20 scaphoid non-union cases treated with plating. Eleven patients underwent dorsal and nine volar plating. Only one patient had persistent non-union patient with subsequent hardware removal. Despite promising results and wide use in Europe the late 80s and early 90s, the Ender plate has all but vanished from the scaphoid literature. The decline of the Ender plate is likely a consequence of the clinical introduction and rapid uptake of the Herbert screw in 1984.

Outcomes for volar, locking plating has been equally promising (Dodds et al., 2014, Ghoneim, 2011, Leixnering et al., 2011). Cumulative union for volar plating is 93% (Ghoneim, 2011, Leixnering et al., 2011) at approximately 4 months. For dorsal plating, recent preliminary published data on 10 scaphoid fractures shows 90% union rate (Bain et al., 2015).

Recommendations

In patients with (1) high-energy injuries with associated scaphoid fractures, (2) non-union where previous treatment has failed or (3) in high demand patients:

- An angle-stable plate can provide a more rotationally stable construct than a single compression screw can [Overall Quality – Moderate]
- Plate fixation can yield high union rates in select patients [Overall Quality – Low]
- Scaphoid plate positioning depends on the fracture configuration and surgeon preference [Overall Quality – Low]

Further research needs to be done to assess biomechanical properties of scaphoid plates and their expected union rates.

Conclusion

Scaphoid plating has been used since the 1970s and its use has recently seen some renewed interest. Plating of the scaphoid remains an area of ongoing research and is currently reserved for challenging high-energy injuries, non-unions with previously failed non-operative or surgical management and for patients that have high wrist demands. Adequate screw fixation into both fracture fragments remains an important part of fixation. Volar or dorsal plate placement depends on fracture configuration and stability. Operative and radiological assessment for impingement is imperative for scaphoid plating. Further work needs to be done to compare scaphoid plate to screw constructs and to assess radiological as well as clinical outcomes of scaphoid plating.

Author's Preferred Technique

PANEL 2: Author's Preferred Techniaue

The case example (Figures 1 & 2) shows a relatively young patient with a non-united scaphoid fracture due to a delayed presentation. The preferred method is:

- Bony evaluation with a pre-operative CT to assess fracture configuration and bone stock
- A dorsal plate was chosen in this case due to the delayed presentation and the obliquity of the fracture rendering it unsuitable for single screw fixation
- Post-operatively the patient was followed up with serial X-rays and a CT to assess for union

Pearls and Pitfalls

PANEL 3: Pearls and Pitfalls

Pearls:

- Pre-operative CT and 3-D reconstruction to plan for most suitable fixation
- Use K-wires as joysticks or a laminar spreader to allow debridement of scar tissue and impaction of bone graft into fracture site
- Image the proposed plate position early to allow for trimming of prominent screw holes and for consideration of plate in-setting to avoid impingement

Pitfalls:

- If the plate is too prominent or screws in the neighboring joints, impingement and secondary joint degeneration will require revision surgery or early removal of the plate
- If the fracture is too distal or too proximal preventing at least three screws to be placed into each fragment, consider alternative fixation options

Figures

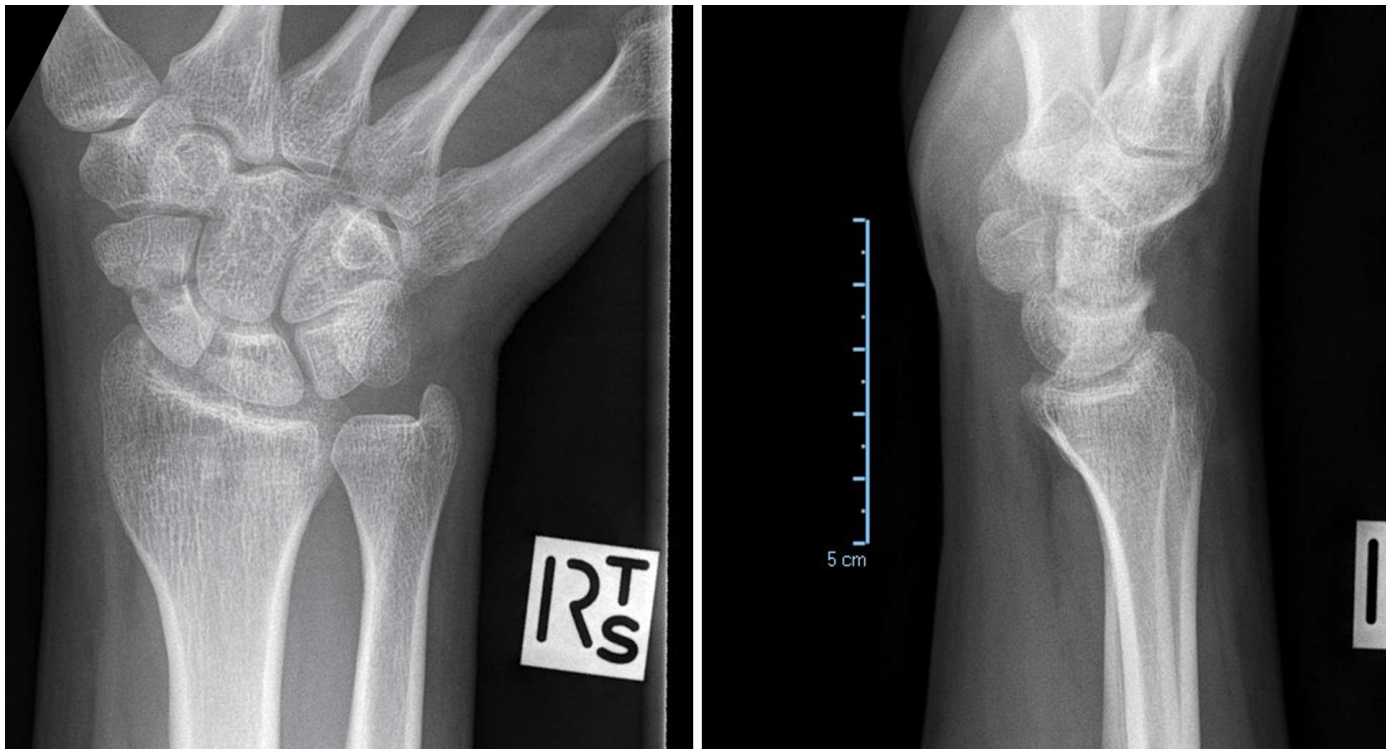


Figure 3.1: Plain radiographs of 30yo male with right wrist pain after a repeat fall onto his outstretched hand.



Figure 3.2: Dorsal scaphoid plating - Post-operative x-rays of patient from Figure 3.1

[This image has been removed due to copyright restriction. Available online from: [https://doi.org/10.1016/s0363-5023\(10\)80160-1](https://doi.org/10.1016/s0363-5023(10)80160-1)]

Figure 3.3 – (A) Hooked Ender Compression plate with a drill guide for the hook; (B) Ender plate in a non-united scaphoid (Huene and Huene, 1991)

[This image has been removed due to copyright restriction. Available online from <https://doi.org/10.1097/ta.0b013e3181f65721>]

Figure 3.4 – Volar scaphoid plating of a previously non-united scaphoid waist fracture (from Leixnering et al. 2011) (Leixnering et al., 2011)

[This image has been removed due to copyright restriction. Available online from: <https://digital.library.adelaide.edu.au/dspace/handle/2440/37935>]

Figure 3.5 – (A) Rotating type scaphoid: Arrangements of DIC and radiocapitate (RC) ligaments predispose the scaphoid to rotation; (B) Flexing/ extending type scaphoid: Direct attachment of DIC and a radioscapnocapitate ligament limit rotation; (S) Scaphoid, (R) Radius. (Fogg, 2004)

Chapter Four – Dorsal scaphoid plating

Study III – Technique description: Dorsal plating of unstable scaphoid fractures and non-unions ~

Gregory I. Bain^{1,2} MBBS, FRACS, PhD; Arthur Turow² MBBS; Joideep Phadnis² MBChB,

¹ Flinders University, Adelaide, South Australia, Australia

² Department of Orthopaedic Surgery, Flinders Medical Centre, Adelaide, Australia

Abstract

Achieving stable fixation of displaced acute and chronic non-united scaphoid fractures continues to be a challenge for the treating surgeon. The threaded compression screw has been the mainstay of treatment of these fractures for the last three decades; however, persistent non-union following screw fixation has prompted development of new techniques. Recent results of volar buttress plating have been promising. We describe a novel technique of dorsal scaphoid plating. In contrast to volar plating, the dorsal plate is biomechanically more favourable as it utilises the tension side of the scaphoid bone for dynamic compression. Dorsal scaphoid plating provides a more stable construct than the traditional Herbert screw and mitigates the need for vascular or corticocancellous bone grafting in most cases.

Introduction

The management of scaphoid fractures remains controversial. Scaphoid waist fractures can be managed non-operatively with a reported non-union rate of 5-15% (Prosser and Isbister, 2003, Langhoff and Andersen, 1988). With internal fixation the reported incidence of non-union is 2-28% (Merrell et al., 2002, Kilic et al., 2011, Ramamurthy et al., 2007, Symes and Stothard, 2011).

Surgical options

The headless compression screw has been the mainstay of treatment, since the Herbert screw became popular (Herbert and Fisher, 1984, Leixnering et al., 2011). There have been many variations of the compression screw since; however, the underlying principles have remained the same. Merrell and colleagues (Merrell et al., 2002) have reported scaphoid non-union rates after screw fixation to be 6%; however, non-union for the Herbert screw appears to be much more frequent (Oduwole et al., 2012). In addition, the increased propensity at which scaphoid revision surgery has been recently reported (Moon et al., 2013), may indicate that non-union rates of screw fixation are more common than originally thought.

Two screws (Garcia et al., 2014) or an anti-rotation wire (Adolfsson et al., 2001, Soubeyrand et al., 2010, Bond et al., 2001) can be used to minimise interfragmentary rotation and therefore increase fixation stability. However, there is limited literature that assesses outcomes of two headless compression screws. Furthermore, given the complex shape of the scaphoid and the importance of accurate screw placement (McCallister et al., 2003, Luria et al., 2012a, Guo et al., 2014) for adequate fracture compression, insertion of two screws can be very challenging.

Staple fixation is an alternative method to achieve fracture fixation. An early study has shown staples to yield satisfactory union rates; however, there were concerns about long-term degenerative changes secondary to hardware impingement (Korkala et al., 1992). Clinical data or biomechanical analyses on fixation strength have been lacking.

Plate fixation has been first introduced by Ender in 1977 (Ender, 1977) for treatment of scaphoid non-union and volar bone loss. The Ender compression plate is a beaked plate. It is hooked on the proximal scaphoid fragment and affixed to the distal portion of the scaphoid with a screw. Huene and Huene (Huene and Huene, 1991) reported on their experience with the Ender plate. The authors treated twenty patients, nine of which had previous unsuccessful surgical fixation, and report of only one persistent non-union. More recently, a volar, pre-contoured plate (Medartis AG, Austrasse, Basel, Switzerland), utilising the volar non-articulating area has been introduced (Dodds et al., 2014, Leixnering et al., 2011, Ghoneim, 2011). Leixnering and colleagues (Leixnering et al., 2011) reported on eleven patients that had symptomatic scaphoid non-union. Patients underwent concurrent cancellous bone grafting and, in all cases, the scaphoid united after an average of four month.

The described technique originated from the early good outcomes of plate fixation of the scaphoid and the assumption that a plate would provide a more stable construct than a compression screw. The potential advantages of stable plate fixation are likely to be greater in unstable fractures such as those that are oblique, comminuted or non-unions with bone loss. A recent computerised 3-dimensional analysis, examined 124 computed tomography scans of acute scaphoid fractures (Luria et al., 2015). The authors found that most waist fractures were horizontal oblique, rather than transverse, illustrating that oblique scaphoid waist fracture are more frequent than originally reported (Green and Wolfe, 2011, Slutsky and Slade, 2011) and that screw fixation might not be the optimal fixation method for waist fractures.

Biomechanics

Headless compression screws are capable of producing and maintaining inter-fragmentary compression when placed perpendicular to the fracture line (Luria et al., 2010) and resist bending forces (Carter et al., 1991, Toby et al., 1997, Rankin et al., 1991, Shaw, 1987). Torsional resistance has been evaluated amongst different screw designs in scaphoid models (Newport et al., 1996, Wheeler and McLoughlin, 1998); however, given the complex kinematics and torsional forces that

the scaphoid experiences (Fogg, 2004), there are no in vivo studies to assess rotational stability of screw fixation. Our hypothesis is that plating resists rotational displacement to a far greater degree when compared to single screw fixation.

The dorsal position of the plate, compared to volar plating, is biomechanically preferable, as it is on the tension side of the scaphoid. A dorsal plate can act as a tension band plate during wrist mobilisation, achieving dynamic compression (Müller et al., 1992). This, however, requires an intact, non-comminuted volar cortex. In cases with volar comminution, the plate acts as a neutralisation plate. Despite being biomechanically more preferable, anatomical consideration cannot be overlooked. Placement of a dorsal plate invariably affects the major blood supply of the scaphoid. Care should be taken not to dissect the entire non-articulating area when placing a plate. In addition, compression through the plate should be avoided as this requires interference between the dorsal bone and the undersurface of the plate. This could likely result in obliteration of arterial inflow.

Anatomy

More than 80% of the surface area of the scaphoid is articular surface with small non-articular areas on the volar and dorsal aspects (Schmidt and Lanz, 2004). Much of the non-articular surfaces are covered in ligamentous attachments, which are important for carpal stability and kinematics. This includes the dorsal scapho-lunate ligament and the volar radioscaphocapitate ligament.

The scaphoid receives the majority of its blood supply from the radial artery. All of the proximal pole and about 70-80% of the internal vascularity of the scaphoid are supplied by dorsal vessels. Dorsal vessels enter the scaphoid via the dorsal ridge and these are vulnerable during a dorsal surgical approach. The distal pole and the remaining 20-30% of the internal vascularity are supplied by volar vessels (Gelberman and Menon, 1980).

Indications

Stable scaphoid fractures can be managed with a cast or a single screw. Fractures that would be stable with a single screw should be managed with the screw.

The indications for plating scaphoid fractures are evolving, and include those fractures in which greater stability is an advantage. Examples include fractures where (a) stability is difficult to obtain, (b) where greater stability will avoid the need to immobilize the wrist, (c) patients with higher demands who need stable fixation to return to sport or work.

Acute comminuted or oblique fractures

Dorsal plating is suitable for unstable fractures, such as Herbert type B (Green and Wolfe, 2011). A dorsal plate can prevent collapse and shortening as well as resist torsion, making it well suited for comminuted (Herbert B5) and displaced fractures (Herbert B2 & B4). Oblique fractures (B1) can be demanding to fix by any method. Positioning the plate to form an "axilla" with the fracture can be used to neutralise shear forces across the fracture and prevent shortening or collapse (Figure 4.1).

Complex wrist injuries such as trans-scaphoid perilunate fracture dislocations are likely to have better stability with plate fixation. This would also allow earlier mobilisation.

Non-union

Non-union is the most common indication for dorsal plate fixation. Non-united fractures usually require greater stability for a longer period of time than acute injuries. Plating is superior to screw fixation in this regard. For non-unions, we use cancellous autologous bone graft from the ipsilateral distal radius. Corticocancellous grafts are usually not necessary. This avoids graft site morbidity from the iliac crest.

Contraindications

In general, presence of radiocarpal degeneration is contraindicated for scaphoid reconstruction and, hence, plating (Reigstad et al., 2009, Smith and Cooney, 1996). In cases with mild radiocarpal osteoarthritis, plating can be performed in conjunction with a radial styloidectomy. However, in patients where degenerative changes are advanced, salvage procedures are preferred.

Scaphoid fractures that involve either the proximal or distal pole, where there might not be adequate fragmentary purchase, are not suitable for plate fixation.

In select non-union cases, other surgical options might be more appropriate. For example, fibrous scaphoid union or non-union with no displacement and minimal sclerosis has been shown to unite with a single screw (Slade et al., 2003). Furthermore, volar cortical loss and severe humpback deformity are not ideal for dorsal plating. Nevertheless, plating with cancellous bone graft might still be an option in such cases. Cancellous bone grafting has been used for scaphoid non-union with concurrent humpback deformity by several authors (Finsen et al., 2006, Kirkham and Millar, 2012, Park et al., 2013, Stark et al., 1988) with union rates as high as 96% after only ten weeks (Kirkham and Millar, 2012).

Technique

Incision

The patient is placed in a supine position, the hand exsanguinated with an Esmarch bandage and an upper arm tourniquet inflated to 250mmHg. A dorsal wrist incision is made just ulnar to the third dorsal extensor compartment. The extensor retinaculum is incised, revealing the third extensor compartment. Extensor pollicis longus is retracted radially and the extensor digitorum released to expose the dorsal capsule. A longitudinal incision of the joint capsule is then made and the flaps retracted radial and ulnar, exposing the dorsal surface of the scaphoid. Care is taken to preserve the scapholunate ligament. The non-union site is then debrided with a curette and prepared for bone grafting and fixation (Figure 4.2).

Fracture preparation

The fracture is reduced and stabilised with provisional fixation, usually with a K-wire. Supplementary bone grafting may need to be performed. If no cavitary defect is present, we prefer to curette the granulation tissue and use cancellous bone from the distal radius (Figure 4.3). In cases of a humpback deformity, bone grafting varies, depending if the deformity is acute or chronic. In the acute case, the deformity can be corrected, and is likely to demonstrate minimal cortical bone loss. In this instance, we use cancellous bone graft, which is packed into the volar and dorsal aspects of the fracture. Dorsal cancellous bone grafting has been used for scaphoid fractures even with chronic volar cortical bone loss by several authors in the past (Finsen et al., 2006, Kirkham and Millar, 2012, Park et al., 2013) with excellent results. Nevertheless, in the chronic case, with significant volar cortical bone loss (Oka et al., 2005b) we use a corticocancellous bone graft from the iliac crest. The graft can usually be inserted through the same dorsal approach, utilising joystick K-wires to achieve adequate exposure. We have not required to perform an additional volar approach to correct a humpback deformity.

Plating

A titanium, locking mini-plate (Medartis AG, Austrasse, Basel, Switzerland) was used for plating. We have used a trapezoidal eight to ten hole-plate that is contoured to conform to the dorsal shape of the scaphoid. The anatomic shape is dome-like with a slight helical twist secondary to lateral contouring (Figure 4.4). In some instances, one of the proximal and/or distal screw holes are cut from the plate to prevent plate impingement. If the plate is cut, sharp edges need to be filed. The plate is then placed on the dorsal surface, spanning from the proximal pole, across the fracture and bone graft to the distal pole. For distal waist fractures, the increasing convexity of the scaphoid can be a challenge for plate placement. In these cases, the plate can be inset in order to allow appropriate fracture spanning and avoid plate impingement distally.

The plate is then held in position with 1.25mm K-wires and position confirmed with fluoroscopy. We aim to have at least three screws either side of the fracture. The fracture is compressed with an AO bone reduction clamp and the plate and screws are secured using dynamic plate techniques (Figure 4.5). The screws should be aimed away from the fracture site. We expect that the superior fixation provided with a plate is likely to decrease the need for corticocancellous grafting and that cancellous grafting will suffice.

Once fixation is complete, the wrist is closely examined clinically and under fluoroscopy to ensure that the plate and screws do not impinge in any wrist position. This includes identifying if (a) the plate impinges on the dorsal radius in wrist extension, (b) the screws violate the articulations including the STTJ and mid-carpal joints and (c) if screws protrude excessively through the volar cortex (Figures 4.6 & 4.7).

The wound is irrigated and sutured in layers.

Complications

An injury to the superficial branch of the radial nerve should be avoided. Plate impingement on the radius, in particular in extension, and screw penetration into adjacent joints can occur but are avoided with careful technique. The wrist is assessed in multiple planes with fluoroscopy to avoid incorrect screw placement. Plate impingement is avoided with careful positioning and identifying sites of impingement intra-operatively. In addition, plate prominence may be avoided by inseting of the plate into the scaphoid, thereby minimising the profile of the plate.

Persistent non-union may occur with dorsal plating of the scaphoid. Volar plating has been shown to have good clinical outcomes (Leixnering et al., 2011, Ghoneim, 2011, Dodds et al., 2014). We have plated 10 scaphoid fractures. Preliminary results show that one patient had radiologically delayed union. He is active and remains comfortable. All other patients are clinically and radiologically united. A more detailed analysis of the clinical outcome of these patients, including time to union, fracture type and functional scores is pending. Salvage procedures, such as four-corner fusion, scaphoidectomy or proximal row carpectomy are options in patients with persistent pain due to arthritis, non-union or other carpal pathology. This has not been required in our cases.

Rehabilitation

The patients are provided with a removable wrist splint, but are allowed to mobilisation of the wrist.

We discourage lifting of more than 2kg for the first eight weeks. The patients are reviewed at one- and 8-weeks post-surgery with radiographs. A longitudinal CT scan is performed at three months to confirm fracture union. A hand therapy referral is initiated only if the patient fails to mobilise adequately. We aim for unrestricted mobilisation by three months.

Figures

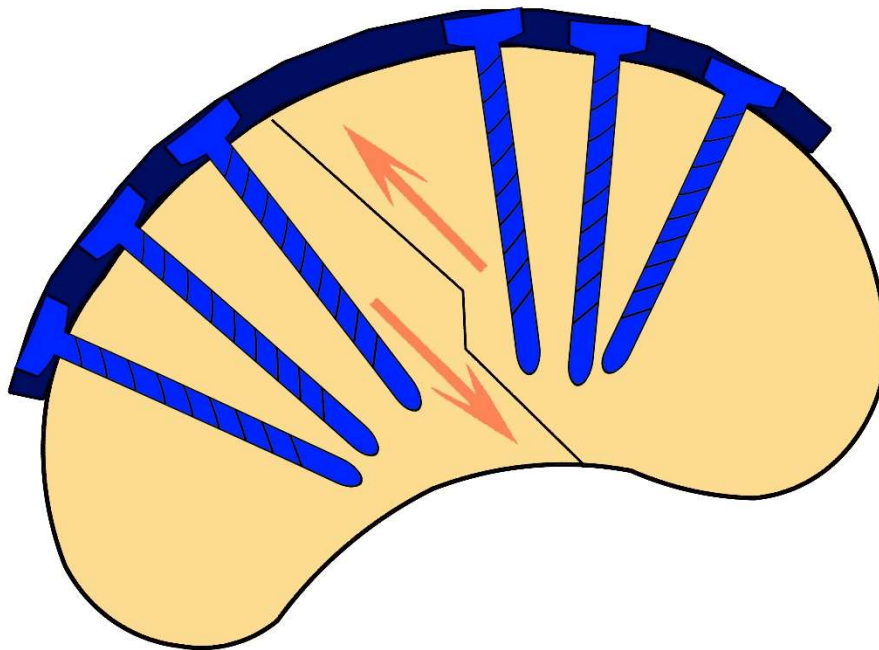


Figure 4.1 Diagram of an oblique scaphoid fracture: arrows indicating shear stress across fracture; dorsal plate with locking screws in each fracture fragment

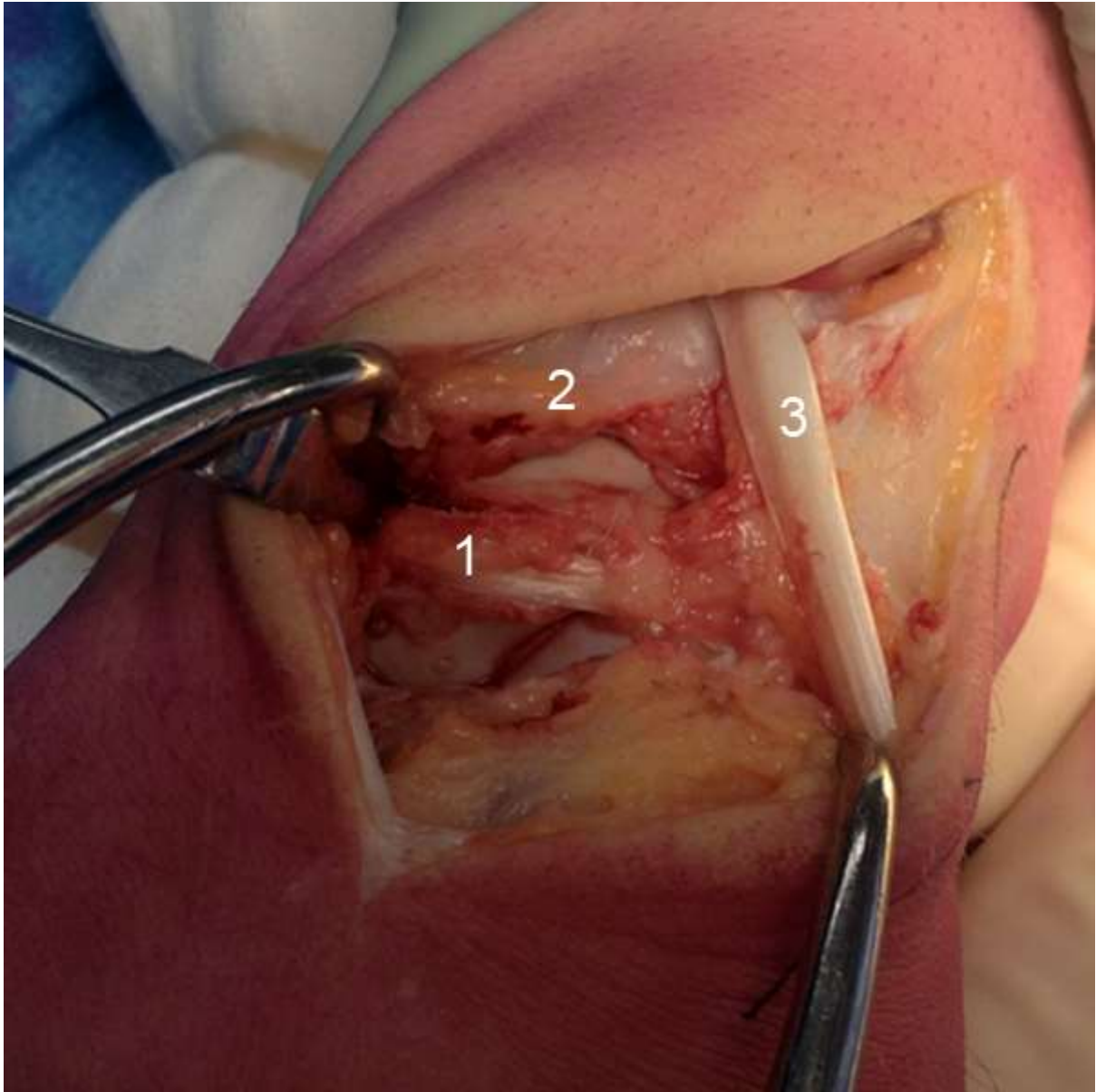


Figure 4.2 Dorsal approach to left wrist for acute displaced scaphoid waist fracture: retracted extensor indicis pollicis (3), the dorsal capsule (2) is retracted; the dorsal ridge of the scaphoid (1) is then visualised

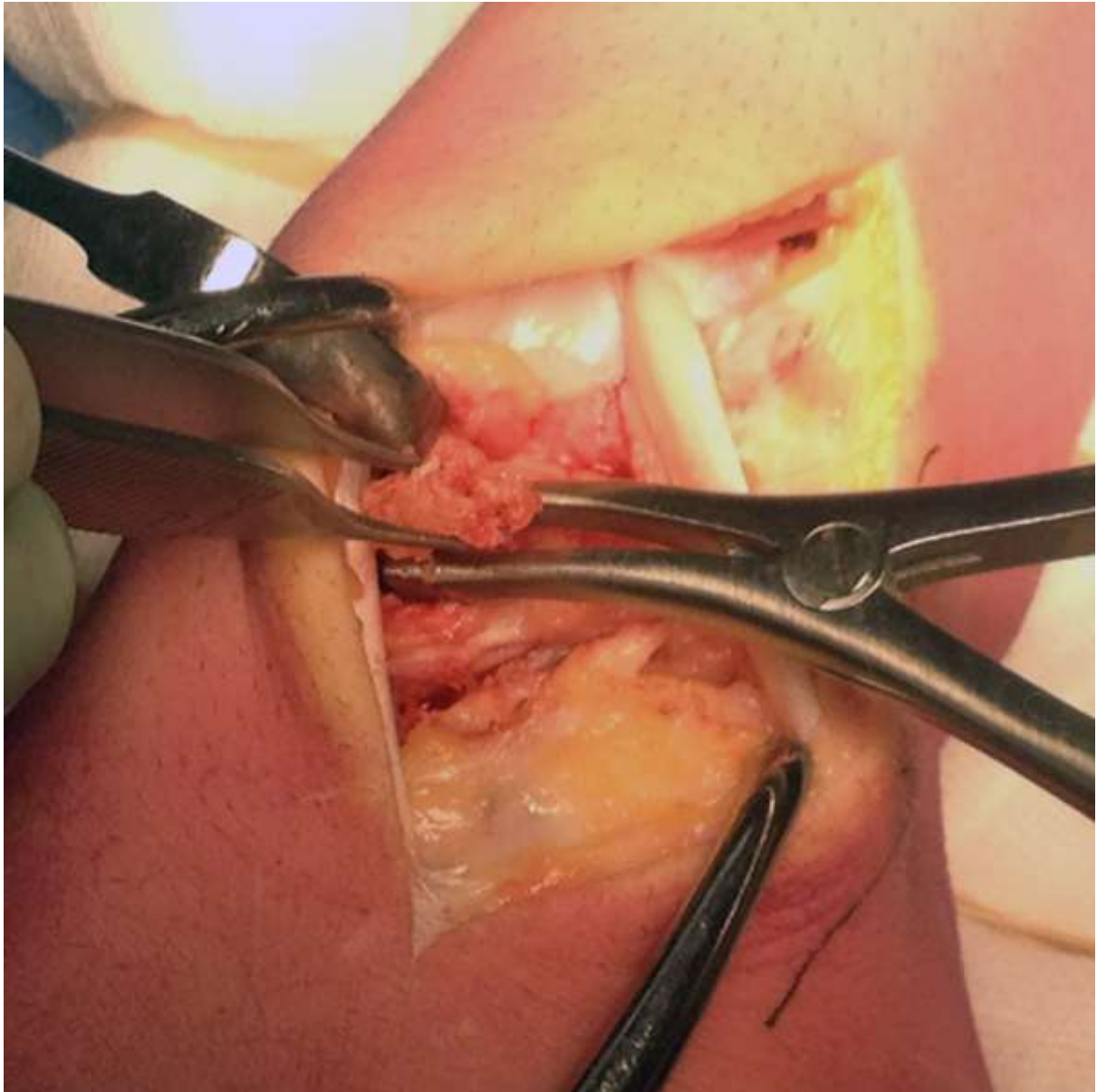


Figure 4.3 Bone grafting: Cancellous bone is taken from the distal radius through the same incision; the fracture is separated with a laminar spreader and the bone graft impacted into the fracture



Figure 4.4 Plate contouring: The plate is contoured to fit the dorsal surface of the scaphoid; in some cases, a screw hole may need to be removed to avoid impingement

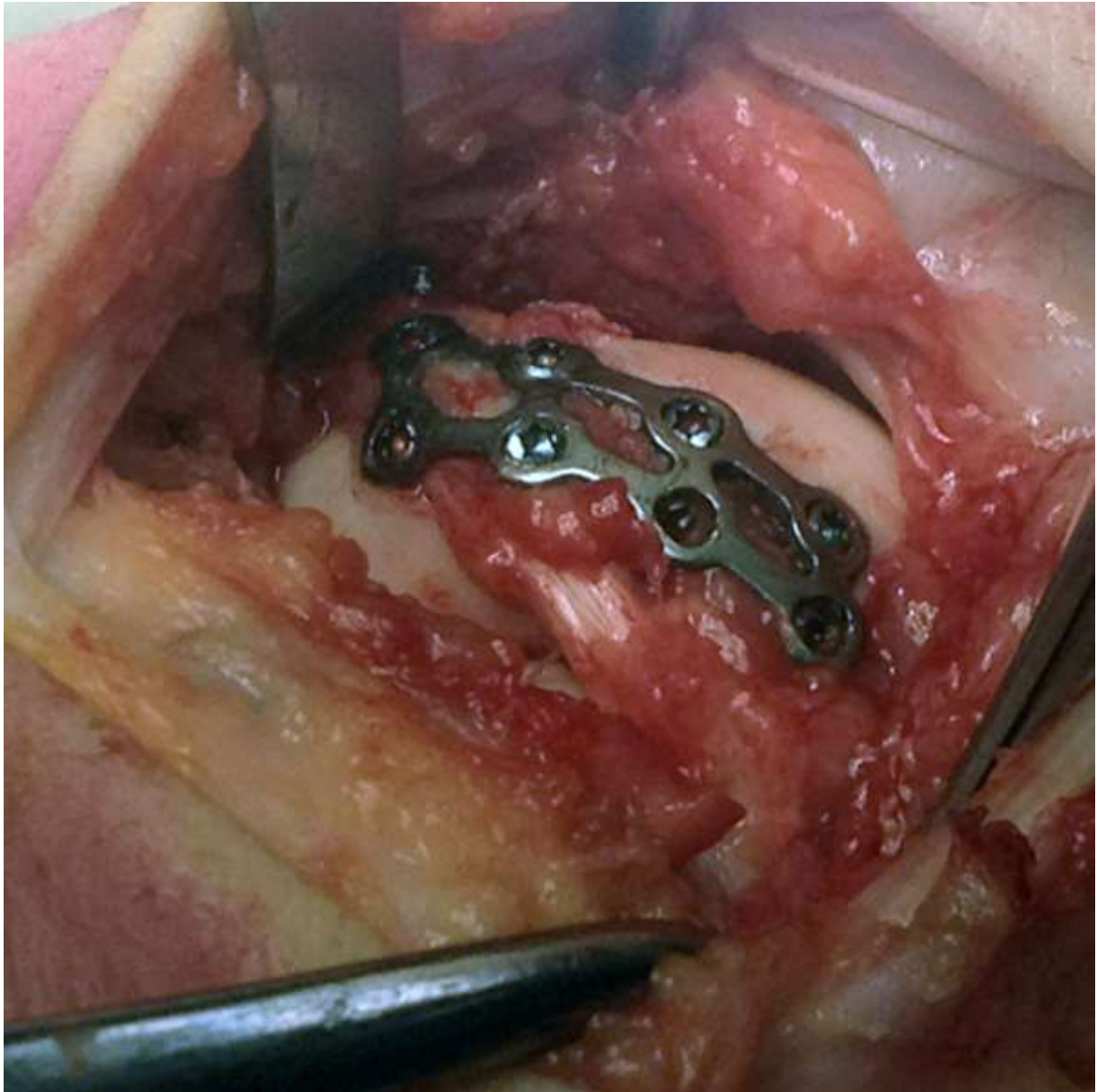


Figure 4.5 Final position of the plate on the dorsum of the scaphoid; at least three screws are positioned into each fracture fragment and aimed away from the fracture



Figure 4.6 CT images showing a pre-operative neglected, non-united right scaphoid fracture with cystic change and humpback deformity (A & B); post-operative X-rays of the same patient (C & D) showing the plate and screw position as well as the distal radial bone done site

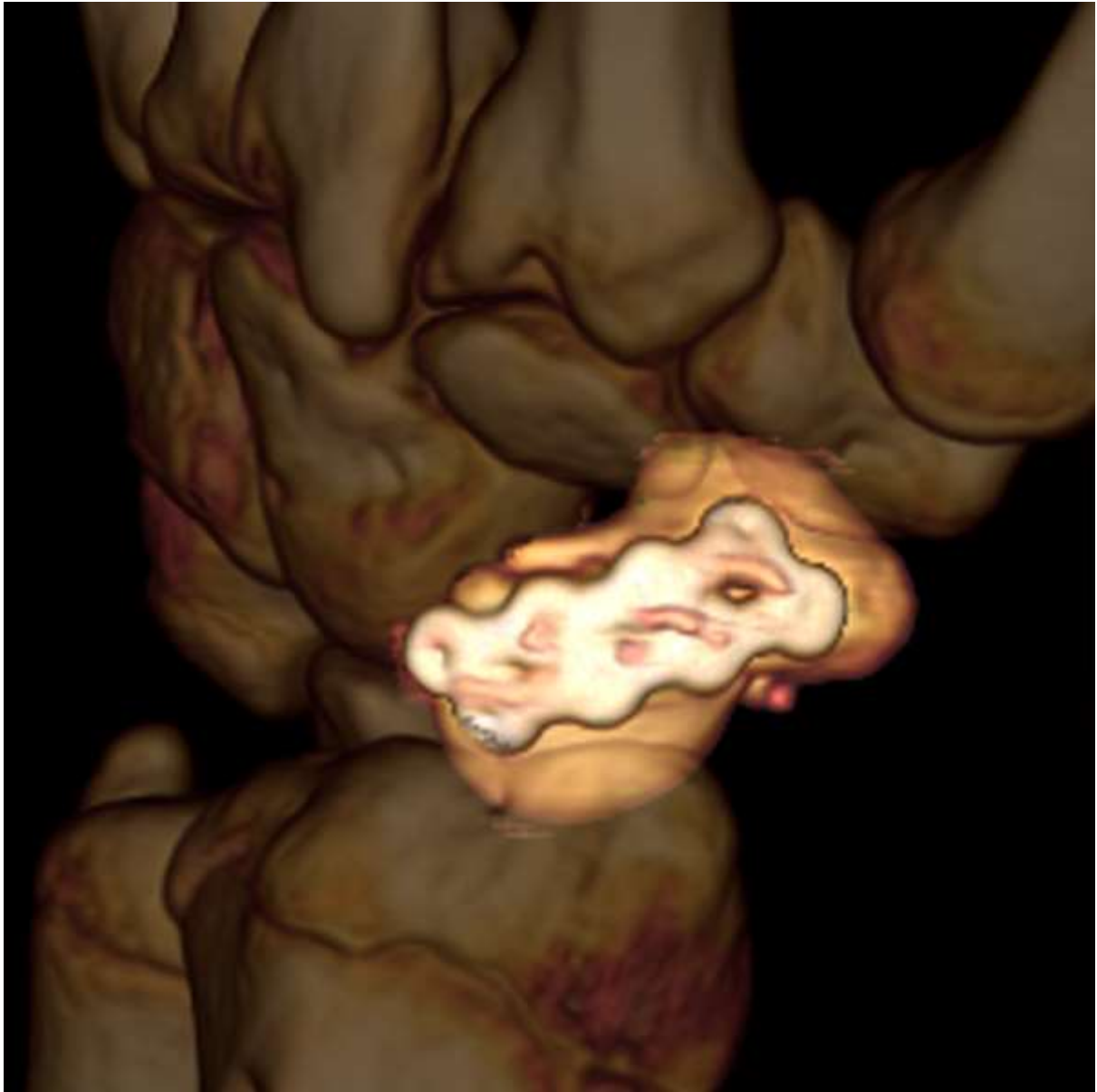


Figure 4.7: Post-operative 3D CT reconstruction of left wrist showing plate position on dorsal bare area

Chapter Five – Imaging the STTJ

Evaluation of the STTJ is an important part of scaphoid fracture fixation. Radiographic assessment of STTJ arthrosis is required in scaphoid non-union management or following fracture fixation with persistent base of thumb symptoms. Furthermore, dedicated STTJ imaging should be obtained intra-operatively and during post-operative care in order to avoid or monitor implant penetration into the STTJ.

STTJ Imaging

The STTJ is usually imaged as part of investigation of radial-sided wrist or base of thumb pain. The standard wrist series includes PA and lateral X-rays (XR) in anatomical neutral wrist positions. A semi pronated oblique view with the radial side of the wrist elevated 45° off the XR cassette is recommended for the STTJ (International Wrist Investigators' Workshop Terminology, 2002). The semi pronated view is aimed at imaging the dome-shaped STTJ with minimal overlap between the distal scaphoid, trapezium and trapezoid. Several improvements to the semi pronated view have been introduced in order to address the volar inclination of the STTJ. Wollstein and colleagues addressed this by placing the wrist in maximal ulnar deviation (Wollstein et al., 2005). Ulnar deviation is known to result in scaphoid extension (Short et al., 1997); hence, presenting the STTJ in profile. However, carpal kinematics are complex and ulnar deviation alone is unlikely to address the volar inclination. Kinematic studies have confirmed that the degree of scaphoid extension in wrist ulnar deviation is variable (Moojen et al., 2002, Craigen and Stanley, 1995). Moreover, the scaphoid might undergo little movement when the wrist is placed in ulnar deviation along the dart thrower's motion arc (Crisco et al., 2005). The semi pronated view was modified further by DeGeorge and colleagues (DeGeorge et al., 2018). The authors placed the thumb in maximal abduction while maintaining the wrist in maximal ulnar deviation. To date, no study has addressed the volar inclination of the STTJ in the neutral wrist position; hence, avoiding the complexities of carpal kinematics.

STTJ Osteoarthritis

The thumb builds the basis for fine and gross motor function of the hand. Thumb function is so crucial that Comcare, the statutory authority of the Australian Federal Government administering workers' compensation claims, assigns significant degree of impairment to patients with thumb pathology (Comcare, 2017). An ankylosed thumb, for example, is assigned more whole person impairment than ankylosis of all four finger metacarpophalangeal joints combined. The thumb is subjected to multiplanar forces throughout range of motion and is prone to degeneration with work, recreational activities and following trauma. It affects 33% of women and 12.5% of men (Green and Wolfe, 2011). The majority of patients with base of thumb osteoarthritis have osteoarthritis of the STTJ (Crosby et al., 1978). The symptoms of STTJ arthritis include pain, stiffness, dexterity loss of thumb movement and weakness. Initial investigations of the thumb start with plain radiography. The standard projections of the STTJ, the PA, lateral and oblique views, have been defined by the International Wrist Investigator's Workshop (International Wrist Investigators' Workshop Terminology, 2002). The PA view is obtained with the wrist in the anatomical neutral position, i.e. no flexion, extension, radial or ulnar deviation. For this, the shoulder is abducted to 90°, the elbow is flexed to 90° and the middle finger metacarpal is aligned with the longitudinal axis of the radius. The lateral radiograph is obtained in shoulder adduction against the torso and maintained elbow flexion similar to the PA view. The semi-oblique view is achieved with the ulnar border against the cassette and the forearm pronated to 45°. The wrist is placed in full ulnar deviation while maintaining a neutral flexion/extension position. Stress views of thumb can also be obtained by resisted abduction against the contralateral thumb; however, stress views are typically used to assess ligamentous integrity of the thumb carpometacarpal joint rather than in the assessment of the STTJ.

Radiographic staging of STTJ osteoarthritis is based on the Eaton and Glickel classification system of thumb carpometacarpal osteoarthritis. Its three stages of progressive joint narrowing and secondary

changes, such as cyst and osteophyte formation, have been modified (Table 5.1) to include subtle joint widening in early disease (Brown et al., 2003, Geurts et al., 2011).

Table 5.1: Radiological staging of the STTJ osteoarthritis

Stage 1	Normal joint/ joint space widening due to synovitis
Stage 2	Mild joint space narrowing with subchondral sclerosis
Stage 3	Marked joint space narrowing; loose bodies & osteophytes of <2mm
Stage 4	Loose bodies/ osteophytes >2mm, subchondral cysts, ankylosis

Radiographic changes of the STTJ in osteoarthritis and clinical symptoms are often variable. Several cadaveric and clinical studies have investigated the correlation between visual inspection of STTJ cartilage and radiographs (Glickel et al., 1992, North and Eaton, 1983, Brown et al., 2003). Agreement between visual joint pathology and radiographic stage lacked sensitivity, ranging between 33-67.5%. Part of the difficulty in accurately identifying and staging STTJ osteoarthritis can be attributed to the anatomic changes that the distal carpus undergoes with progressive degeneration (Crosby et al., 1978). In a clinical follow-up study of 49 patients, Crosby and colleagues identified a rotatory subluxation of the DAS of the scaphoid against the trapeziotrapezoidal (TT) articulation as the STTJ undergoes degeneration. The authors demonstrated on lateral radiographs, with the thumb in neutral position, that the scaphoid underwent extension while the trapezium and trapezoid translated volar. The surrogate marker for this change was a decreased scapholunate angle. It was observed to be less than 45° in 84% and less than 35° in 24% of patients. It was noted that the severity of these rotatory changes was correlated with the stage of osteoarthritis. In a large cadaveric study, Moritomo and colleagues described the radiographic changes to the degenerate STTJ further (Moritomo et al., 2000b). On semi-supinated PA radiographs, the TT inclination, an angle between the proximal TT articular surface and the long axis of the middle finger metacarpal, was measured. The TT inclination was used to estimate coverage of the DAS of the scaphoid by the

TT articulation. It was found to be significantly greater in STTJ osteoarthritis, indicated volar migration of the TT complex and greater under-coverage of the DAS compared with non-degenerate cases.

In summary, despite clearly defined parameters to obtain STTJ plain radiographs, imaging of the degenerate STTJ can be challenging. Clinical cohort studies demonstrated poor correlation with standard imaging protocols and anatomic changes to the carpus have identified why such low sensitivity might exist in the evolution of the osteoarthritic STTJ.

STTJ Osteoarthritis in Scaphoid fractures

The natural history of untreated scaphoid non-union results in a predictable pattern of degenerative radiocarpal osteoarthritis. It has been well described more than three decades ago (Mack et al., 1984) and has been subsequently termed scaphoid non-union advanced collapse (Kraakauer et al., 1994). Stages of joint arthrosis resemble those of scapholunate advanced collapse (SLAC). In scaphoid non-union advanced collapse (SNAC) degenerative changes start at the radial styloid (stage 1), then progress to the scaphocapitate joint (stage 2) and the midcarpal joint (stage 3). The final stage is pan-carpal arthrosis with preservation of the radio-lunate joint. Frequently, the only differentiation between SNAC and SLAC wrists is the sparing of articulation between the proximal pole and the radius (Shah and Stern, 2013). With an intact SLIL in SNAC, the proximal pole acts as an extension of the lunate, follows the load distribution subjected to the lunate and results in preservation of its and the corresponding radial articular surface. Surgical treatment of scaphoid non-union has been regarded as the treatment of choice to halt degenerative changes observed in SNAC (Filan and Herbert, 1996). However, earlier fixation techniques using headed screws (Trumble et al., 1996) or interposition bone grafts (Russe, 1960) may have predisposed patients to joint arthrosis. The standard technique for interposition bone grafting in scaphoid non-union has been the

Matti-Russe graft. It requires debridement of the fibrous non-union site and preparation of both fracture fragments so that a corticocancellous bone graft can be inserted. This restores scaphoid length and introduces new osteocytes to the fracture site to stimulate bone healing (Russe, 1960, Green and Wolfe, 2011). Preparation of the scaphoid for interposition bone grafting can result in inadvertent cartilage damage and lead to osteoarthritis (Barton, 2004). Consequently, long-term benefits of fracture fixation might not be as clear-cut as expected. Long term outcome studies have confirmed that joint arthrosis could not be fully prevented by fracture fixation (Martini and Schiltewolf, 1995, Jiranek et al., 1992). Stark and colleagues followed up 43 patients treated with the Matti-Russe technique (Stark et al., 1987). The pre-operative osteoarthritis rate of 18% increased to 82% at final follow-up (mean 12 years). Newer fixation techniques using headless compression screws and wedge-shaped bone grafts predispose the scaphoid to less articular damage (Barton, 2004). Nonetheless, the gradual process of articular degeneration cannot be fully halted. Filan and Herbert followed up 163 out of 431 patients treated for non-union using the original Herbert screw (Filan and Herbert, 1996). The pre-operative osteoarthritis rate of 40% increased to 49% at final follow-up; however, severe arthritis more than doubled from 3% to 7%.

The STTJ has not been described as part of the sequelae of scaphoid non-union; however, controversy exists with regards to the role of scaphoid trauma and subsequent fracture fixation in the development of STTJ osteoarthritis. The prevalence of STTJ degeneration is high. It has been reported to be as high as 83% in a cadaveric study of largely elderly wrists (Bhatia et al., 1996). Consequently, the incidence of STTJ osteoarthritis observed following scaphoid trauma may be unrelated to the scaphoid fracture and could have occurred irrespective of the initial injury. Further to that, arthrosis of the STTJ might have already been present at the time of injury. Pre-existing osteoarthritis of the STTJ is infrequently reported on. Inoue and colleagues examined 160 patients with established scaphoid non-union (Inoue et al., 1997). They were able to identify 30 patients (19%) who had STTJ osteoarthritic prior to commencement of any treatment. This highlights a lack of

clear causality between scaphoid fracture and STTJ osteoarthritis. Insertion of a headless compression screw through the distal pole requires mobilisation of soft tissues, including the radial aspect of the scapho-trapezial ligaments, partial exposure of the joint surfaces and with the original Herbert screw, attachment of an insertion jig. Any of these intra-operative steps can, in theory, damage articular surfaces of the STTJ. Instrumentation of the STTJ might not be a prerequisite for articular degeneration, though. Jiranek and colleagues, for example, examined 26 wrists 7-18 years after Russe interposition bone grafting (Jiranek et al., 1992). STTJ osteoarthritis was observed in ten wrists (38%). Reported STTJ osteoarthritis following screw fixation ranges from 0-60% (Nicholl and Buckland-Wright, 2000, Saeden et al., 2001). Nicholl and Buckland-Wright followed-up 23 scaphoid fractures managed with cast immobilisation and 18 fractures with a single Herbert screw and bone grafting (Nicholl and Buckland-Wright, 2000). There was no increase in osteoarthritis between the two treatment modalities after a minimum five-year follow-up. The only finding in the operative group was a more likely development of distal osteophytes. Saeden and colleagues examined 62 fractures 12 years following injury. A subset of patients was evaluated using CT. In the non-operative group, four patients (25%) had signs of STTJ osteoarthritis. In contrast, 14 patients (60%) treated with the Herbert screw via the volar approach showed STTJ osteoarthritis.

As headless screw designs matured, percutaneous fixation techniques became popular, promising quicker union times and less surgical exposure (Bond et al., 2001, McQueen et al., 2008).

Subsequently, screw fixation strength has been shown to be increased with centrally placed screws (Dodds et al., 2006, McCallister et al., 2003). This allowed for maximal use of available cancellous bone in both fracture fragments and distribution of rotational forces along the entire scaphoid, reducing strain at the fracture site (Slutsky and Slade, 2011). This is of interest, as the trapezium usually obstructs central screw placement in volar percutaneous screw fixation. Several options to overcome this exist. Part of the trapezium can be excised or the STTJ can be opened so that a better entry point can be achieved with manipulation of the distal pole. Another technique is the trans-

trapezial approach (Meermans and Verstreken, 2008). The screw trajectory is determined by intra-operative fluoroscopy, marking guide wire placement on the skin in the AP and lateral planes. The intersection of the lateral and AP directions, determines the starting point of the screw. Compared with traditional techniques, this starting point is chosen based on the axis of the scaphoid and is not influenced by the location of the extra-articular tubercle. Consequently, the guide wire, cannulated drill and the screw transverse the STTJ. Meermans and Verstreken reported 100% union after an average of 6.4 weeks. There was no changes to the STTJ at short-term follow-up (Meermans and Verstreken, 2008). The same patient cohort was followed up 6.1 years after fixation (Geurts et al., 2011). Despite six cases of screw protrusions into the STTJ (18%), only three patients with osteoarthritis were identified (8%). The authors concluded that trans-trapezial percutaneous screw fixation does not lead to symptomatic osteoarthritis at medium-term follow-up. Screw length might not be the only reason to insert a screw through the STTJ, though. Traditional teaching for lag and compression screw placement demands screws to be placed perpendicular to the fracture plane (Müller et al., 1992). A screw that is not inserted perpendicular to the fracture will displace the fracture fragments as the screw is tightened. Luria and colleagues examined the stiffness of headless compression screws placed across oblique scaphoid osteotomies (Luria et al., 2012b). Screws placed perpendicular to the fracture site, performed similar to those placed in the central axis of the scaphoid axis through the DAS. Construct stiffness was in fact higher for screws perpendicular to the fracture site (148N vs 137N).

Study IV - A New Radiographic View of the Scaphotrapeziotrapezoid Joint **

Arthur Turow^{1,2} MBBS; Joideep Phadnis^{2,3} MBChB; Gregory I. Bain^{1,2} MBBS, FRACS, PhD

¹Flinders University of South Australia, Adelaide, Australia

² Department of Orthopaedic Surgery, Flinders Medical Centre, Adelaide, Australia

³ Brighton & Sussex University Hospitals, Brighton, United Kingdom

Abstract

Background – The STTJ has a complex osseous and ligamentous anatomy. Precise radiographic assessment is paramount when assessing osteoarthritic, post-traumatic or post-operative patients. There has been no described technique to image the STTJ without any wrist movement, unobscured by the rest of the carpus. The aim of this study was to define an optimal radiographic method to assess the STTJ while maintaining the wrist in neutral position.

Methods – Computed tomography 3-D reconstructions of three uninjured wrists were initially used to determine an approximate beam angle. Serial radiographs of twelve cadaveric wrists were taken. The forearms were positioned in varying degrees of pronation and supination. The beam angle was concurrently adjusted to varying degrees of caudal tilt. From the images obtained, we assess if the adjacent carpus obscured the view of the STTJ.

Results – Optimal STTJ imaging was in the semi-pronated wrist and the with the X-ray beam tilted caudal. We found that the STTJ was best visualised at 48° supination from a fully pronated wrist and a caudal beam angle of 22°.

Conclusion - The described wrist and beam orientation can aid in achieving an unobstructed view of the STTJ with little technical effort. This can aid in imaging ambulatory patients where symptoms prevent using other imaging techniques as well as patients in the theatre room where imaging timing can be critical.

Introduction

The STTJ is a multi-facet articulation, formed by the distal, triangular shaped articular surface of the scaphoid, the trapezium and the trapezoid (Fogg, 2004). The trapezoid articulates with the adjacent trapezium and capitate. Routine PA radiographs usually show the scaphoid in a slightly flexed profile with its distal articular surface obscured by the concave trapezium and trapezoid articulations (Feipel et al., 1999, Wollstein et al., 2005). A dedicated STTJ view could aid to better visualise the joint in acute trauma or in degenerative conditions.

Plain X-ray assessment has been limited to standard PA, lateral, semi-pronated and ulnar deviation views as used for evaluating scaphoid pathology. Several studies have used these standard views, namely PA radiographs, to identify the severity of osteoarthritis (Geurts et al., 2011, Melville et al., 2015, Scordino et al., 2014); however, PA radiographs have been shown to have a low sensitivity for the detection of pathology (Brown et al., 2003).

Morimoto and colleagues (Moritomo et al., 2000b) have developed the scaphoid axial view for kinematic evaluation of the STTJ, placing the wrist in 45° of supination in order to evaluate TT inclination. The International Wrist Investigators' Workshop (International Wrist Investigators' Workshop Terminology, 2002) has suggested a similar view with the addition of some ulnar deviation. Both views isolate the STTJ but fail to achieve clear depiction of the scapho-trapezial articulation. More recent studies have focused on improving those techniques. Wollstein and colleagues (Wollstein et al., 2005) described a STTJ view, where the wrist is placed in full ulnar deviation and maximal extension. Their technique achieved good visualisation of the TT joint, at the expense of an unobstructed visualisation of the distal scaphoid. A recent study has modified the STTJ view described by Wollstein (Wollstein et al., 2005) by imaging the wrist in 45° pronation in order to evaluate post-operative STTJ osteoarthritis following scaphoid fracture screw fixations (Geurts et al., 2011). This modified view still showed some overlap with the trapezium. DeGeorge and colleagues

(DeGeorge et al., 2018) added thumb abduction at 40° of forearm pronation and maximal wrist ulnar deviation. Thumb abduction allowed the authors to get a better, yet still incomplete, scapho-trapezium-trapezoid identification with preservation of the TT articulation.

Patient presenting with STTJ pathology frequently are not able to achieve full wrist extension, ulnar deviation or thumb movement due to pain, especially where concurrent wrist pathology is present. Similarly, trauma or post-operative patients are usually unable to achieve full range of motion.

The aim of this study was to achieve ideal STTJ visualisation using serial radiographs while maintaining the wrist in neutral position. The results could then be used for trauma, surgical patients or those with osteoarthritis.

Materials & Methods

Sample preparation

Twelve embalmed adult cadaveric upper limbs were supplied by the Department for Anatomy & Histology at Flinders University, South Australia. Ethics approval was granted from the Southern Adelaide Clinical Human Research Ethics Committee (Approval SAC HREC EC00188). Twelve cadaveric right upper limbs of six males and six females (mean age 81; range 57-95) were studied. Each specimen was embalmed in neutral wrist position.

Imaging

Initial assessment included review of three CT 3-D reconstructions of non-pathological wrists of alive patients in neutral position using the RadiAnt DICOM Viewer™. This was to streamline radiographic imaging of the cadaveric specimens. The angle for best beam placement was determined by rotating from the neutral, anterior reconstruction positions (Figure 5.1A) until a uniform, clear-space was seen across the STTJ (Figure 5.1B). Rotation angles were recorded for each CT series and averages calculated. This revealed that the STTJ was positioned at an angle 40° oblique to the coronal and 20° caudal to the axial plane of the forearm.

Each embalmed upper limb was secured on an imaging table. Initial wrist placement was in line with routine PA wrist radiographs: full pronation, palm in contact with imaging receptor, 100cm from the X-ray tube (Whitley et al., 2016). The X-ray beam was limited to caudal and cranial tilt only.

Supination and pronation were achieved by changing placement of the wrist on the imaging table with the aid of positioning blocks. The placement of the wrists was confirmed using a digital accelerometer, placed across the diaphysis of the radius and the ulna 5cm proximal to the wrist joint. The starting position was 40° of forearm supination and 20° of caudal beam orientation as determined by the initial CT assessment. Serial X-rays were taken in 2° increments of beam tilt and 5° of forearm rotation.

Image assessment

The scapho-trapezial and the scaphoid-trapezoid joint spaces were assessed separately. The primary end-point was STTJ clear-space between the scaphoid and the TT complex (Figure 5.2). Three parameters were used to assess quality of that clear-space: (1) any narrowing or obliteration along the distal scaphoid, (2) width uniformity of scapho-trapezial and the scaphoid-trapezoid joint spaces and (3) continuity across the trapezium and trapezoid. In cases of clear-space obliteration and discontinuity (Figure 5.3A) or differing widths of clear-spaces at the trapezium or trapezoid (Figure 3B), the forearm position and beam orientation were adjusted. Imaging of the STTJ was deemed satisfactory when the scapho-trapezial and the scaphoid-trapezoid joint spaces were uniform in width and when these spaces were continuous with each other (Figure 5.2). Osteoarthritis was assessed according to the modified Eaton and Glickel classification (Brown et al., 2003, Geurts et al., 2011). As the primary aim was to determine joint space uniformity in different wrist position, rather than the degree of joint degeneration, osteoarthritis was recorded in binary format. Each image was reviewed separately for joint space quality and presence or absence of osteoarthritis by two investigators (an orthopaedic surgical trainee and a fellowship trained orthopaedic surgeon). Any discrepancies were re-assessed until consensus was reached. Differences in the forearm and beam angle orientation between samples were analysed using the Mann-Whitney U test. A result was considered statistically significant when the p-value was less than 0.05.

Results

A summary of the results is presented in table 5.1. Osteoarthritis of the STTJ was present in 50% of the specimens (Figure 5.4). All of those specimens had concurrent base of thumb osteoarthritis.

In order to achieve an unobscured view of the STTJ, the mean angles measured were: supination 48° (range: 45-55°) and a caudal beam angle 22° (range 15-30°) from the initial wrist position (Figure 5.5). There were no significant differences in forearm rotation ($p=0.70$) or beam tilt ($p=0.82$) between males and females. Equally, angular parameters were statistically similar in osteoarthritic and non-osteoarthritic specimens (forearm rotation: $p=0.82$; beam tilt: $p=0.48$).

Discussion

The standard PA view of the wrist has been the mainstay of STTJ imaging; however, this view is not ideal due to substantial overlap of carpal bones, preventing clear visualisation of the dome-shaped STTJ. The PA oblique view, as proposed by International Wrist Investigators' Workshop (International Wrist Investigators' Workshop Terminology, 2002), can unfold the STTJ to a degree, but still suffers from joint-space obliteration and discontinuity. In this study, we identified a radiographic view that avoids these difficulties and allows for clear imaging of the STTJ. Wollstein and colleagues (Wollstein et al., 2005) described an alternative STTJ view; however, this view depended on mobilising the wrist into extremes of extension and ulnar deviation. A modified oblique pronation view of Wollstein's view was described as part of a percutaneous trans-trapezium scaphoid fixation cohort study (Geurts et al., 2011). That view also required wrist mobilisation to 45° of flexion and ulnar deviation. Our view has the advantage that the wrist can be kept in a neutral position with no required movement at either the wrist or carpal joints. It is able to achieve an unobstructed view of the distal scaphoid with no overlap with the trapezium or trapezoid. As an additional benefit, the TT joint can also be visualised with little bony overlap (Figure 5.2). This can be useful when assessing STTJ fusion outcomes (Srinivasan and Matthews, 1996, Wollstein and Watson, 2005).

Our STTJ view can be easily reproduced during surgical procedures as well as in the ambulatory setting. Most modern outpatient X-ray machines can be orientated in at least one axis of rotation.

This allows wrists to be imaged flat on the imaging table with only adjustment of supination from the standard posterior-anterior position, avoiding calibration of the X-ray beam in several axes. This allows for more efficient and reliable imaging, even in situations where patients' symptoms would not allow any movement of the wrist or thumb.

Adequate imaging of the STTJ is paramount in scaphoid fracture fixation. There is evidence to suggest that screw placement through the distal pole of the scaphoid can lead to STTJ osteoarthritis (Barton, 2004, Geurts et al., 2011, Kehoe et al., 2003). Screw prominence, in particular when placed in a proximal to distal direction, needs to be assessed to avoid STTJ damage. Recent use of both volar (Dodds et al., 2014, Leixnering et al., 2011) and dorsal (Bain et al., 2015) plates for comminuted or non-united fractures, makes intra- and post-operative STTJ imaging even more important. Intra-operative fluoroscopy frequently depends on small adjustments, while holding a fracture reduced or while placing implants. With the described view, patients' wrists can be placed palm-down on the fluoroscopy intensifier. Supination and elevation of the forearm (Figure 5.5) achieves our described view while maintaining the wrist and carpus in a fixed position.

The limitations of our study include sampling bias and the use of embalmed specimens. Sampling bias occurs due to its relatively small sample size. However, the rather uniform distribution of pronation and beam angles across genders and in wrists with STTJ osteoarthritis is reassuring. Usage of embalmed cadavers could predispose to measurement errors due to potential tissue distortion as part of the embalment process. By not relying on ligamentotaxis or articular movements when obtaining X-rays, such errors were kept to a minimum. Furthermore, usage of a digital accelerometer across the specimens and incremental adjustments of the beam angle tilt allowed reproducible and accurate specimen positioning. Finally, as the starting pronation and beam angulations were derived from the CT analysis, not all wrist positions were tested. A future study could evaluate the unfolding of the STTJ from the standard, fully pronated PA to our described wrist position. This could allow for a more detailed analysis of the effects of pronation and beam orientation on the STTJ space. An

inter-observer analysis of all variants of the STTJ view when compared to standard PA and PA oblique radiographs could further define the value of dedicated STTJ imaging in osteoarthritis assessment and classification.

Conclusion

Precise imaging techniques of the wrist play an important role in evaluating the complex osseous and ligamentous anatomy of the wrist. Our described radiographic view achieves an unobstructed view of the STTJ with little technical effort. It can be used for ambulatory patients where wrist or thumb movement is prohibitive due to pain or in the theatre setting where accurate imaging is frequently time-critical.

Acknowledgments

The authors thank the Department for Anatomy & Histology at Flinders University of South Australia for providing the cadavers, in particular Prof. Rainer Haberberger and Gregory Souter for their continued support of this study.

Figures

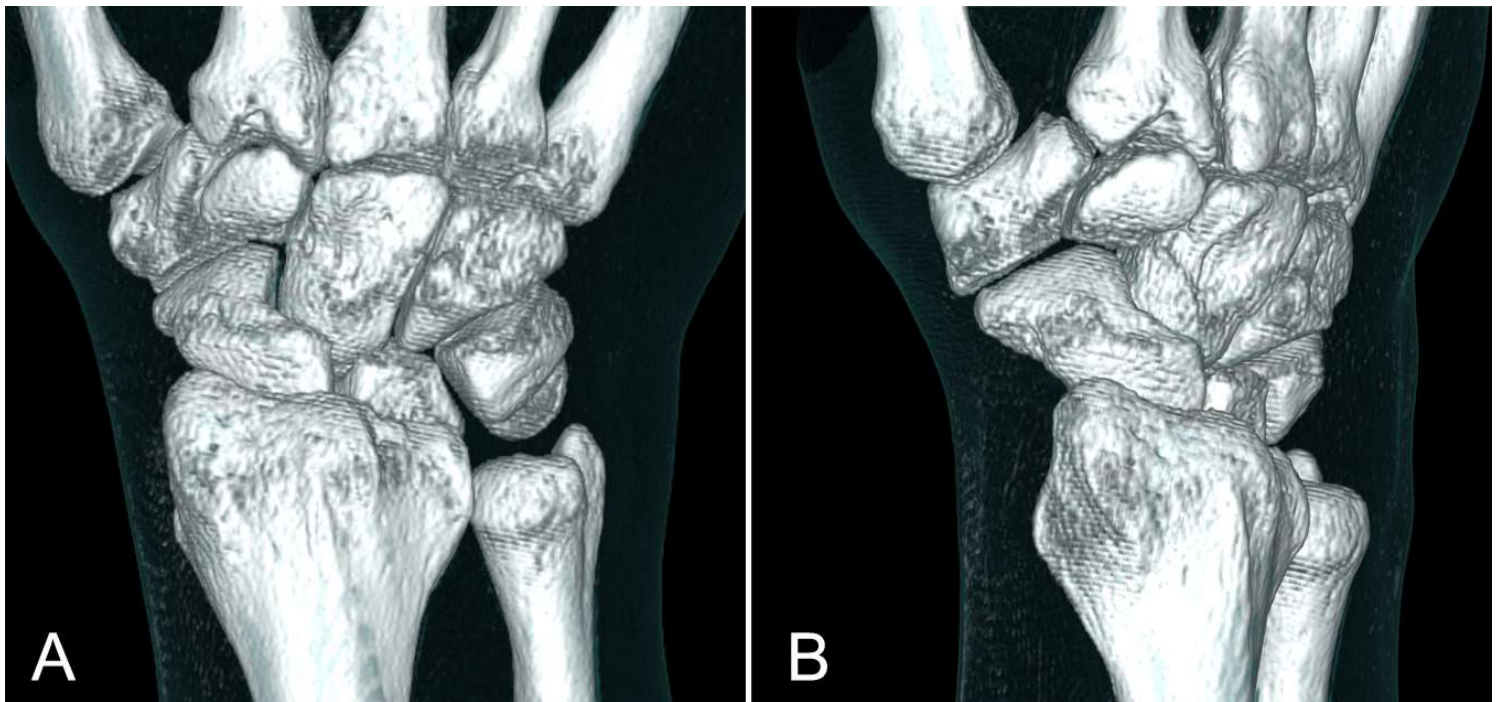


Figure 5.1: 3-D reconstruction of one of the CTs used for initial orientation assessment: A: dorsal view of a normal wrist in neutral position; B: after 40° coronal and 10° axial rotation, the STTJ can be seen unobscured from the trapezium and trapezoid.

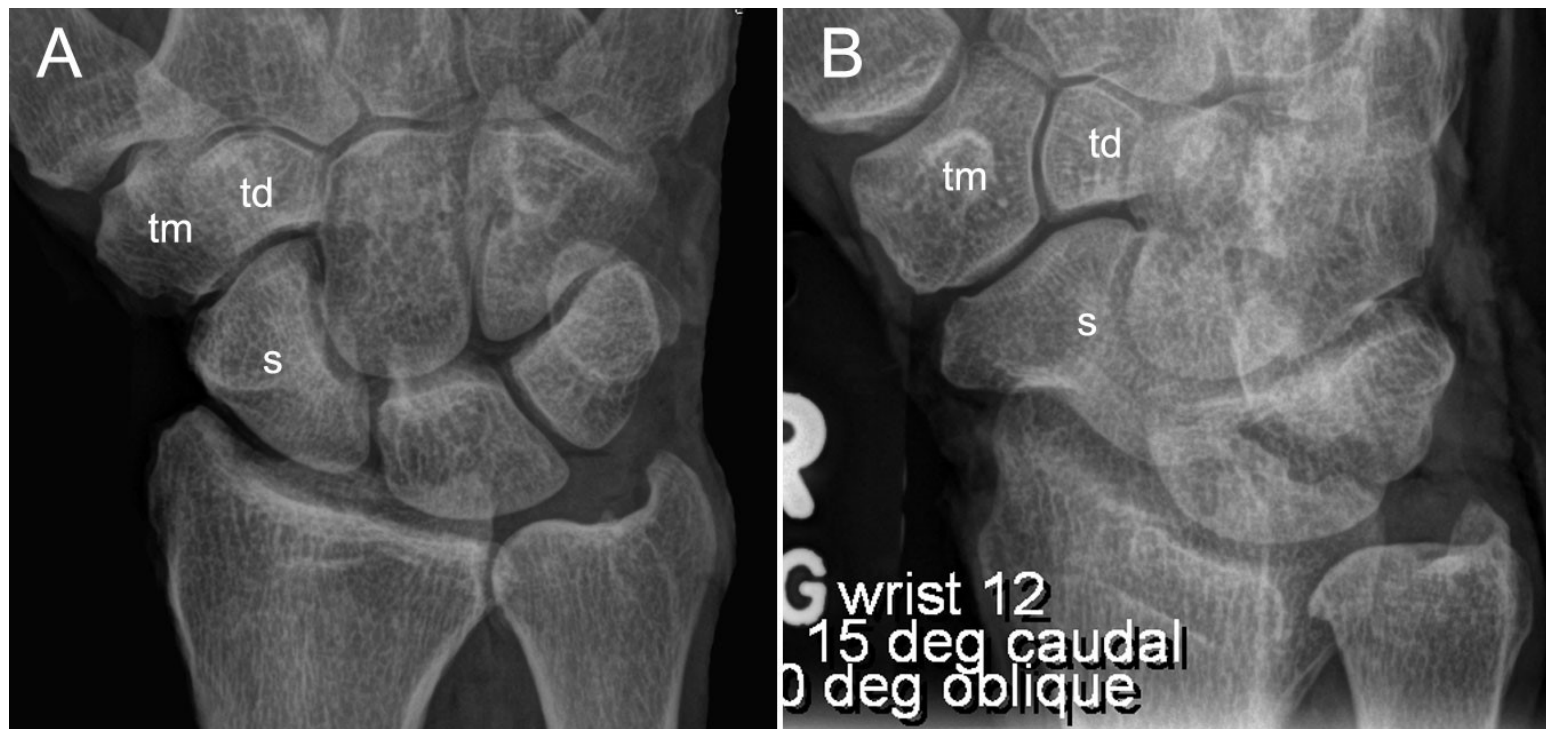


Figure 5.2: X-rays of a right cadaveric wrist taken in: (A) standard PA view, demonstrating trapezium [tm], trapezoid [td] and scaphoid [s] overlap; (B) Supination 40° and 15° caudal beam tilt showing an unobstructed STTJ

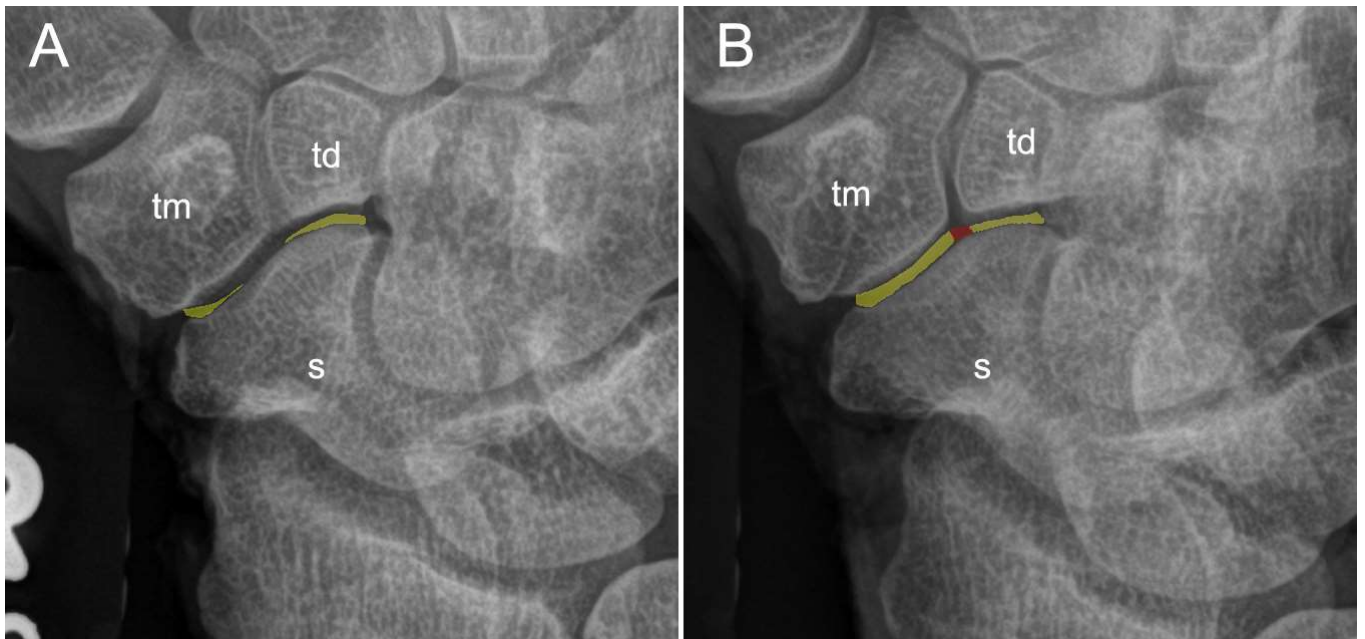


Figure 5.3: X-rays of the same cadaveric wrist as in Figure 5.2. Both radiographs were taken in 15° of caudal beam angulation. The supination angles are 5° away from the chosen image (Figure 2B): (A) 35° of supination, (B) 45° of supination. Unobstructed joint spaces are highlighted in yellow. Red highlights the continuation of those spaces across the tm/td joint. trapezium [tm], trapezoid [td] and scaphoid [s]

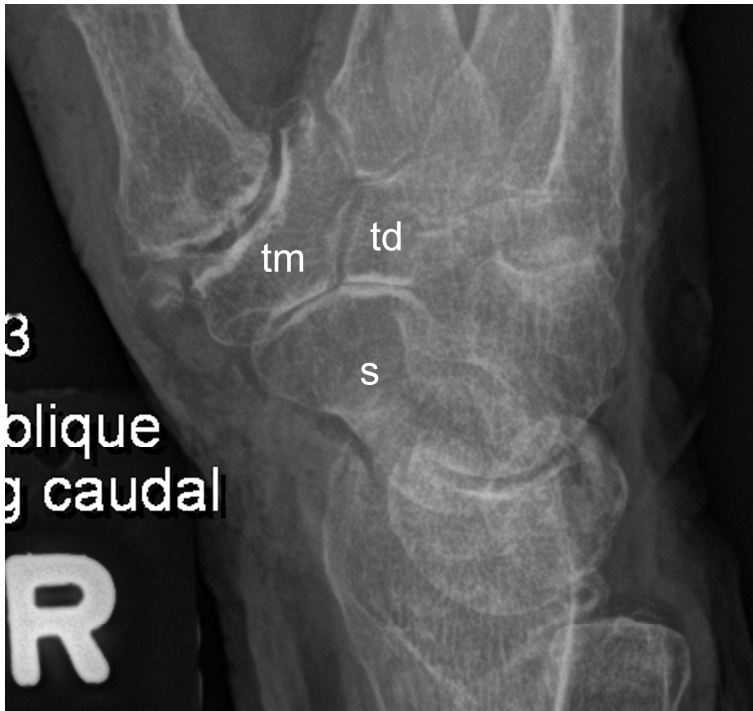


Figure 5.4: Example X-ray of a wrist with advanced STTJ and concurrent carpometacarpal osteoarthritis. trapezium [tm], trapezoid [td] and scaphoid [s]

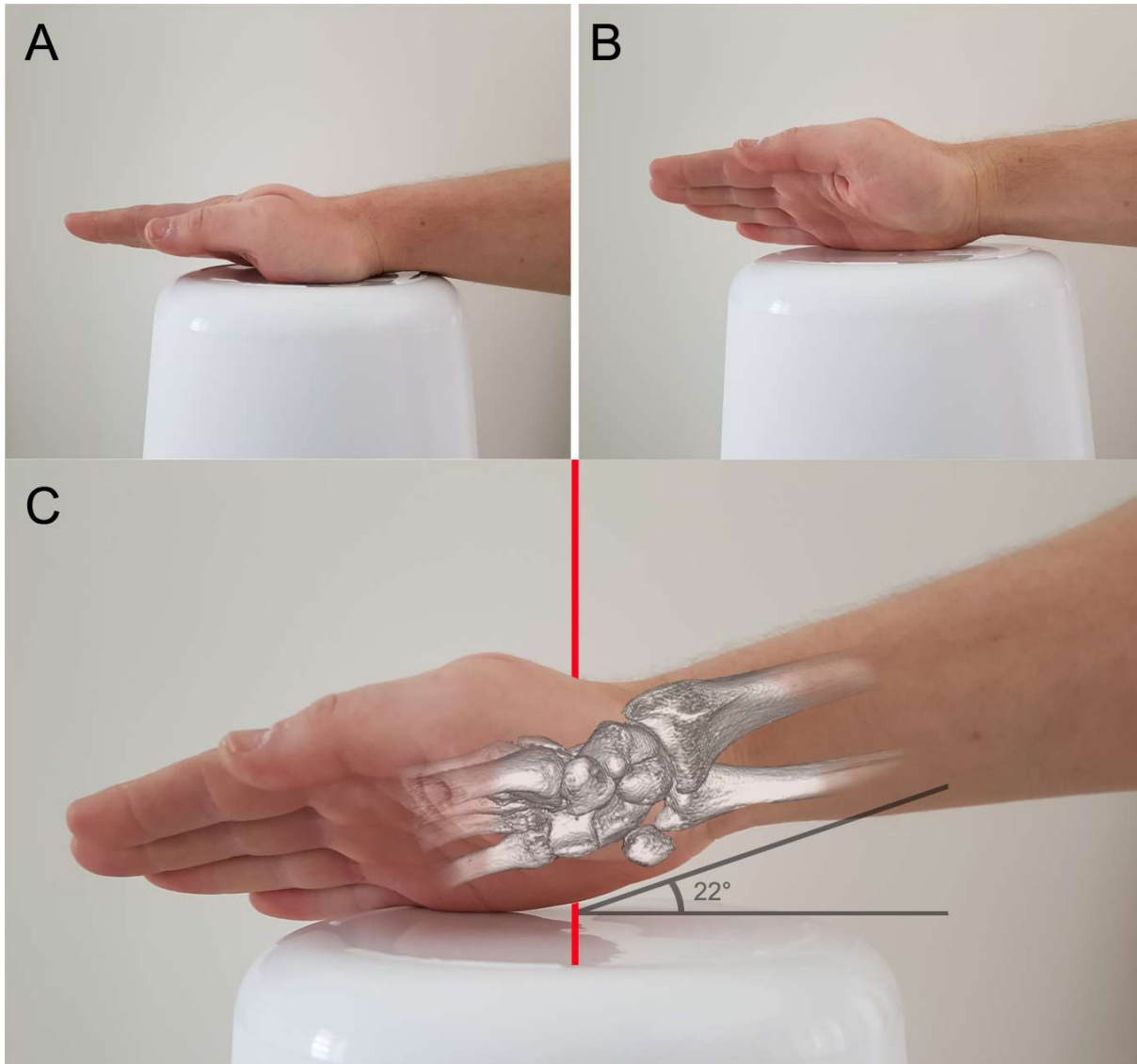


Figure 5.5: Serial positioning of the wrist for imaging; Red line indicates X-ray beam direction. (A) Full pronation position with palm-down for routine PA radiographs; (B) supination of 48° from the starting position; (C) forearm elevation to 22° while maintaining a neutral wrist position

Table 5.1: Specimen details, including presence of osteoarthritis (OA), concurrent carpometacarpal osteoarthritis (CMC OA) as well as the forearm pronation and the beam tilt (values in degrees; beam directed caudal in all wrists)

Wrist	Age	Sex	OA	Supination	Beam
1	79	M	No	55	25
2	90	F	Yes	45	20
3	67	M	No	45	30
4	91	F	Yes	55	30
5	75	M	No	45	15
6	88	F	No	50	20
7	95	M	Yes	45	30
8	83	F	Yes	50	25
9	83	M	Yes	45	15
10	79	F	Yes	45	18
11	57	M	No	40	15
12	88	F	No	48	15

Chapter Six – CT analysis of the scaphoid fracture

Fracture mapping

Fracture identification and description has been the mainstay of orthopaedic surgery since the discovery of XR in 1895 by Wilhelm Conrad Roentgen (del Regato, 1975). The uptake of XR in the medical field was almost instantaneous (Lane, 1895). Since then, plain radiography of bony pathology became the backbone of orthopaedic surgery. CT became available in 1973 (El-Khoury et al., 2004). In the late 1970s, its availability became wide-spread. This improved the understanding of fracture patterns and revolutionised three-dimensional imaging of fractures (Fishman et al., 1991). CT was initially used for complex trauma, where plain XR proved to lack diagnostic sensitivity (Sausser et al., 1980, Shirkhoda et al., 1980). However, early CTs only provided limited resolution. In addition, only the scanned plane, usually the transverse, was available for use (Sausser et al., 1980). As computers increased in processing power and decreased in costs, it was possible to obtain fine, axial data of an anatomical area. A modern wrist CT, for example, typically generates 200-400 slices. The obtained data set is viewed as a volume, rather than as individual images. Post-processing allows manipulation of these data sets in order to allow visualisation of the scanned area in different planes or in 3D (El-Khoury et al., 2004). Multiplanar reconstruction allows the display of stacked axial images in any desirable two-dimensional plane, e.g. coronal or sagittal. The availability of fine-slice CT produces isotropic volume data, where the volumetric pixel of the obtained data is cubic. This means that reformation of data does not suffer from resolution loss, retaining detail of the original axial image. This facilitates reformation of data in any desired plane. In addition to two-dimensional multiplanar reconstruction, modern CT allows three-dimensional images being displayed. The two types are volume rendering and surface rendering. Volume rendering creates a representation of the

surface of a scanned structure by examining every volumetric pixel, i.e. voxel, from the whole data set and assigning colours and shading to each voxel. This creates a summarised view of the whole data set. Most modern CT scanners use automated volume rendering to generate 3-dimensional images (El-Khoury et al., 2004). The downside of volume rendering is that the generated images cannot be manipulated, measured or segmented (Slutsky and Slade, 2011). In surface rendering, boundaries of anatomical structures are identified and overlaid with a polygonal mesh. This mesh can then be used to generate interactive 3-dimensional objects, such individual fracture fragments or various anatomical structures. The downside to surface rendering is that the process is frequently not fully automated, requiring manual segmentation or alteration to thresholds. This alters surface rendering impractical and too time consuming in the acute clinical setting.

The developments made in three-dimensional CT have helped to advance fracture analysis in 3D. Fracture mapping using 3D has expanded in recent years and has evolved from overlaying 2D images of volume rendered fractures onto a 2D anatomical model (Armitage et al., 2009, Cole et al., 2013, Hasan et al., 2017) to using surface rendering, virtual reduction and precise mapping onto a 3D template (Mellema et al., 2014, Xie et al., 2017). One of the first was Armitage and colleagues, who examined 90 scapula fractures (Armitage et al., 2009). Volume rendered scapula fractures were overlaid onto a scapula template and fracture lines transferred. The authors identified common fracture patterns not previously described. Their technique was used as the basis for 3D fracture mapping. Xie and colleagues examined 75 Hoffa fractures (Xie et al., 2017). The authors used 2D fracture overlays to identify common fracture configurations. More detailed analysis followed in 3D. Fractures were virtually reduced and transferred onto an intact femur model. This allowed for a detailed 3D fracture analysis and identification of comminution zones.

Scaphoid fracture classifications

The first attempt at grouping scaphoid fractures came from Destot in his monograph on wrist injuries (Destot, 1925). His description of scaphoid fractures covered his experience with more than 220 clinical cases. He did not make any mention about the timing of fractures. Furthermore, his predominate focus was on scaphoid fractures with associated pathology, such as distal radius, lunate or capitate fractures. He identified that fracture lines were variable and most frequently involved the middle third of the bone. He divided fractures into proximal third, middle third and distal third fractures. Further to that, he identified that fractures could be undisplaced or segmental. He noted difficulties in identifying fragments due to bony overlap in comminuted or very displaced cases. The first formal classification of scaphoid fractures followed in 1954 by Böhler and colleagues (Böhler et al., 1954). The authors identified 1113 scaphoid fractures between 1925 and 1952. A clear distinction was made between chronic and acute injuries. Chronic fractures and complex perilunate dislocations were excluded from the classification. Type one fractures were those of the extra-articular tubercle. The authors described tubercle fractures as harmless, never posing any problems, and recommended cast immobilisation for three weeks. Consequently, they excluded tubercle fracture from their treatment and outcome analysis. Type two fractures were intra-articular. Intra-articular fractures were further classified based on the fracture location and the fracture type (Table 5.2). The correlation between fracture location and fracture type was limited to some pertinent observations. Transverse fractures were predominately observed in the middle and central thirds of the scaphoid. Only a small proportion of these were comminuted. The distribution of horizontal oblique fracture was grouped around the central third of the scaphoid. The middle and peripheral thirds showed similar rates of horizontal oblique and transverse types. The vertical oblique fracture was uncommonly observed in the central third.

Table 5.1: Classification of acute, intra-articular scaphoid fractures, adapted from Böhler and colleagues (Böhler et al., 1954)

<i>Classification basis</i>	<i>Class</i>	<i>Frequency</i>
<i>Fracture location</i>	Central third	11%
	Middle/central third	8%
	Middle third	65%
	Middle third with a comminuted wedge fragment	5%
	Peripheral third	11%
	<i>Fracture type</i>	Horizontal oblique
	Transverse	50%
	Vertical oblique	3%

Russe adapted Böhler’s classification in 1960 by simplifying the fracture location subtypes (Russe, 1960). He divided fracture location into three groups: proximal, middle and distal third. The technical aspects of how to divide the scaphoid into thirds were not specified. No alterations to the fracture types were made.

McLaughlin and Parkes introduced the concept of fracture stability (McLaughlin and Parkes 2nd, 1969). In an observational study of 19 patients, three categories or classes of fractures were identified. Class A fractures were incomplete fractures. Class B fractures propagated along the entire width of the scaphoid, not involving its entire circumference. Both class A and B fractures were considered stable. Class C fractures showed displacement and were, consequently, characterised as unstable. With regards to displacement quantification, the authors noted: “The amount of displacement is of secondary importance to the fact that any displacement indicates an unstable fracture”. Some years later, Cooney and colleagues expanded on the definitions of stability and

displacement (Cooney et al., 1980). Undisplaced fractures or those with intact peri-ostial structures were regarded as stable. Fractures with dorsal opening, but an intact volar peri-ostial hinge were also viewed as stable. In contrast, unstable fractures demonstrated displacement of more than 1mm on either AP or oblique radiographs. In addition, any signs of carpal instability, namely DISI, altered the fracture unstable. Carpal instability was assessed on lateral radiographs. A lunocapitate angle of >15 or a scapholunate angle of >45 was chosen as cut-offs for instability. More recently, the relationship of fracture morphology to surrounding ligamentous structures was proposed in the assessment of stability (Garcia-Elias and Lluch, 2001, Moritomo et al., 2008).

Herbert and Fisher combined Böhler's classification of fracture location and orientation with the concepts of fracture instability into a new systematic description of fractures (Herbert and Fisher, 1984). Herbert later modified his classification system to exclude uncommon fractures (Figure 6.0) (Filan and Herbert, 1996).

Type A
Stable acute

A1 - Tubercle



A1 - Incomplete

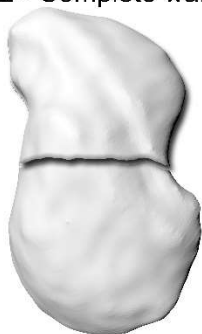


Type B
Unstable acute

B1 - Distal oblique



B2 - Complete waist



B3 - Proximal Pole



B4 - Perilunate

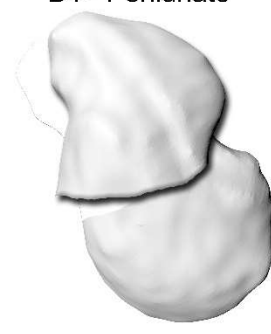


Figure 6.0: Herbert and Fisher's classification system of acute scaphoid fractures (adapted from (Herbert and Fisher, 1984))

Further developments in scaphoid fracture assessment and description were made with the use of CT. Varying scaphoid morphology as well as its radial convexity and ulnar concavity made accurate assessment challenging. Furthermore, early CT scans only allowed the scanned plane to be assessed. Orthogonal planes required additional scans to be performed and had to be examined separately. Sanders pioneered accurate CT assessment of the scaphoid by utilising the longitudinal scaphoid axis (Sanders, 1988). The longitudinal axis of the scaphoid is approximated by the longitudinal axis of the fully extended thumb. A scout image confirms the desired plane and changes to the hand position can be made before the scan is commenced. As CT technology evolved, scanning along the longitudinal axis of the scaphoid became obsolete. Fine-slice CTs allowed for multiplanar reconstructions (MPR) in any plane from the original axial data set. During this time of evolution, assessment of the three-dimensional scaphoid fracture patterns continued to advance. Compson, for example, correlated plain radiography to the three-dimensional fracture morphology (Compson, 1998). He examined 91 scaphoid fractures on plain radiographs and transcribed fractures onto representative methyl methacrylate scaphoid models. Ten scaphoid models were used in anticipation of considerable morphological variability. Compson noted tubercle fractures to be difficult to trace and, consequently, excluded those. Additionally, in eleven out of 91 cases, fractures could not be accurately transferred onto a model as they were either incomplete or appeared united on some of the available radiographic views. He identified three fracture types: surgical waist, dorsal sulcus and proximal pole. He sub-divided the dorsal sulcus fracture into three variants, depending on associated comminution, but noted challenges in accurately locating comminuted fragments. With the availability of the 3D CT, fracture assessment and reduction could be done at a workstation. The focus shifted from fracture classification to identification of nuances not previously identified by plain radiography or two-dimensional CT. Luria and colleagues examined the fracture plane orientation in 124 acute scaphoid fractures (Luria et al., 2015). Angles subtended between the

fracture plane and the longitudinal scaphoid axis were assessed. The average angle for waist fractures was found to be 56°. Consequently, contrary to earlier classification systems, the authors concluded that most waist fractures were horizontal oblique rather than transverse. Similarly, Schwarcz and colleagues studied fracture displacement patterns in 3D (Schwarcz et al., 2017). The premise that the distal fragment undergoes pronation, flexion and ulnar deviation was investigated. With the aid of a computer coordinate system, the proximal and distal fracture fragments were marked and examined in relation to the radius. The authors found that the proximal fragment displaced into extension, supination and volar translation while the distal fragment was anchored to the trapezium and demonstrated no movement.

Study V - Scaphoid Fracture Mapping – a 3D Computed Tomography Analysis^{##}

Arthur Turow^{1,2} and Anne Eva Bulstra^{1,3}; Miriam Oldhoff⁴; Batur Hayat^{1,3}; Job Doornberg^{1,2,3}; John White^{1,2}; Ruurd L. Jaarsma^{1,2}; Gregory I. Bain^{1,2}

¹Flinders University of South Australia, Adelaide, Australia

² Department of Orthopaedic Surgery, Flinders Medical Centre, Adelaide, Australia

³ University of Amsterdam, Amsterdam UMC, Amsterdam, the Netherlands

⁴ Delft University of Technology, Delft, the Netherlands

Abstract

Background. Scaphoid fractures have traditionally been described using plain radiography.

The aim of this study was to characterise acute scaphoid fracture morphology using three-dimensional CT.

Methods & Materials. A retrospective, multicentre database search was performed to identify CT studies of acute scaphoid fractures. CT scans of scaphoid fractures less than six weeks from time of injury were included in this retrospective, multicentre study. CTs were segmented and converted into three-dimensional models. Following virtual fracture reduction, fractures were mapped onto a three-dimensional scaphoid model.

Results. Seventy-five CT scans were included. The median delay from injury to CT was 29 days. Most studies were in male patients (89%). Most fractures were comminuted (52%) or displaced (64%). 73% of displaced fractures had concomitant comminution. Waist fractures had higher rates of comminution and displacement when compared to all other fractures. Comminution was located along the dorsal ridge and the volar scaphoid waist.

Conclusion. Treatment of waist fractures should include careful examination of these anatomical areas. Inspection of the three-dimensional anatomy of the fracture plane, concurrent comminution and direction of displacement can be a valuable tool in scaphoid fracture management.

Introduction

Scaphoid fractures have traditionally been described on plain radiography. From the first description of the scaphoid fracture in 1925 by Destot (Destot, 1925), various classification systems have been developed (Ten Berg et al., 2016). The most commonly used classification systems are Herbert (Herbert and Fisher, 1984), Mayo (Cooney et al., 1980) and Russe (Russe, 1960). They take fracture location, stability and chronicity into consideration; however, given the heterogeneity of fracture patterns, accurate fracture description remains challenging.

The scaphoid shows considerable size and shape variation (Ceri et al., 2004) and has complex kinematics (Craig and Stanley, 1995, Garcia-Elias et al., 1995). Consequently, despite being the preferred initial imaging modality in suspected scaphoid fractures (Shenoy et al., 2007), plain radiography has limitations in fracture description and diagnosis (Tiel-van Buul et al., 1992, Hunter et al., 1997). The correlation between fracture characteristics and clinical outcomes has been well established (Amirfeyz et al., 2011, Eastley et al., 2013, Grewal et al., 2013). Accurate fracture description is, therefore, paramount in management choice and operative planning.

There has been a paucity of studies investigating acute scaphoid fracture morphology. A recent computerised 3-dimensional analysis examined acute scaphoid fractures and found that most waist fractures were horizontal oblique, rather than transverse (Luria et al., 2015), which is contrary to previous reports that this fracture pattern is uncommon (Green and Wolfe, 2011, Slutsky and Slade, 2011). Scaphoid fracture comminution has been shown to exist in certain fracture types (Compson, 1998). Comminution has been associated with fracture instability, longer time to union and higher rates of non-union (Clementson et al., 2015, Buijze et al., 2012, Grewal et al., 2016). However, literature about comminution patterns in various fracture types has been lacking. Furthermore, despite 3D CT being known for increased reliability in fracture evaluation (Hu et al., 2009), only a limited number of studies has investigated the scaphoid fracture in 3D. The aims of this study were to describe acute fracture morphology, to map these fractures onto a 3D scaphoid model and to correlate this to scaphoid anatomy.

Material and methods

In this multicentre, retrospective study, scaphoid fractures investigated with a CT scan between 2008 and 2018 were examined. CT scans underwent initial assessment for comminution and displacement. Subsequently, CTs were segmented, 3D models prepared and virtually reduced. Fractures were mapped onto an intact scaphoid model and fracture patterns and comminution were assessed.

Subjects

CT scans of adult patients (≥ 18 years) presenting with a scaphoid fracture were reviewed. CT scans within six weeks of the index injury were included. Patients that had pre-existing scaphoid pathology, such as previously documented scaphoid trauma, were excluded. Only CT scans of adequate quality were considered for further 3D analysis. The parameters included slice thickness of at most 1mm on axial imaging, no motion artefact and complete visualization of the scaphoid and all its articulations. A previously published grading system for high resolution peripheral computed tomography was utilised (Pialat et al., 2012). Only grade one (no motion artefact) or grade two scans (minor motion artefact) were included for analysis. Seventy-five patients were included for analysis. Age, sex, concurrent carpal or wrist fractures and scan delay following injury were recorded.

Initial CT assessment

Axial imaging was reviewed together with MPR in the coronal and sagittal planes. The following criteria for bone fracture on CT were used: (1) a step in the cortex, (2) cortical discontinuity, (3) any displacement or comminution of bone fragments. All CT scans were assessed by the two primary investigators (A.T and A.B.) and any discrepancies were re-assessed and referenced with the associated report by the radiology consultant. Particular care was taken to assess trabecular discontinuity without any cortical disruption, as this CT pattern is frequently associated with nutrient vessels (Davies et al., 2011). Comminution was defined as more than two fracture fragments or two

fracture fragments with signs of impaction. A fracture was considered displaced if it was translated $\geq 1\text{mm}$ in any plane. This was based on previous radiographic scaphoid assessment (Temple et al., 2005) and clinical observations that scaphoid fractures with more than 1mm displacement have a higher non-union rate and require early, surgical fixation (Cooney et al., 1988).

Displacement was measured for each scaphoid with two separate MPR protocols using the Radiant DICOM Viewer™ (Version 4.6.9; Poznań, Poland). First, source axial images underwent coronal and sagittal multiplanar reconstructions. The longitudinal axis of the radius as well as a line from the radial to the ulnar styloid were used as reference. In cases where scans were not performed in a fully pronated, neutral wrist position, MPR were orientated from a line perpendicular to the deepest part of the sigmoid notch, bisecting the radial styloid. A second assessment was performed with MPR in the central, longitudinal axis of the scaphoid as described by Sanders (Sanders, 1988).

CT segmentation

Included CT scans were retrieved through PACS. De-identified scans were exported in the Digital Imaging and Communication in Medicine (DICOM) format and loaded into 3D Slicer (Version 4.8.1; Boston, MA, USA). All scaphoid fragments were manually segmented using the Threshold and Paint tools. Criteria from the initial CT assessment were carried over to the segmentation process. Additionally, a fracture fragment was defined separate from another fragment, when fracture lines were visible and continuous in all three planes. Incomplete fractures were defined as cases where fracture lines faded into normal trabecular bone without continuity to the nearest cortex. Comminuted fragments were segmented separately. Impacted fragments were identified in locations where there was sharp increase in density, not consistent with normal, surrounding, trabecular bone. It was not possible to segment impaction due to bone continuity with at least one of the fracture fragments. Segmentations were reviewed by three investigators (A.T., A.B. and M.O.). Any discrepancies were re-assessed and changes to segmentation made accordingly.

Three-dimensional model preparation

The data from 3D Slicer was exported into Rhinoceros™ (Version 5.4.2; McNeel, Seattle, WA, USA) in a stereolithography (STL) format. All fractures were re-assessed in 3D. In order to facilitate fracture mapping, the fragments were virtually reduced via translation and angulation of the fragments. Reductions were assessed according to pre-defined anatomical landmarks. A reduction was deemed anatomical when the following anatomical aspects of the scaphoid were restored: (1) concavity of the capitate fossa; (2) concavity of the radial and ulnar aspects of the scaphoid waist; (3) convexity of the radial and ulnar aspects of the proximal and distal poles; (4) alignment of the dorsal ridge. Comminuted fragments were measured and assessed by three separate authors (A.T, A.B. & J.W.). Fragments less than 2mm were excluded from further assessment. Fragments larger than 2mm were reduced into the corresponding cortical void after the major fragments were reduced. Impacted bone fragments were reduced. Consequently, care was taken to restore scaphoid length and rotation without resulting in excessive interfragmentary flexion.

Model alignment

The reduced scaphoid fragments were aligned to a standard scaphoid 3D template. This scaphoid template was segmented with 3D Slicer and imported into Artec Studio™ (version 3.5, Autodesk, Inc). All left-sided scaphoid models were mirrored using Meshmixer™ (version 3.5, Autodesk, Inc) and each scaphoid subsequently imported into Artec Studio™. Each fractured scaphoid was aligned onto the scaphoid template in two sequential steps. First, six anatomical landmarks, as described by Schwarcz and colleagues (Schwarcz et al., 2017), were marked on both the template and the fractured model. Second, the non-rigid Mesh Alignment Tool was used to calculate the best fit of the fractured scaphoid mesh and the template scaphoid mesh. Correct alignment was verified by two authors (A.T and A.B.). Any discrepancies were re-assessed, and alignment re-adjusted to ensure best fit. Only correctly

reduced 3D models would allow for the six anatomical landmarks to align correctly. Hence, correct alignment was also used as a secondary checkpoint for the virtual fracture reduction performed earlier.

Fracture mapping

After successful model alignment, assessment was continued in Rhinoceros™. The template was rotated 45° along its longitudinal axis, creating eight standardised viewpoints to allow for reproducible and accurate fracture line mapping across all fractured scaphoids. Direct face-on views of the distal and proximal articulating surfaces were also added in anticipation of any scaphoid tubercle or scapholunate ligament avulsion fractures. Fracture lines were then transposed from the fractured scaphoid onto the scaphoid template. Where there was any opening of the fracture, the lines were drawn at the halfway point between the fracture fragments. Any impaction or comminution was marked separately.

The main fracture patterns were defined based on the dorsal ridge as viewed from the radial aspect of the scaphoid (Figure 6.1 and 6.2). The dorsal ridge was chosen for fracture description from preliminary mapping analysis. This demonstrated fracture grouping based on the dorsal ridge. In contrast, fracture patterns of the volar scaphoid as well as the capitate fossa did not display any defining features. Preliminary analysis also showed angular difference between fractures involving the dorsal ridge. Fracture lines that followed the dorsal ridge closely were near parallel to the ridge. Angles measured between the ridge axis and the fracture lines were less than 30°. In contrast, fractures with a short path through the dorsal ridge were more obtuse with angles measuring 50° and more.

Fractures passing proximal to the dorsal ridge, were defined as proximal pole fractures. Fractures crossing the dorsal ridge were defined as waist fractures. Waist fractures were sub-classified further based on their angular morphology. For each fracture line, a line of best fit between the most radial

and ulnar extents was drawn. Angles between this line and the longitudinal axis of the dorsal ridge were measured. Transverse waist types were defined as those that subtended angles of more than 30° and oblique fractures less than or equal to 30° (Figure 6.3). Involvement of the most dorsal and ulnar non-articulating part of the scaphoid, the scaphoid apex (Moritomo et al., 2008), was noted. The dorsal scapholunate ligament and part of the dorsal intercarpal ligament attach to the scaphoid apex (Oka et al., 2005a). It has been proposed that fractures passing proximal to the scaphoid apex are associated with carpal instability (Moritomo et al., 2008). Fractures distal to the transverse ridge were defined as distal pole and tubercle fractures. These distal fractures were divided further into intra- and extra-articular based on the classification by Prosser et al. (Prosser et al., 1988). Articular anatomy was adapted from previous morphological work (Fogg, 2004) and transcribed onto the scaphoid 3D model (Figure 6.1).

Incomplete fractures showed cortical discontinuity only on one aspect of the scaphoid with the fracture line fading within the trabecular bone. In cases with three or more dominant fracture fragments, the fracture was classified as segmental.

Statistical Analysis

Categorical variables were examined using Fisher's exact test and continuous variables were compared by analysis of variance (ANOVA). To determine predictors of fracture type, univariate analysis was performed on comminution, fracture displacement and presence of concurrent wrist injuries. Waist fractures were examined separately to compare their obliquity with reference to the dorsal ridge axis. Angles subtended were assessed using the independent sample t-test. A p-value of <0.05 was considered statistically significant.

Results

Seventy-five CT scans fulfilled the inclusion criteria (Table 6.2; Figure 6.4 and 6.5). The mean age was 36 years (range 18-84). The majority of fractures were seen in males (n=66, 88%). The fractures

involved the left (n=39, 52%) and right (n=36, 48%) wrists. The mean delay from injury to CT was 12 days (range 0-42).

Proximal pole

There were seven proximal pole fractures (9%; Figure 6.7). One fracture was displaced, and one had comminution. All fractures showed similar patterns. Radially, the fractures passed obliquely from the proximal/dorsal to the distal/volar border. The scaphoid apex was spared in all cases (Figure 6). At the dorsal border, fractures appeared to either be proximal to the dorsal scapholunate ligament (dSLL) footprint or to be extending directly into its attachment. The only case with comminution had a small fragment just proximal to the scaphoid apex, likely representing an avulsion of the dSLL. On the volar aspect, the fractures continued a more distal path, approaching the scaphoid waist. Proximal pole fractures ran obliquely across the capitate fossa between the palmar scapholunate ligament (pSLL) and the dSLL. On the volar aspect, most fractures (n=5, 71%) involved the pSLL, with the remainder exiting through an area between the RSC and the pSLL. With the exception of this dSLL and pSLL involvement, proximal pole fractures were purely intra-articular. None of the fractures involved the proximal capitate ridge.

Waist Fractures

Most scaphoid fractures had their dominant fracture line at the waist (n=51, 69.3%). With respect to the dorsal ridge axis, oblique waist fractures (n=24; 32%) subtended an average angle of 15.4° (range 6-28°) and transverse fractures (n=28; 37%) an average angle of 51.1° (range 30-77°).

Transverse

Dorsally, transverse fractures were confined to the proximal half of the dorsal ridge (Figure 6.6). They were aggregated around the dorsal concavity, with 29% (n=8) involving the scaphoid apex. This was mirrored on the volar side, with fractures exiting between the widest part of the proximal

scaphoid and the most concave waist. Fractures were uniformly distributed around the waist of the scaphoid. The capitate fossa was fractured at its middle with sparing of the proximal capitate ridge. Comminution was present in 54% (n=15) of cases. The capitate fossa showed comminution in a transverse direction, similar to the overall fracture morphology (Figure 6.8).

Oblique

Oblique waist fractures involved almost the entire dorsal ridge (Figure 6.6). Most oblique waist fractures involved the scaphoid apex (n=18, 78%). Dorsally, oblique waist fractures showed to be more distal than their transverse counterparts, extending into the distal pole. Fracture morphology was similar across the capitate fossa when compared to transverse waist fractures. It was not possible to make clear distinctions between the two waist types in this region. Comminution was present in 70% (n=16) of cases and this was largely located dorsally. Comminuted fragments tended to be large at 6-10mm and spanned most of the dorsal ridge. Comminution across the capitate fossa followed a more oblique pattern and was more frequent than in transverse types (Figure 6.9).

Distal Pole

Nine distal pole fractures were identified (12%). Only one fracture ran transversely across the widest portion of the distal pole. In this case, dorsal and ulnar comminution was present. The remainder of fractures involved the tubercle. Of those, 25% (n=2) were extra-articular and 75% (n=6) were intra-articular. All intra-articular fractures involved the radial half of the STTJ. Larger articular fragments were associated with comminution and fracture displacement (Figure 6.10). Distal fragment size was on average 3.5mm for extra-articular and 8.2mm for intra-articular tubercle fractures.

Incomplete

Three incomplete fractures were included. Two were traversing across the narrowest part of the scaphoid waist. Their dorsal and volar morphology approximated that of transverse waist fractures.

One incomplete fracture followed the dorsal ridge as was seen in oblique waist fractures. No comminution or displacement was present.

Segmental

Segmental fractures represented 7% of all examined fractures (n=5). All were displaced.

Comminution spanned the entire dorsal ridge across the waist and distal pole of the scaphoid. The capitate fossa demonstrated fracture morphology similar to waist fractures. None of the segmental fractures involved the proximal pole. The proximal capitate ridge and the lunate articular surface that articulated with the lunate remained spared, just like in waist and proximal pole fractures.

Displacement

More than half of fractures were displaced (n=48, 64%). All segmental fractures were displaced; however, due to small numbers in this subgroup, this did not reach statistical significance when comparing to all other fracture types (p=0.153). There was a strong correlation between displacement and comminution (p<0.001; Figures 11 and 12), with 90% of comminuted fractures being displaced. Transverse waist fractures were more frequently displaced (n=22, 79%) than were oblique waist fractures (n=15, 65%). Transverse waist fractures showed the highest rate of displacement amongst any fracture type (p=0.042). In comparison, proximal pole fractures were less likely to be displaced when comparing to other fracture types (29%, p=0.040). Three displaced tubercle fractures (38%) were identified. Their comparative displacement rates were similar to other fracture types (p=0.128).

Comminution

Fifty-two percent of fractures were comminuted. Transverse and oblique waist fractures showed comparable comminution rates (39% and 41%, respectively). However, oblique waist fractures

demonstrated higher rates of comminution (70%) when comparing to other fracture types (44%, $p=0.043$). Higher rates of comminution were also observed when grouping all waist fractures together (61%, $p=0.026$). In contrast, proximal pole fractures were less comminuted (14%, $p=0.042$). Similarly, the rate of comminution in tubercle fractures (13%) was significantly lower when comparing to other fracture types (57%, $p=0.025$).

Scaphoid comminution did not appear to be random but was localised to specific anatomical areas of the scaphoid (Figure 6.13). Radially, comminution was highest along the proximal half of the dorsal ridge. This was in-line with the axis of the ridge and extended into the scaphoid apex. The DIC finds attachment to the proximal ridge and, in part, to the scaphoid apex. On the ulnar aspect, comminution was aggregated between the attachments of the RSC ligament and the pSLL. Comminution was distributed at near right angles to the longitudinal axis of the scaphoid. The highest rate of comminution was seen at the isthmus of the scaphoid waist. The narrowest part of the scaphoid corresponds to an area of inflection. At this point, the relatively shallow concavity of the waist tapers into a sharp convexity as the waist transitions into the distal pole.

Concurrent Fractures

Almost half of all scaphoid fractures had an associated wrist injury (45%). In ten cases, a scaphoid fracture was present as part of a greater arc, perilunate dislocation. Subgroup analysis showed that a greater percentage of segmental fractures (40%) were associated with a perilunate dislocation than proximal pole (33%), oblique waist (13%) or transverse (11%) fractures; however, concurrent fractures were not significantly associated with a particular fracture type ($p=0.613$).

Discussion

One of the first scaphoid studies to look at 3D fracture morphology came from Compson who combined plain radiography with anatomical landmarks (Compson, 1998). The author chose ten representative methyl methacrylate scaphoid models and transcribed 91 acute scaphoid fracture onto these models. He excluded tubercle fractures due to technical difficulties of tracing these fractures and was unable to determine the fracture pattern in 11 out of the 91 cases. For the remainder, he found three main fracture types: dorsal sulcus, surgical waist and proximal pole. He made attempts at including comminution in his study but noted that classifying scaphoid fractures in three dimensions to be challenging. Nakamura and colleagues expanded on this concept and studied 3D CT scaphoid fracture anatomy (Nakamura et al., 1991). The authors examined fracture displacement in largely sub-acute and chronic cases. They found the distal fragment to be translated either dorsal or volar onto the proximal fragment. A more recent study on three-dimensional fracture displacement found that translation occurs at the proximal fragment (Schwarcz et al., 2017). The authors utilised a computer coordinate system with anatomical markers on the distal and proximal scaphoid fragments as well as the distal radius. They showed the proximal fragment to undergo extension, supination and volar translation in relation to the distal radius. In contrast, the distal fragment demonstrated no movement.

There has been a paucity of studies investigating acute fracture morphology with CT. Luria and colleagues examined 124 acute scaphoid fractures (Luria et al., 2015). Following virtual reduction, angles subtended between the fracture plane and the longitudinal axis of the scaphoid, as determined by a principle component analysis algorithm, were measured. The authors found waist fractures to be oriented on average 56° from the scaphoid axis. They concluded that most waist fractures were horizontal oblique rather than transverse. Garala and Dias (Garala and Dias, 2019) utilised CT in a study adapted from the early work done by Compson (Compson, 1998). The authors examined 379 acute scaphoid fractures and superimposed a 3-dimensional scaphoid model onto plain radiography images. They demonstrated waist fractures to be oriented on average 63° to the

scaphoid axis; confirming obliquity of waist fractures. Our study confirmed a spectrum of waist fractures ranging from transverse and oblique types. Furthermore, it is the first study to correlate 3D morphology of acute scaphoid fractures to displacement and comminution.

Proximal pole fractures are traditionally regarded as challenging to treat, unstable and with a high risk of non-union (Trumble and Vo, 2001). Our results demonstrate that acute proximal pole fractures are undisplaced and have low rates of comminution. The only comminution was seen proximal to the scaphoid apex, likely representing a dorsal scapholunate ligament (dSLL) avulsion. Dorsally, fractures involved the proximal extent of the dSLL attachment and followed the distal extent of the proximal articulating surface. On the volar aspect, proximal pole fracture ran either through or just distal to the palmar scapholunate ligament (pSLL) attachment. Low rates of displacement could be explained by fractures running between the attachments of the dSLL and pSLL. Fibres of the corresponding SLL would lie on either side of the fracture and could aid in preventing proximal pole extension relative to the distal fragment. The proximal pole is mostly articular and is known to have the thickest trabeculae of the entire scaphoid (Su-Bum et al., 2012). As a fracture would propagate through the proximal pole, a single fracture line is created. The bordering thick trabeculae would prevent secondary fracture propagation.

In contrast to proximal pole fractures, waist fractures had the highest rates of comminution and displacement of any fracture type. This is consistent with the pathomechanisms resulting in scaphoid waist fractures. Most commonly, the scaphoid fractures with wrist extension and concurrent axial loading (Weber and Chao, 1978). Axial loading of a neutral wrist or forced hyperextension of an unloaded wrist can also result in a scaphoid waist fracture (Green and Rayan, 1997, Horii et al., 1994). As the scaphoid is locked between the capitate and the distal radius, the degree of ulnar or radial wrist deviation can determine the resultant fracture morphology (Apergis and SpringerLink, 2013). The ensuing forces on the scaphoid create a volar tension and a dorsal compression side. Dorsal compression results in comminution. With wrist mobility, extension of the lunate and the

proximal scaphoid fragment occurs (Schwarcz et al., 2017). This can result in volar collapse and further comminution, producing a humpback deformity in the chronic setting. The sequelae of volar collapse, in particular volar bone loss, have been confirmed by quantitative and qualitative 3D CT (Oka et al., 2005b). Our study confirms these initial observations and aids in identification of areas with high rates of comminution.

In our study, comminution was predominantly localised to dorsal ridge. The DIC and the dorsal capsule attach at the proximal dorsal ridge (Green and Wolfe, 2011). The DIC can have different insertion patterns depending on the dorsal ridge morphology (Fogg, 2004). In a rotating scaphoid (type 1), the DIC bypasses the dorsal ridge and finds attachment near the scaphotrapeziotrapezoid joint. During an injury of a type 1 scaphoid, the DIC can act a fulcrum over which the dorsal scaphoid extends, causing depression and comminution of the entire dorsal ridge. In a flexing scaphoid (type 2), the DIC inserts directly onto the proximal crest. As a type 2 scaphoid fractures, the DIC acts as the dorsal check for the capitate (Green and Wolfe, 2011). During injury, hyperextension is followed by scaphoid flexion resulting in tensioning of the DIC. This causes avulsion of its attachment at proximal dorsal ridge only (Figure 6.14).

Volarly, comminution was localised between the RSC and the pSLL. The RSC lies on the volar concavity of the scaphoid waist, acting as a fulcrum around which the scaphoid rotates (Green and Wolfe, 2011). Volar comminution was aggregated at this concavity, representing the scaphoid isthmus (Figure 6.15). Comminution was at near right angles to the longitudinal axis of the scaphoid. Most fractures were located either at the attachment of the pSLL or just distal to it. The RSC was spared in the majority of fractures. Only a few fractures extended more proximally into the membranous SLL or more distally into the attachment of the RSC. Comminution and its orientation in this area can be explained by (1) the direction of the RSC in this area, (2) the scaphoid pivoting over the RSC during flexion and (3) by an abrupt change in cortical thickness at the waist (Su-Bum et al., 2012).

Some areas of the scaphoid were observed to be either protected against fracturing or experienced low rates of displacement and comminution. The distal pole was one of those areas. The distal scaphoid is stabilised by strong volar ligaments: two limbs of the scapho-trapezium-trapezoid ligament, the scapho-capitate ligament and the capitate-trapezium ligament. This anchors the distal pole between the trapezium-trapezoid complex and the capitate, shielding it from the forces experienced during an injury. This is reflected by the low frequency of distal pole fractures (12%), a finding that has been observed by previous epidemiological work (Russe, 1960).

There were no fractures that involved the proximal ridge of the capitate fossa. The osseous microarchitecture in this area is likely the reason for this finding. The proximal pole is widest in this part of the scaphoid. Su-Bum and colleagues examined the trabecular structure and bone density of the scaphoid using micro-CT (Su-Bum et al., 2012). The authors found the proximal capitate fossa to have the highest bone mineral density and the largest number of trabeculae of the entire scaphoid.

Scaphoid fractures are known to have concurrent injuries of the carpus as well as the distal radius and ulna. Leslie and colleagues reported that 12.5% of their 247 scaphoid fractures had an associated injury (Leslie and Dickson, 1981). We observed associated fractures in 45% (n=34) of cases. Our cohort is likely corresponding to patient presenting with higher energy injuries, resulting in a higher rate of concurrent fractures.

The limitations of this study include sampling bias and the retrospective nature of this review. Most of the CT exams obtained for this cohort came from a level one trauma centre. Consequently, fracture types associated with high energy injuries are likely overrepresented. Transcription of fracture lines onto a representative scaphoid model is another limitation of this study. However, throughout this laborious aspect of the study, great care was taken to ensure accuracy of transcription. This was performed by two assessors, any differences were re-assessed and, hence, imprecisions avoided.

Our study is the first of its kind to investigate acute scaphoid fracture morphology using 3D CT. It is also the first study to examine scaphoid fracture comminution and to correlate this to displacement and fracture type. Furthermore, we have shown waist fractures to have high rates of comminution and displacement. Hence, treatment of waist fractures, should include careful examination of the dorsal ridge and the volar waist for comminution. Finally, with modern CT scanners and imaging software, automated 3D reconstruction has become easily accessible. Inspection of the 3D anatomy of the fracture plane, concurrent comminution and direction of displacement can be a valuable tool in scaphoid fracture management.

Figures

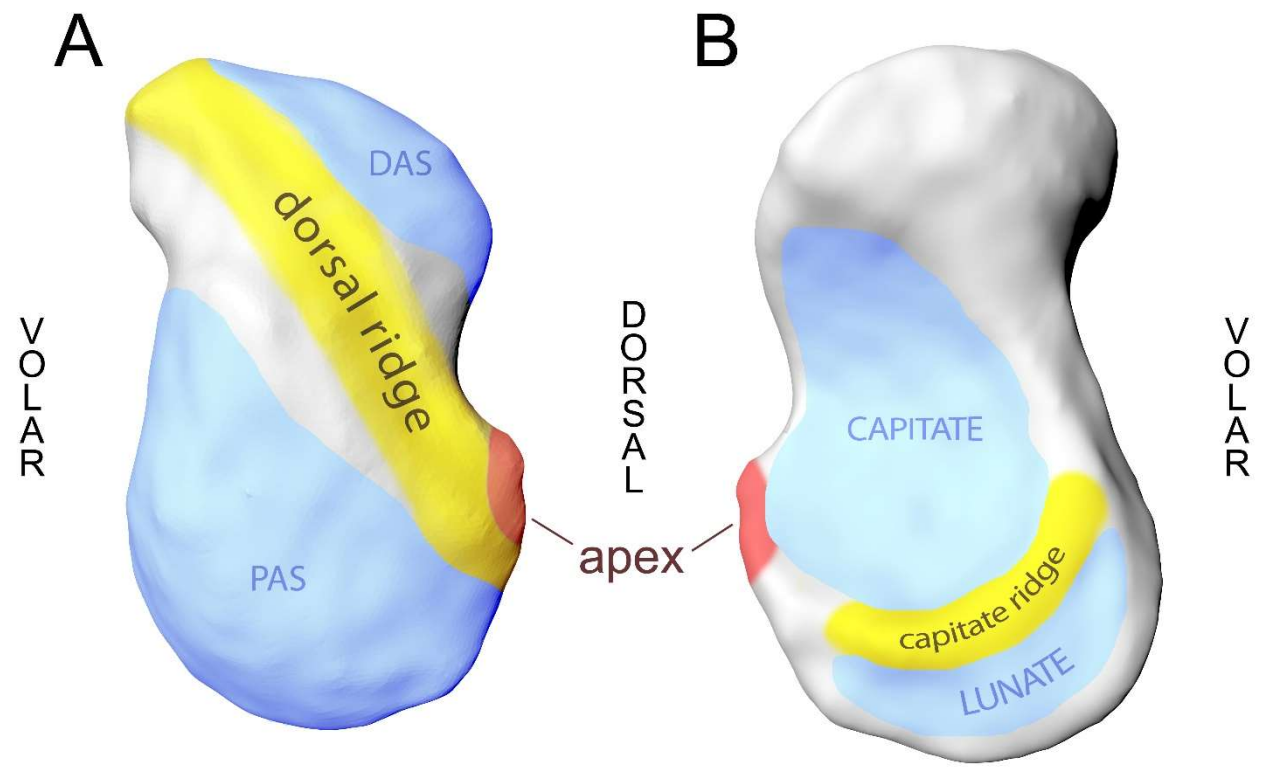


Figure 6.1: Scaphoid templates with anatomical areas as seen from the radial (A) and ulnar (B) views. Articular surfaces were adapted from Fogg (Fogg, 2004) and are marked *blue*. DAS: Distal articular surface; PAS: Proximal articular surface

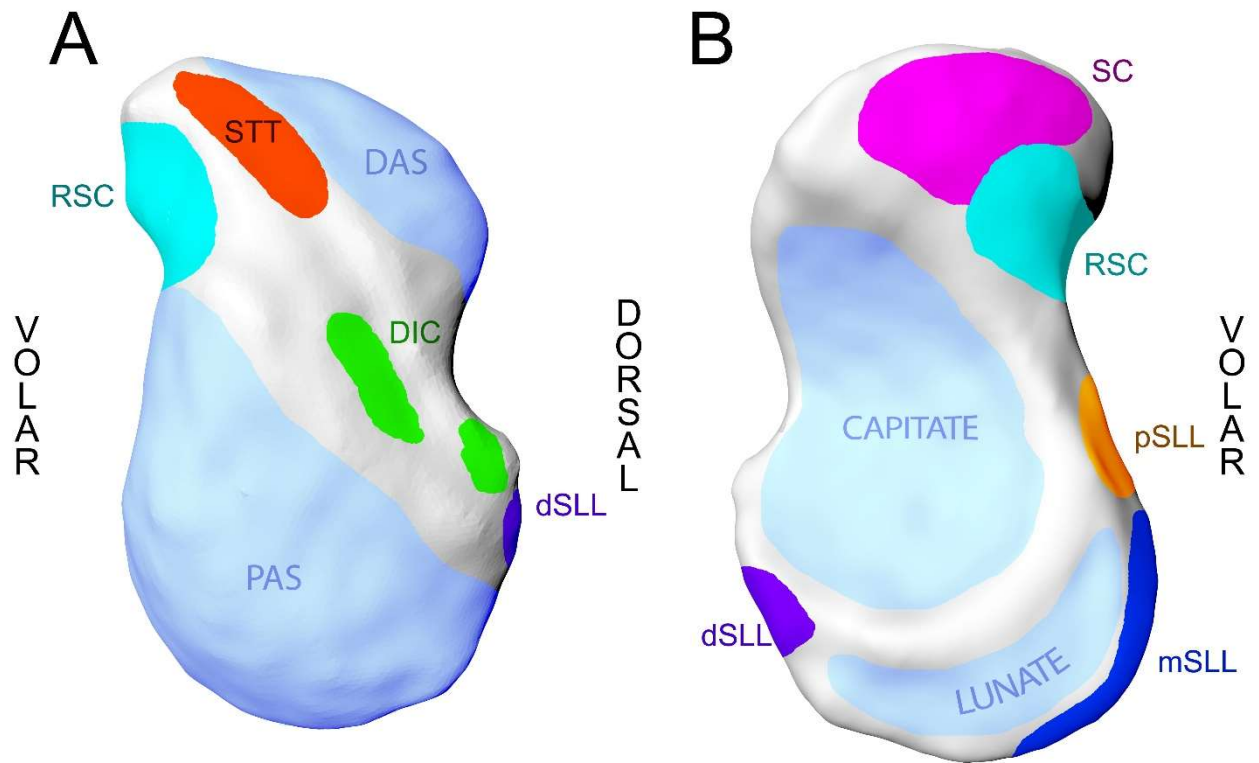


Figure 6.2: Ligament attachments from the radial (A) and ulnar (B) views used for fracture description. Adapted from Fogg (Fogg, 2004) and Kijima et al. (Kijima and Viegas, 2009). Articular surfaces are marked *blue*. DAS: Distal articular surface; PAS: Proximal articular surface; STT – scaphotrapezotrapezoid ligament complex; RSC – radioscaphocapitate ligament; DIC – dorsal intercarpal ligament; SC – scaphocapitate ligament; dSLL, mSLL, pSLL – dorsal, membranous and palmar scapholunate ligaments

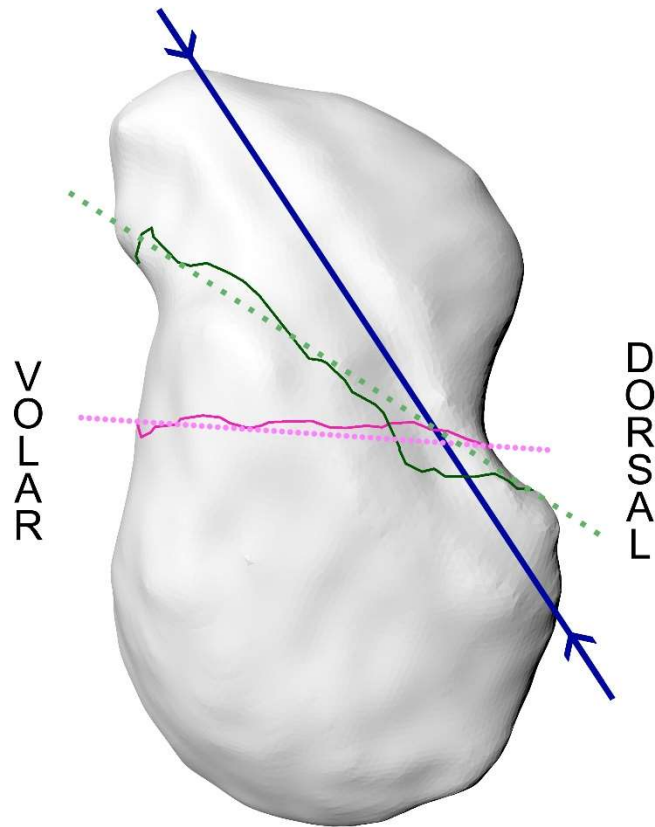


Figure 6.3: Angular assessment of waist fractures. A representative transverse waist fracture (*red*) and its line of best fit (*dotted red*) as well as an oblique waist fracture (*green*) with its line of best fit (*dotted green*) are shown. Angular measurements were made against the dorsal ridge axis (*blue*).

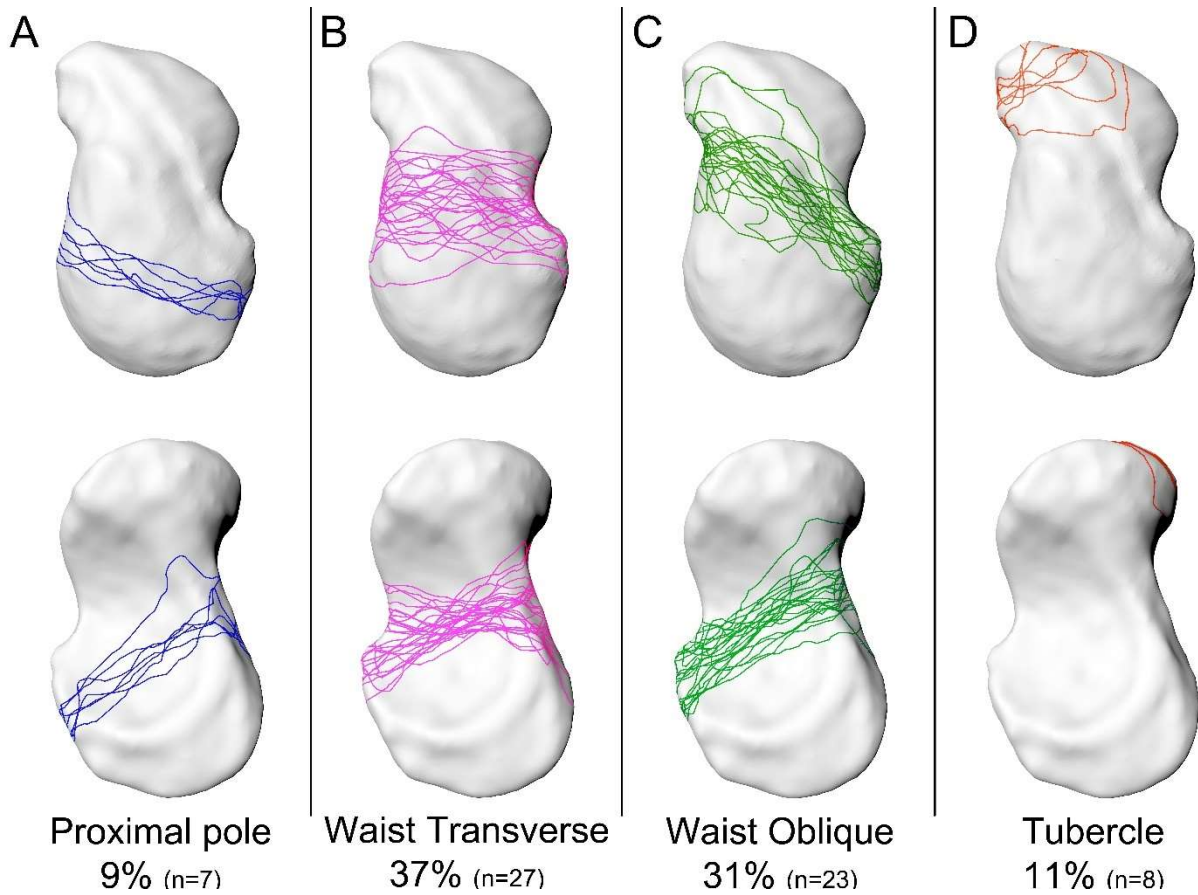


Figure 6.4: The four main fracture types. Fractures shown from the radial (top row) and the ulnar (bottom row) views.

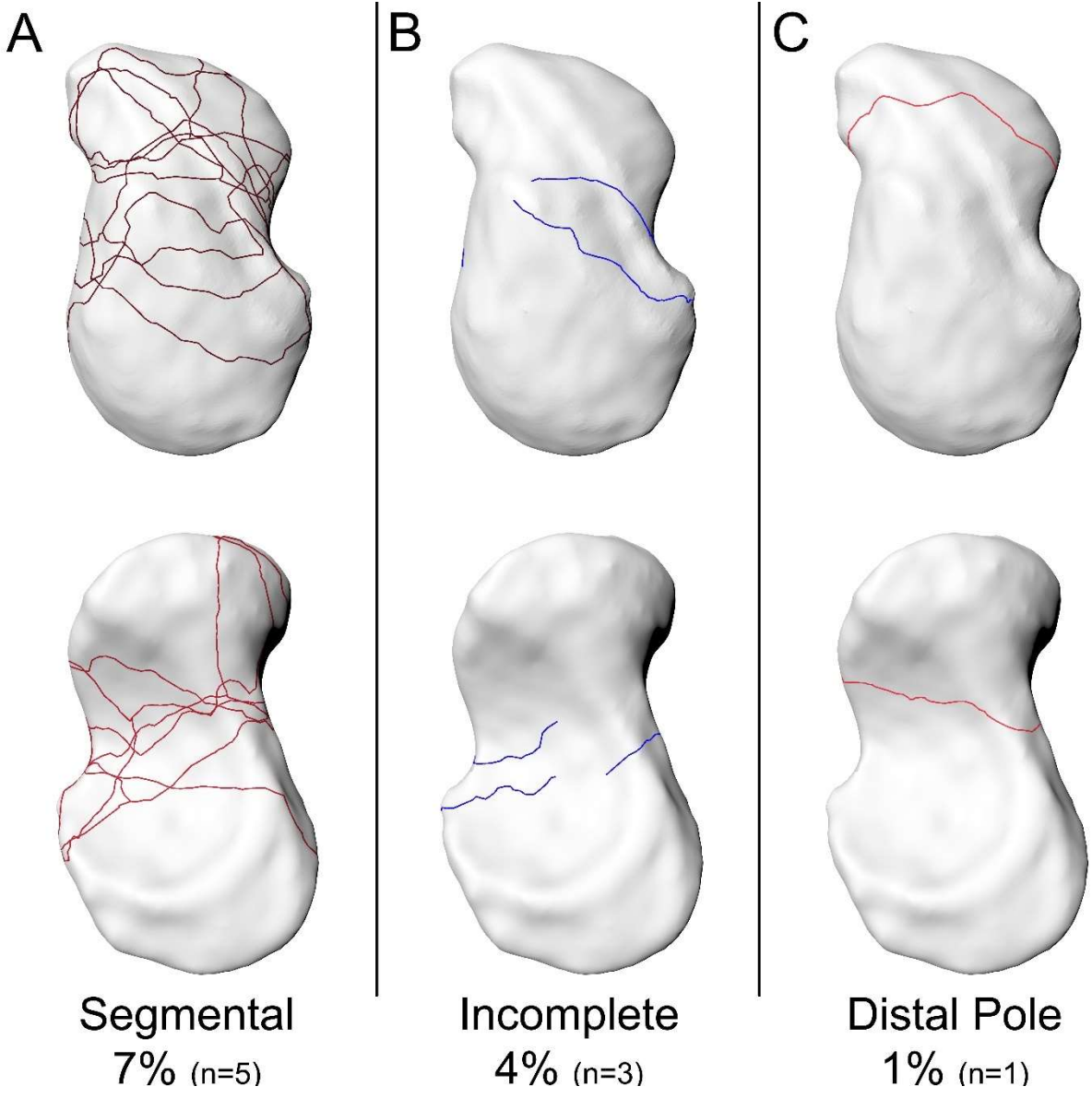
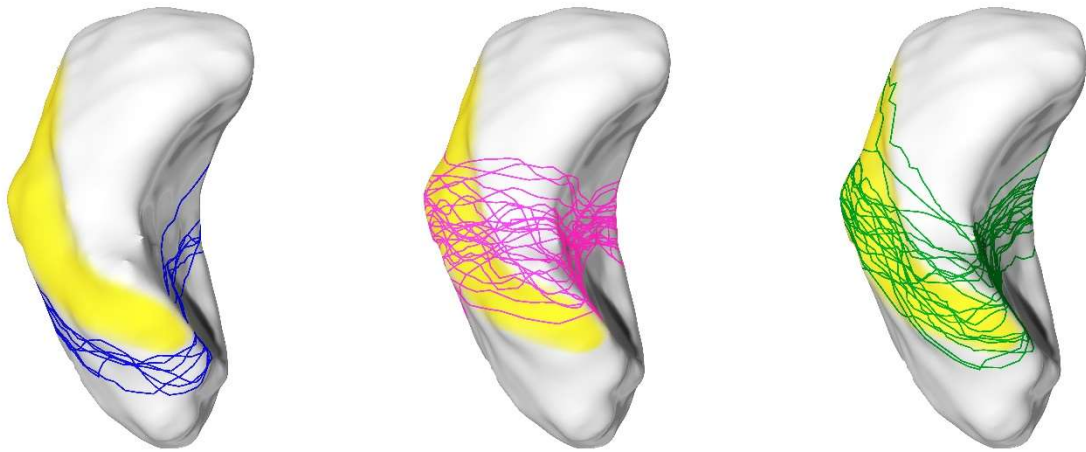


Figure 6.5: Uncommon fracture types. Fractures shown from the radial (top row) and the ulnar (bottom row) views



Proximal Pole

Waist Transverse

Waist Oblique

Figure 6.6: Dorsal ridge involvement in proximal pole, transverse waist and oblique waist fractures. Dorsal ridge is outlined in *yellow*.

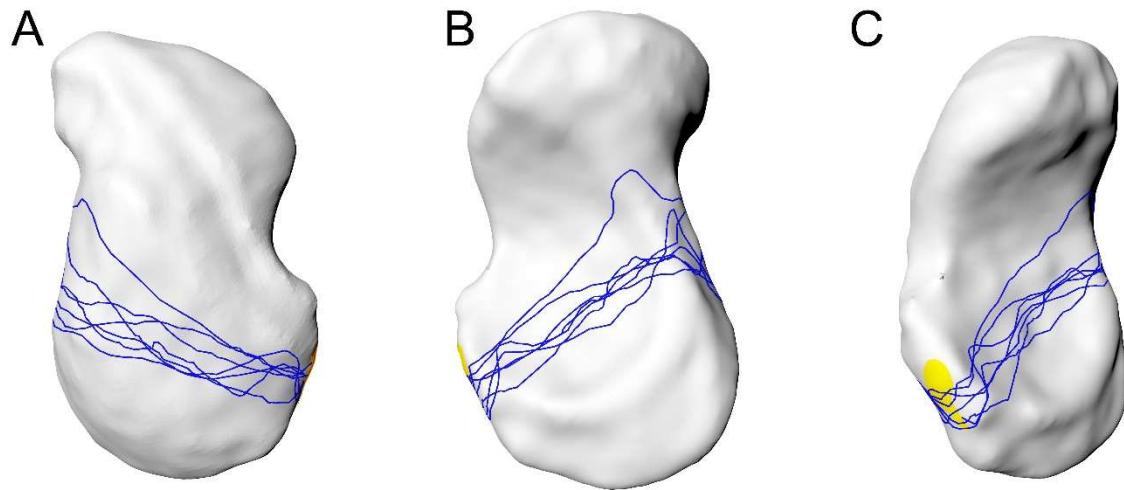


Figure 6.7: Proximal pole fractures as seen from the radial (A) and ulnar (B) aspects of the scaphoid. The radial border (C) is shown to better illustrate the site of comminution. Comminution is marked in *yellow* and was only seen in one case.

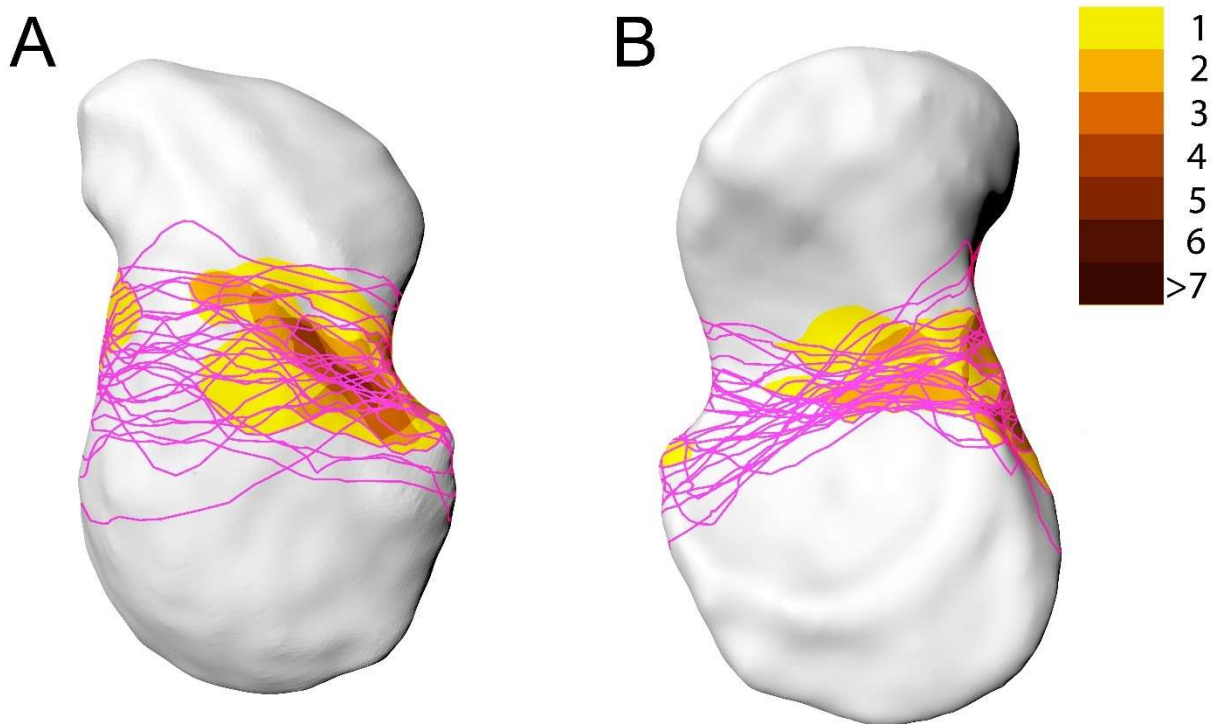


Figure 6.8: Transverse waist fractures and their comminution from the radial (A) and ulnar (B) aspects of the scaphoid. Comminution is marked in *yellow*, with overlapping cases allocated darker colour.

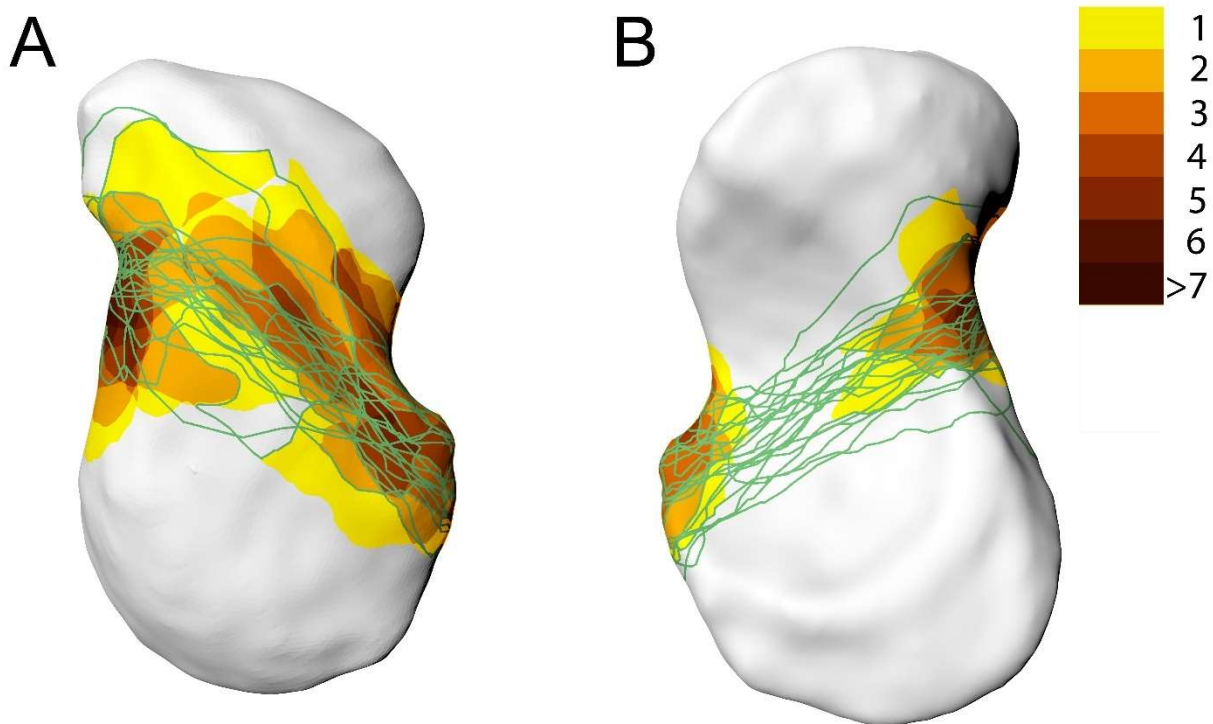


Figure 6.9: Oblique waist fractures and their comminution from the radial (A) and ulnar (B) aspects of the scaphoid. Comminution is marked in *yellow*, with overlapping cases allocated darker colour.

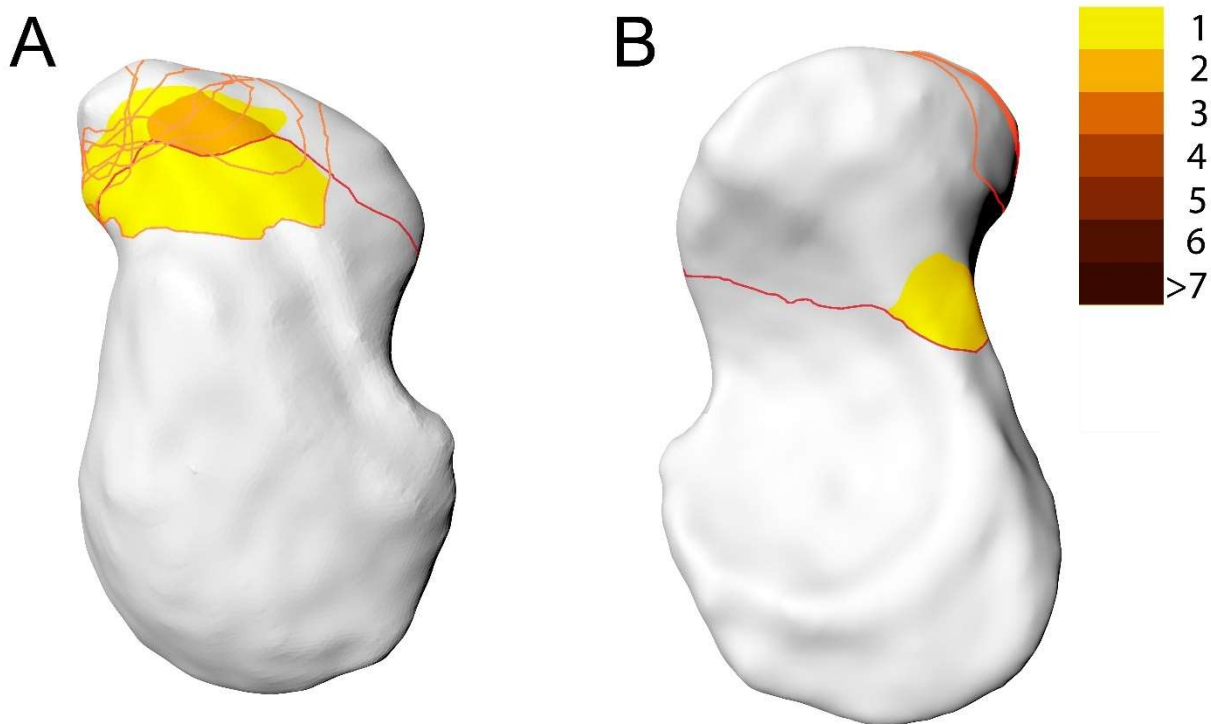


Figure 6.10: Distal pole fractures and their comminution from the radial (A) and ulnar (B) aspects of the scaphoid. Comminution is marked in *yellow*, with overlapping cases allocated darker colour.

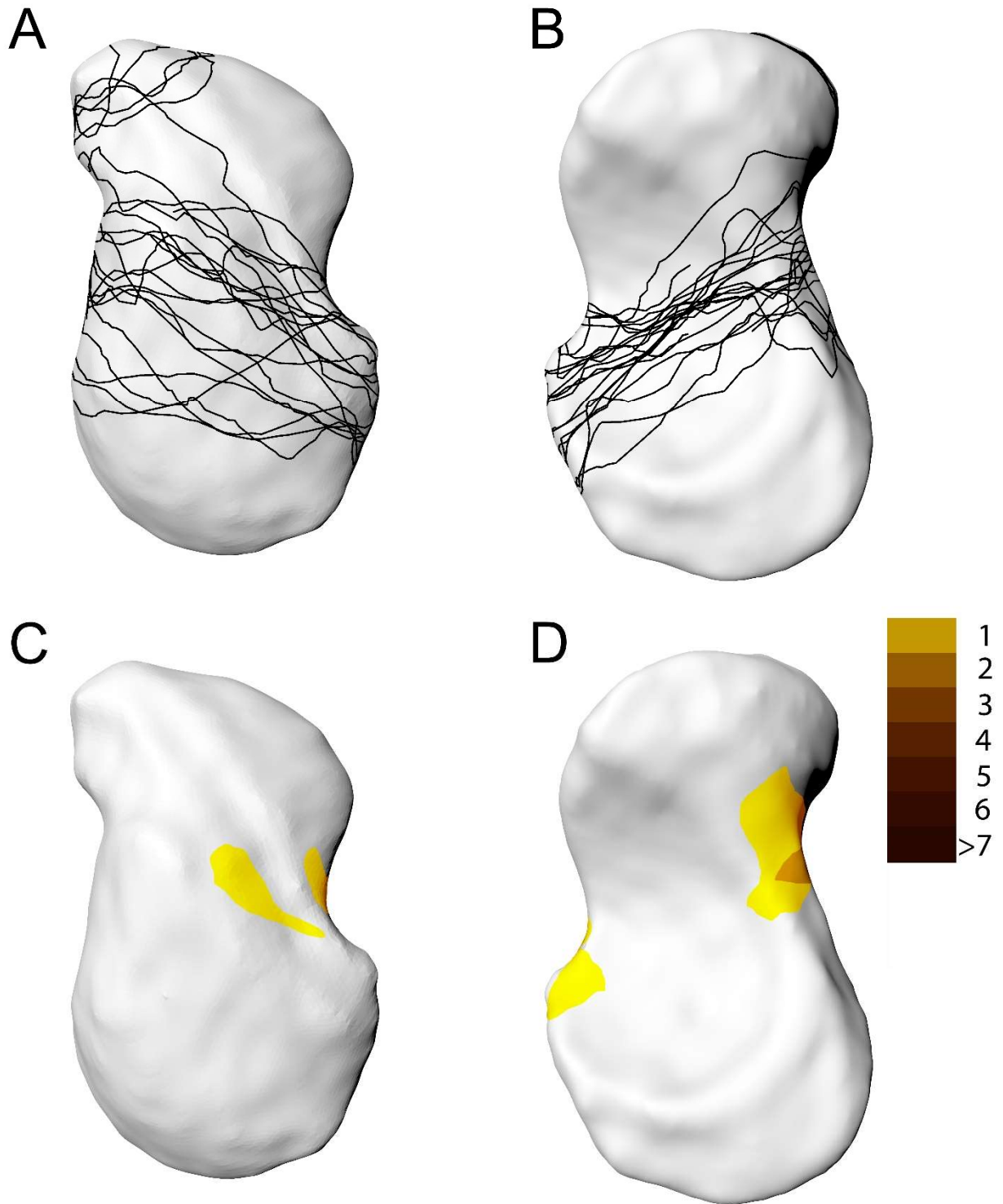


Figure 6.11: Un-displaced fractures and their associated comminution. The radial (A, C) and ulnar (B, D) aspects of the scaphoid are shown. Comminution (C, D) is marked in *yellow*, with overlapping cases allocated darker colour. Only four un-displaced fractures with associated comminution were identified.

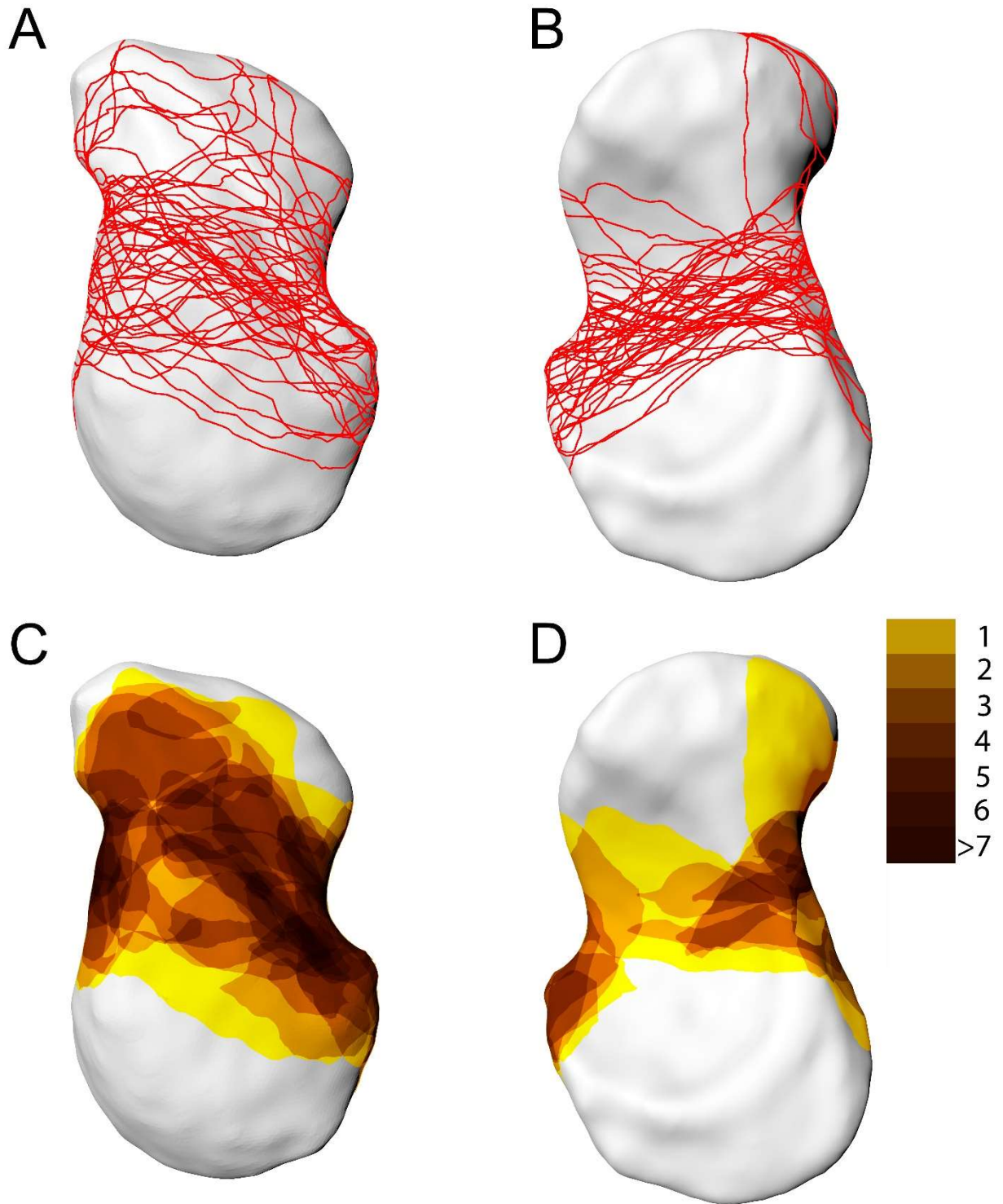


Figure 6.12: Displaced fractures and their associated comminution. The radial (A, C) and ulnar (B, D) aspects of the scaphoid are shown. Comminution (C, D) is marked in *yellow*, with overlapping cases allocated darker colour.

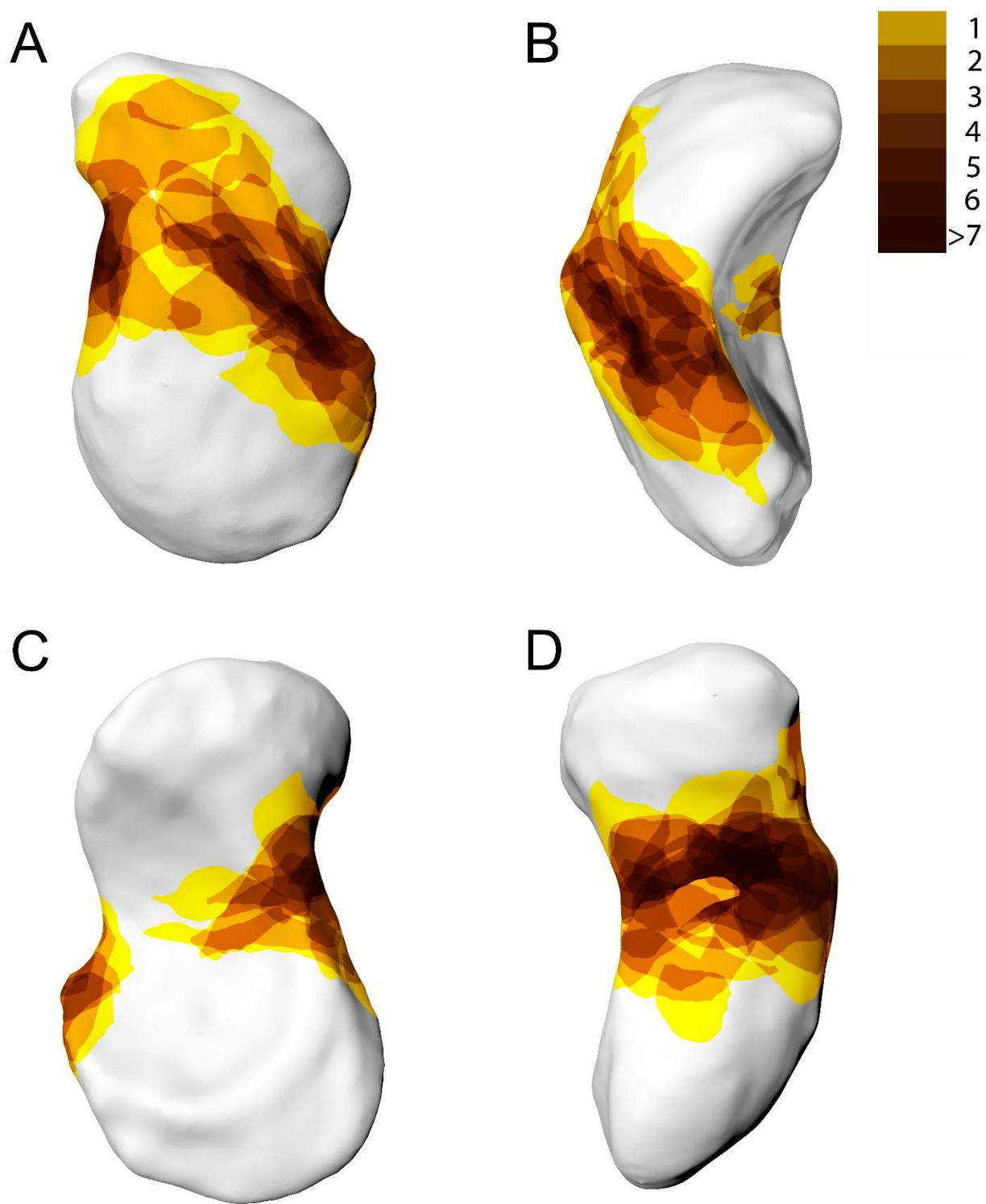
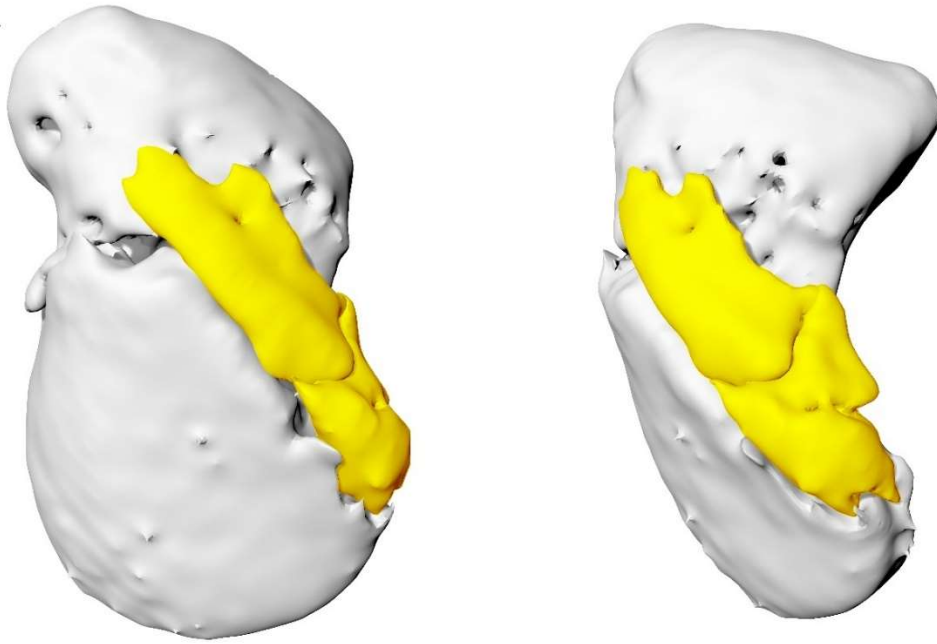


Figure 6.13: Scaphoid fracture comminution. Segmental fractures were excluded from analysis to better visualise comminution patterns. The scaphoid is rotated by 90° from the starting, radial position (A). The defined views are: (A) radial, (B) dorsal, (C) ulnar, (D) volar. Comminution is marked in *yellow*, with overlapping cases allocated darker colour.

A



B

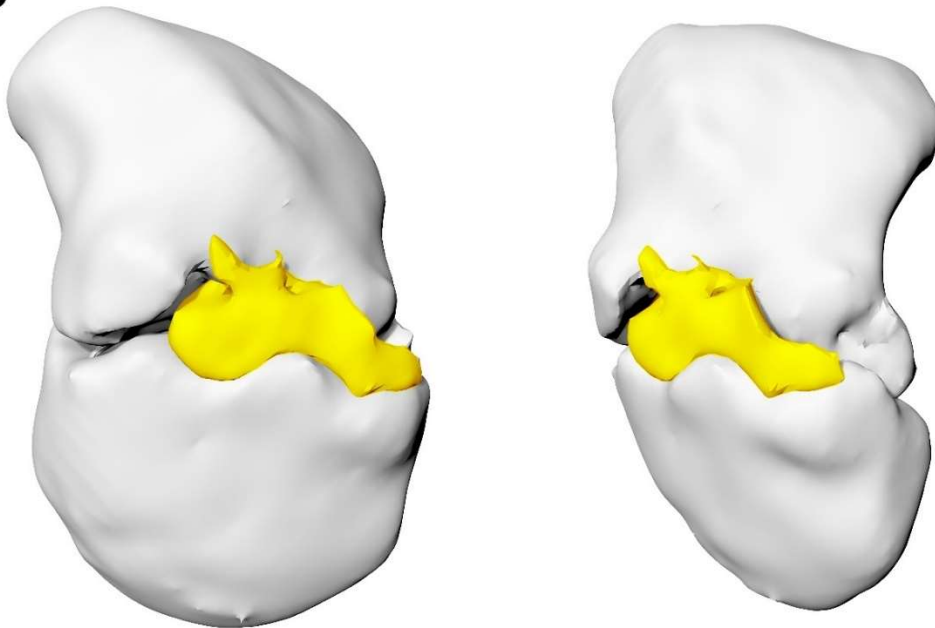


Figure 6.14: Examples of dorsal comminution, marked in *yellow*. (A) A type 1 scaphoid with a single high crest and comminution of the entire dorsal non-articulating area; (B) A type 2 scaphoid with several lower crests and comminution at the DIC insertion only.

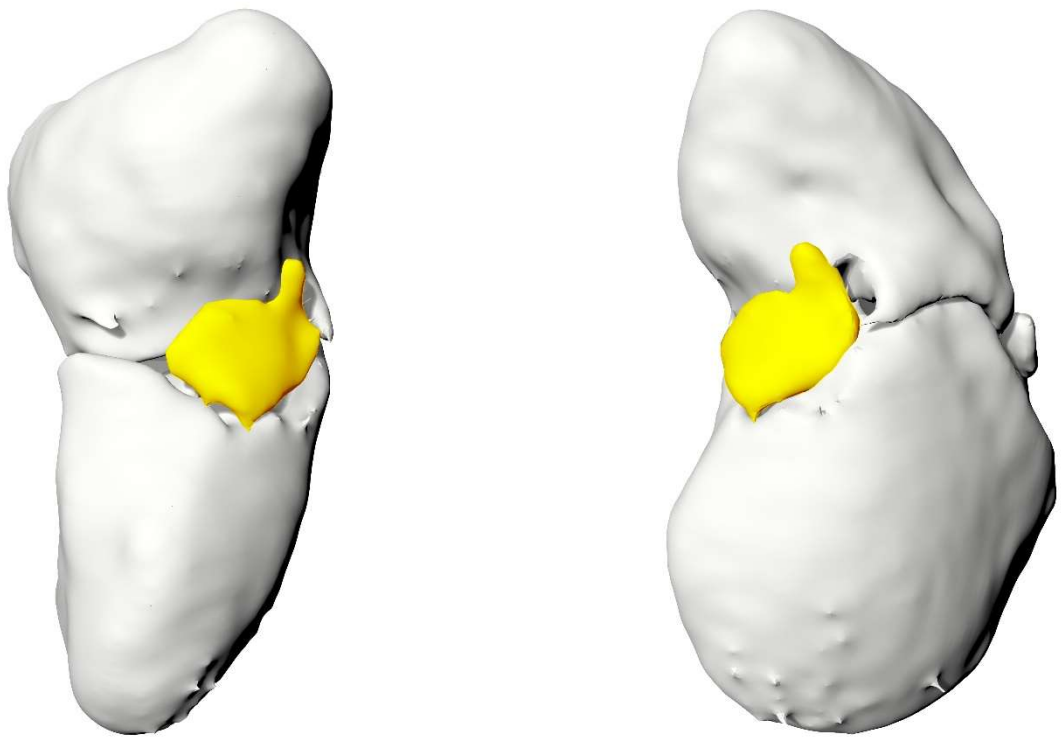


Figure 6.15: Example of volar comminution, marked in *yellow*. Comminution is located at the isthmus of the scaphoid at the junction between waist and distal pole.

Table 6.2: Results of all fracture types and fracture characteristics. Absolute numbers are reported, with percentages of each shown in (). *statistically significant

Fracture Type	Number	Displacement	Comminution	Concurrent #	Perilunate
Proximal Pole	6 (8)	2 (33)	1 (17)	4 (67)	2 (33)
Waist Transverse	28 (37)	22* (79)	15 (54)	10 (36)	3 (11)
Waist Oblique	24 (32)	15 (63)	16* (67)	13 (54)	3 (13)
Distal Pole	1 (1)	1 (100)	1* (100)	0 (0)	0 (0)
Tubercle	8 (11)	3 (38)	1* (13)	3 (38)	0 (0)
Incomplete	3 (4)	0 (0)	0 (0)	1 (33)	0 (0)
Segmental	5 (7)	5 (100)	5* (100)	3 (60)	2 (40)
Total	75	64%	52%	45%	13%

Plate design

The technique description of dorsal plating used a standard lattice, titanium plate. It was contoured to fit the dorsal scaphoid. The technique preceded the cadaveric study; hence, assessments of plate position and plate shape were done intra-operatively. The cadaveric study has shown that the shape of the dorsal non-articulating area resembled that of a lazy-S. It followed an oblique course separated by the DAS and PAS. There were no distinct tapering points along its length; however, the most ulnar aspect, the scaphoid apex, had an oblique take-off, lending to a broader footprint when utilising a plate (Figure 6.16A). The length of the non-articulating area was 26mm. This is similar to the mini-plate used in study III. We identified gender differences in the size of the area of 17%. Consequently, the length of a pre-contoured plate should be undersized by at least that amount in order to avoid impingement.

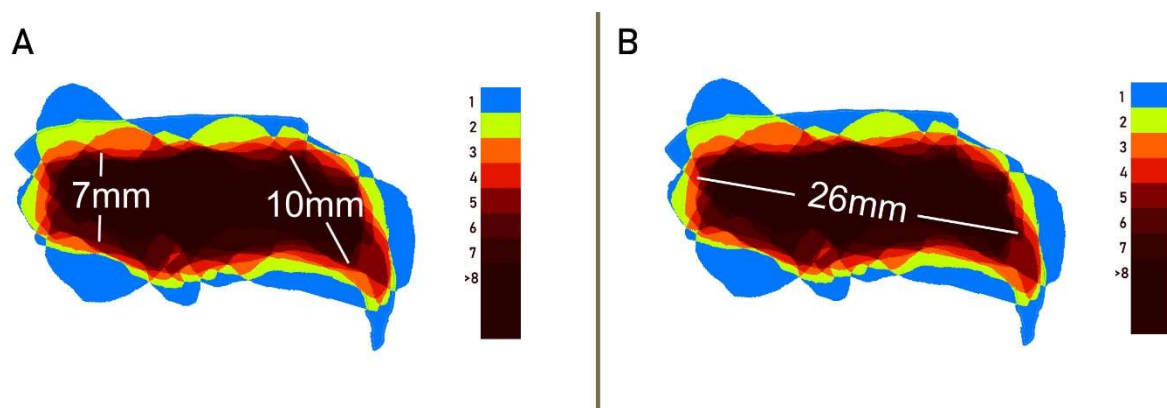


Figure 6.16: Colour heatmap of non-articulating areas identified in study I. More overlap between specimens is allocated a higher wavelength colour, similar to visible light. A: width measurements; B: length measurement

Based on these cadaveric findings a proposed design for a dorsal scaphoid plate is presented in figure 6.17. It maintains a relative constant width, has a gentle S-shape when traced from ulnar to radial and capitalises on the oblique orientation of the scaphoid apex.

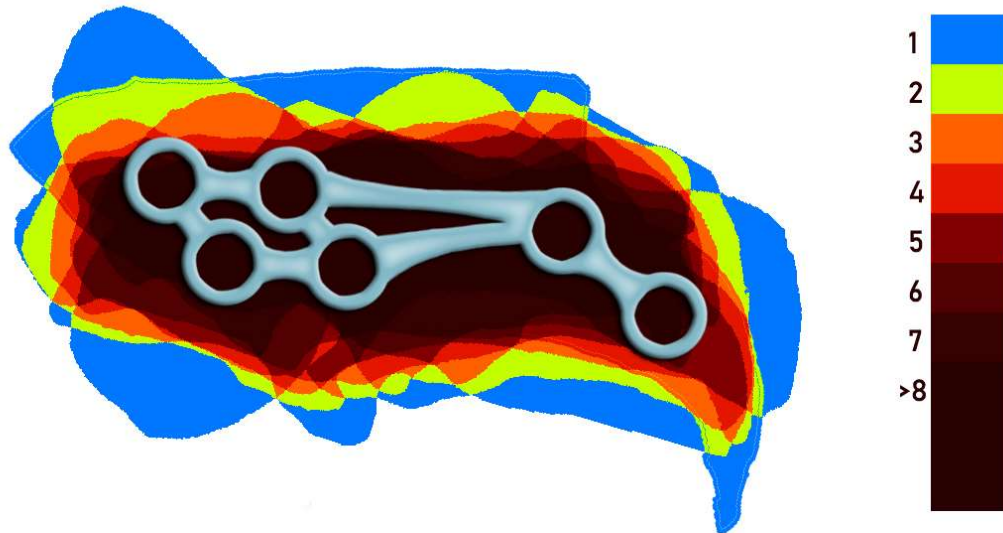
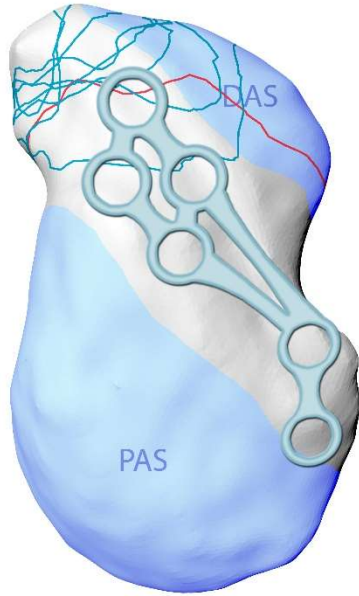


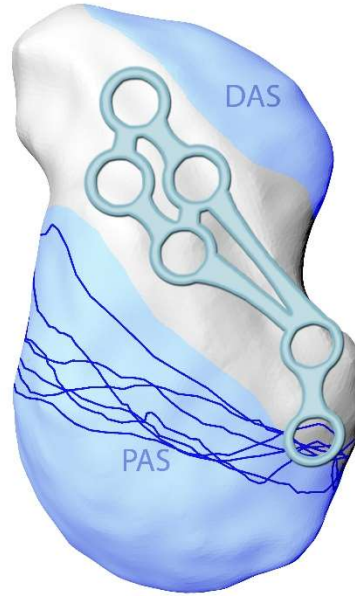
Figure 6.17: Proposed design for a dorsal scaphoid plate. Colour heatmap of non-articulating areas identified in study I. More overlap between specimens is allocated a higher wavelength colour, similar to visible light.

The fracture mapping study lends itself to further elaborate on plate design (Fig. 6.18). Distal pole and proximal pole fractures are not amenable for plate fixation as no sufficient screw purchase could be achieved with a dorsal plate. Transverse waist fractures are best suited for dorsal plating. Oblique waist fractures can be considered for plating; however, the large proportion of scaphoid apex involvement seen in oblique waist fractures needs to be assessed pre-operatively. Similarly, the dorsal comminution patterns observed in transverse waist fractures are more amenable for plating compared with those of oblique waist types (Fig 6.19).

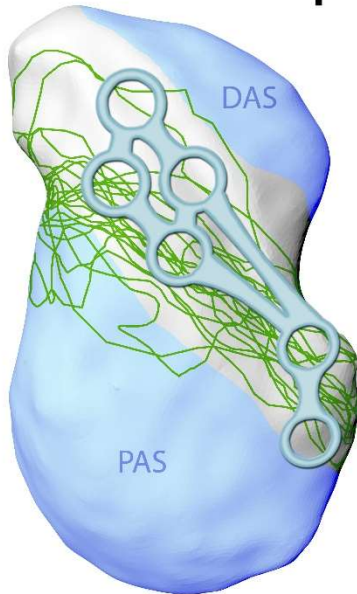
Distal pole



Proximal Pole



Waist Oblique



Waist Transverse

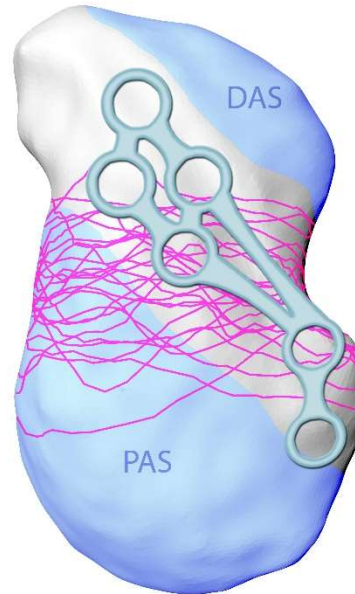
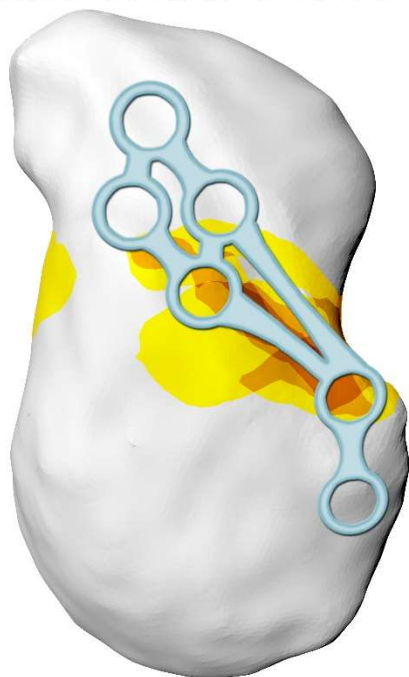


Figure 6.18: Proposed plate design superimposed onto the main fracture types identified in study V. Distal pole and proximal pole fractures do not allow for adequate screw placement into each fragment. Fracture lines of oblique waist fractures involve all screw positions. Transverse waist fractures are best suited for plating.

Waist Transverse



Waist Oblique



Figure 6.19: Proposed plate design superimposed onto comminution observed in waist fractures. Comminution is marked in *yellow*, with overlapping cases allocated darker colour.

Conclusion

The scaphoid is a fascinating bone. It is frequently injured, but its injury can often escape detection.

This thesis sheds light on some aspects of the scaphoid not previously studied. The dorsal non-articulating area is known to provide an anchoring point for carpal ligaments. Understanding its size, shape and position in relation to the radius can aid in guiding surgical exposure. Similarly, with developing implants and surgical techniques, the scaphoid plate placed on the dorsal non-articulating area can be one of the ways to impart more stability to the fractured scaphoid. However, irrespective of implant choice, imaging of the scaphoid will remain the cornerstone of scaphoid fracture treatment. This thesis highlights one radiographic view to image one aspect of the scaphoid, the scaphotrapeziotrapezoid joint. Nevertheless, accurate imaging of the scaphotrapeziotrapezoid joint is paramount for implant insertion, for monitoring post-operative implants complications and

for assessment of post-traumatic arthrosis. Three-dimensional analysis of fracture morphology is in its infancy and is anticipated to advance rapidly. The mapping of acute scaphoid fractures has demonstrated that displacement and comminution are associated with certain fracture types. The correlation of fracture displacement to fracture type as well as description of fracture comminution is novel and will assist in prognosticating fracture outcomes at the time of imaging.

Future Directions

Clinical outcome studies for scaphoid plating, in particular dorsal plating are lacking. Ideally, future studies investigating the merits of scaphoid plating would be randomised and prospective. In addition, our scaphotrapeziotrapezoid joint view should be validated against previously published imaging techniques. A study quantifying and comparing the sensitivity and specificity of different scaphotrapeziotrapezoid joint radiographs would allow to improve carpal imaging. Finally, follow-up studies for 3D scaphoid fracture mapping could investigate displacement in 3D or assess medium- to long-term clinical outcomes based on fracture type, comminution and displacement.

References

- ADLER, J. B. & SHAFTAN, G. W. 1962. Fractures of the capitate. *J Bone Joint Surg Am*, 44-A, 1537-47.
- ADOLFFSON, L., LINDAU, T. & ARNER, M. 2001. Acutrak screw fixation versus cast immobilisation for undisplaced scaphoid waist fractures. *J Hand Surg Br*, 26, 192-5.
- AGGRAWAL, A. 2014. *Textbook of Forensic Medicine and Toxicology*.
- AMIRFEYZ, R., BEBBINGTON, A., DOWNING, N. D., ONI, J. A. & DAVIS, T. R. 2011. Displaced scaphoid waist fractures: the use of a week 4 CT scan to predict the likelihood of union with nonoperative treatment. *J Hand Surg Eur Vol*, 36, 498-502.
- ANNAMALAI, G. & RABY, N. 2003. Scaphoid and pronator fat stripes are unreliable soft tissue signs in the detection of radiographically occult fractures. *Clin Radiol*, 58, 798-800.
- APERGIS, E. & SPRINGERLINK 2013. *Fracture-Dislocations of the Wrist*.
- ARMITAGE, B. M., WIJICKS, C. A., TARKIN, I. S., SCHRODER, L. K., MAREK, D. J., ZLOWODZKI, M. & COLE, P. A. 2009. Mapping of scapular fractures with three-dimensional computed tomography. *JBS*, 91, 2222-2228.
- BAGBY, G. W. & JANES, J. M. 1958. The effect of compression on the rate of fracture healing using a special plate. *The American Journal of Surgery*, 95, 761-771.
- BAIN, G. I. 1999. Clinical utilisation of computed tomography of the scaphoid. *Hand Surgery*, 4, 3-9.
- BAIN, G. I., TUROW, A. & PHADNIS, J. 2015. Dorsal Plating of Unstable Scaphoid Fractures and Nonunions. *Tech Hand Up Extrem Surg*, 19, 95-100.
- BANNERMAN, M. M. 1946. Fractures of the carpal scaphoid bone: An analysis of sixty-six cases. *Archives of Surgery*, 53, 164-168.
- BARTON, N. 1992. Twenty questions about scaphoid fractures. *Journal of hand surgery*, 17, 289-310.
- BARTON, N. 1997. Experience with scaphoid grafting. *Journal of Hand Surgery*, 22, 153-160.
- BARTON, N. J. 2004. The late consequences of scaphoid fractures. *J Bone Joint Surg Br*, 86, 626-30.
- BERGER, R. A. 1997. The ligaments of the wrist. A current overview of anatomy with considerations of their potential functions. *Hand Clin*, 13, 63-82.
- BERGER, R. A. 2001. The anatomy of the scaphoid. *Hand Clin*, 17, 525-32.
- BERGER, R. A. & GARCIA-ELIAS, M. 1991. *Biomechanics of the wrist joint*, Springer.
- BERGER, R. A., IMEADA, T., BERGLUND, L. & AN, K.-N. 1999. Constraint and material properties of the subregions of the scapholunate interosseous ligament. *The Journal of hand surgery*, 24, 953-962.
- BERGH, T. H., LINDAU, T., SOLDAL, L. A., BERNARDSHAW, S. V., BEHZADI, M., STEEN, K. & BRUDVIK, C. 2014. Clinical scaphoid score (CSS) to identify scaphoid fracture with MRI in patients with normal x-ray after a wrist trauma. *Emerg Med J*, 31, 659-64.
- BERLIN, D. 1929. Position in the treatment of fracture of the carpal scaphoid. *New England Journal of Medicine*, 201, 574-579.
- BEUTEL, B. G., MELAMED, E., HINDS, R. M., GOTTSCHALK, M. B. & CAPO, J. T. 2016. Mechanical evaluation of four internal fixation constructs for scaphoid fractures. *HAND*, 11, 72-77.
- BHATIA, A., PISHO, T., TOUAM, C. & OBERLIN, C. Incidence and distribution of scaphotrapezotrapezoidal arthritis in 73 fresh cadaveric wrists. *Annales de Chirurgie de la Main et du Membre Superieur*, 1996. Elsevier, 220-225.
- BOABIGHI, A., KUHLMANN, J. N. & KENESI, C. 1993. The distal ligamentous complex of the scaphoid and the scapho-lunate ligament. An anatomic, histological and biomechanical study. *J Hand Surg Br*, 18, 65-9.
- BOHLER, J. & ENDER, H. G. 1986. [Pseudarthrosis of the scaphoid]. *Orthopade*, 15, 109-20.
- BOHLER, L., TROJAN, E. & JAHNA, H. 1954. Treatment of 734 cases of fresh fracture of the scaphoid bone of the hand. *Wiederherstellungschirurgie und Traumatologie. Reconstruction surgery and traumatology*, 2, 86.
- BÖHLER, L., TROJAN, E. & JAHNA, H. 1954. Behandlungsergebnisse von 734 frischen einfachen Brüchen des Kahnbeinkörpers der Hand. *Reconstr Surg Traumatol*, 2, 86-111.

- BÖHLER, L., TROJAN, E. & JAHNA, H. 2003. The results of treatment of 734 fresh, simple fractures of the scaphoid. *Journal of Hand Surgery*, 28, 319-331.
- BOND, C. D., SHIN, A. Y., MCBRIDE, M. T. & DAO, K. D. 2001. Percutaneous screw fixation or cast immobilization for nondisplaced scaphoid fractures. *JBJS*, 83, 483.
- BOTTE, M. J. 2003. *Surgical anatomy of the hand and upper extremity*, Lippincott Williams & Wilkins.
- BRAUN, C., GROSS, G. & BUHREN, V. 1993. [Osteosynthesis using a buttress plate--a new principle for stabilizing scaphoid pseudarthroses]. *Unfallchirurg*, 96, 9-11.
- BREITENSEHER, M. J., METZ, V. M., GILULA, L. A., GAEBLER, C., KUKLA, C., FLEISCHMANN, D., IMHOF, H. & TRATTNIG, S. 1997. Radiographically occult scaphoid fractures: value of MR imaging in detection. *Radiology*, 203, 245-250.
- BROGAN, D. M., MORAN, S. L. & SHIN, A. Y. 2015. Outcomes of open reduction and internal fixation of acute proximal pole scaphoid fractures. *Hand*, 10, 227-232.
- BROOKS, S., CICUTTINI, F., LIM, S., TAYLOR, D., STUCKEY, S. & WLUKA, A. 2005. Cost effectiveness of adding magnetic resonance imaging to the usual management of suspected scaphoid fractures. *British journal of sports medicine*, 39, 75-79.
- BROWN, G. D., 3RD, ROH, M. S., STRAUCH, R. J., ROSENWASSER, M. P., ATESHIAN, G. A. & MOW, V. C. 2003. Radiography and visual pathology of the osteoarthritic scaphotrapezio-trapezoidal joint, and its relationship to trapeziometacarpal osteoarthritis. *J Hand Surg Am*, 28, 739-43.
- BRYDIE, A. & RABY, N. 2003. Early MRI in the management of clinical scaphoid fracture. *The British journal of radiology*, 76, 296-300.
- BUIJZE, G. A., DVINSKIKH, N. A., STRACKEE, S. D., STREEKSTRA, G. J. & BLANKEVOORT, L. 2011a. Osseous and ligamentous scaphoid anatomy: part II. Evaluation of ligament morphology using three-dimensional anatomical imaging. *The Journal of hand surgery*, 36, 1936-1943.
- BUIJZE, G. A., JØRGSHOLM, P., THOMSEN, N. O., BJÖRKMANN, A., BESJAKOV, J. & RING, D. 2012. Factors associated with arthroscopically determined scaphoid fracture displacement and instability. *The Journal of hand surgery*, 37, 1405-1410.
- BUIJZE, G. A., LOZANO-CALDERON, S. A., STRACKEE, S. D., BLANKEVOORT, L. & JUPITER, J. B. 2011b. Osseous and ligamentous scaphoid anatomy: Part I. A systematic literature review highlighting controversies. *The Journal of hand surgery*, 36, 1926-1935.
- BUSHNELL, B. D., MCWILLIAMS, A. D. & MESSER, T. M. 2007. Complications in dorsal percutaneous cannulated screw fixation of nondisplaced scaphoid waist fractures. *The Journal of hand surgery*, 32, 827-833.
- CARTER, F. M., 2ND, ZIMMERMAN, M. C., DIPAOLO, D. M., MACKESSY, R. P. & PARSONS, J. R. 1991. Biomechanical comparison of fixation devices in experimental scaphoid osteotomies. *J Hand Surg Am*, 16, 907-12.
- CERI, N., KORMAN, E., GUNAL, I. & TETIK, S. 2004. The morphological and morphometric features of the scaphoid. *J Hand Surg Br*, 29, 393-8.
- CHAN, K. W. & MCADAMS, T. R. 2004. Central screw placement in percutaneous screw scaphoid fixation: a cadaveric comparison of proximal and distal techniques. *The Journal of hand surgery*, 29, 74-79.
- CHANG, M. A., BISHOP, A. T., MORAN, S. L. & SHIN, A. Y. 2006. The outcomes and complications of 1, 2-intercompartmental supraretinacular artery pedicled vascularized bone grafting of scaphoid nonunions. *The Journal of hand surgery*, 31, 387-396.
- CHEN, A. C.-Y., CHAO, E.-K., HUNG, S.-S., LEE, M. S.-S. & UENG, S. W.-N. 2005. Percutaneous screw fixation for unstable scaphoid fractures. *Journal of Trauma and Acute Care Surgery*, 59, 184-187.
- CHEN, C.-Y., CHAO, E.-K., LEE, S.-S. & UENG, S. W.-N. 1999. Osteosynthesis of carpal scaphoid nonunion with interpositional bone graft and Kirschner wires: a 3-to 6-year follow-up. *Journal of Trauma and Acute Care Surgery*, 47, 558-563.

- CLAY, N. R., DIAS, J. J., COSTIGAN, P., GREGG, P. & BARTON, N. 1991. Need the thumb be immobilised in scaphoid fractures? A randomised prospective trial. *The Journal of bone and joint surgery. British volume*, 73, 828-832.
- CLEMENTSON, M., JØRGSHOLM, P., BESJAKOV, J., BJÖRKMAN, A. & THOMSEN, N. 2015. Union of scaphoid waist fractures assessed by CT scan. *Journal of wrist surgery*, 4, 049-055.
- CLEMENTSON, M., THOMSEN, N., BESJAKOV, J., JØRGSHOLM, P. & BJÖRKMAN, A. 2017. Long-term outcomes after distal scaphoid fractures: a 10-year follow-up. *The Journal of hand surgery*, 42, 927. e1-927. e7.
- COLE, P. A., MEHRLE, R. K., BHANDARI, M. & ZLOWODZKI, M. 2013. The pilon map: fracture lines and comminution zones in OTA/AO type 43C3 pilon fractures. *Journal of orthopaedic trauma*, 27, e152-e156.
- COMCARE 2017. Guide to the assessment of the degree of permanent impairment. 2.1 ed.: Australian Government
- COMPSON, J. 1998. The anatomy of acute scaphoid fractures: a three-dimensional analysis of patterns. *The Journal of bone and joint surgery. British volume*, 80, 218-224.
- COMPSON, J. P., WATERMAN, J. K. & HEATLEY, F. W. 1994. The radiological anatomy of the scaphoid. Part 1: Osteology. *J Hand Surg Br*, 19, 183-7.
- COONEY, W. P., DOBYNS, J. H. & LINSCHIED, R. L. 1980. Fractures of the scaphoid: a rational approach to management. *Clin Orthop Relat Res*, 90-7.
- COONEY, W. P., LINSCHIED, R. L. & DOBYNS, J. H. 1998. *The wrist: diagnosis and operative treatment*, Mosby.
- COONEY, W. P., LINSCHIED, R. L., DOBYNS, J. H. & WOOD, M. B. 1988. Scaphoid nonunion: role of anterior interpositional bone grafts. *The Journal of hand surgery*, 13, 635-650.
- CRAIGEN, M. & STANLEY, J. 1995. Wrist kinematics: row, column or both? *Journal of Hand Surgery*, 20, 165-170.
- CRISCO, J. J., COBURN, J. C., MOORE, D. C., AKELMAN, E., WEISS, A.-P. C. & WOLFE, S. W. 2005. In vivo radiocarpal kinematics and the dart thrower's motion. *JBJS*, 87, 2729-2740.
- CROSBY, E. B., LINSCHIED, R. L. & DOBYNS, J. H. 1978. Scaphotrapezial trapezoidal arthrosis. *The Journal of hand surgery*, 3, 223-234.
- DANIS, D. R. 1949. *Université de Bruxelles... Théorie et pratique de l'ostéosynthèse: par Robert Danis*, Masson (Niort).
- DAVIES, A. M., GRAINGER, A. J. & JAMES, S. J. 2011. *Imaging of the Hand and Wrist : Techniques and Applications*.
- DAVIS, E. N., CHUNG, K. C., KOTSIS, S. V., LAU, F. H. & VIJAN, S. 2006. A cost/utility analysis of open reduction and internal fixation versus cast immobilization for acute nondisplaced mid-waist scaphoid fractures. *Plastic and reconstructive surgery*, 117, 1223-1235.
- DEGEORGE, B. R., JR., PULOS, N. & SHIN, A. Y. 2018. Obtaining a Reliable Scaphotrapeziotrapezoid Radiograph: Pronation, Ulnar Deviation, and Thumb Abduction. *Tech Hand Up Extrem Surg*, 22, 120-123.
- DEL REGATO, J. A. 1975. Wilhelm Conrad Roentgen. *International Journal of Radiation Oncology• Biology• Physics*, 1, 133-139.
- DESTOT, E. A. J. 1925. *Injuries of the wrist : a radiological study*, London, Benn.
- DIAS, J., BRENKEL, I. & FINLAY, D. 1989. Patterns of union in fractures of the waist of the scaphoid. *The Journal of bone and joint surgery. British volume*, 71, 307-310.
- DIAS, J., TAYLOR, M., THOMPSON, J., BRENKEL, I. J. & GREGG, P. 1988. Radiographic signs of union of scaphoid fractures. An analysis of inter-observer agreement and reproducibility. *The Journal of bone and joint surgery. British volume*, 70, 299-301.
- DIAS, J., WILDIN, C., BHOWAL, B. & THOMPSON, J. 2005. Should acute scaphoid fractures be fixed?: a randomized controlled trial. *JBJS*, 87, 2160-2168.
- DINAH, A. & VICKERS, R. 2007. Smoking increases failure rate of operation for established non-union of the scaphoid bone. *International orthopaedics*, 31, 503-505.

- DODDS, S. D., PANJABI, M. M. & SLADE III, J. F. 2006. Screw fixation of scaphoid fractures: a biomechanical assessment of screw length and screw augmentation. *The Journal of hand surgery*, 31, 405-413.
- DODDS, S. D., PATTERSON, J. T. & HALIM, A. 2014. Volar plate fixation of recalcitrant scaphoid nonunions with volar carpal artery vascularized bone graft. *Tech Hand Up Extrem Surg*, 18, 2-7.
- DORSAY, T. A., MAJOR, N. M. & HELMS, C. A. 2001. Cost-effectiveness of immediate MR imaging versus traditional follow-up for revealing radiographically occult scaphoid fractures. *AJR Am J Roentgenol*, 177, 1257-63.
- DREWNIAKY, J. J., PALMER, A. K. & FLATT, A. E. 1985. The scaphotrapezial ligament complex: an anatomic and biomechanical study. *The Journal of hand surgery*, 10, 492-498.
- DUCKWORTH, A. D., JENKINS, P. J., AITKEN, S. A., CLEMENT, N. D., COURT-BROWN, C. M. & MCQUEEN, M. M. 2012. Scaphoid fracture epidemiology. *J Trauma Acute Care Surg*, 72, E41-5.
- DUNN, J., KUSNEZOV, N., FARES, A., MITCHELL, J. & PIRELA-CRUZ, M. 2016. The Scaphoid Staple A Systematic Review. *HAND*, 1558944716658747.
- EASTLEY, N., SINGH, H., DIAS, J. J. & TAUB, N. 2013. Union rates after proximal scaphoid fractures; meta-analyses and review of available evidence. *J Hand Surg Eur Vol*, 38, 888-97.
- EGOL, K. A., KUBIAK, E. N., FULKERSON, E., KUMMER, F. J. & KOVAL, K. J. 2004. Biomechanics of locked plates and screws. *Journal of orthopaedic trauma*, 18, 488-493.
- EL-KHOURY, G. Y., BENNETT, L. D. & ONDR, G. J. 2004. Multidetector-row computed tomography. *JAAOS-Journal of the American Academy of Orthopaedic Surgeons*, 12, 1-5.
- ENDER, H. G. 1977. [A new method of treating traumatic cysts and pseudoarthrosis of the scaphoid (author's transl)]. *Unfallheilkunde*, 80, 509-13.
- ERHART, J., UNGER, E., SCHEFZIG, P., KRUMBOECK, A., HAGMANN, M., VECSEI, V. & MAYR, W. 2016. In vitro experimental investigation of the forces and torque acting on the scaphoid during light grasp. *Journal of Orthopaedic Research*, 34, 1734-1742.
- FEIPEL, V., RINNEN, D. & ROOZE, M. 1999. Postero-anterior radiography of the wrist: scapholunate ratios and joint projection shape analysis. *Surg Radiol Anat*, 21, 207-13.
- FERNÁNDEZ, A. D. O., TEPIC, S., FRIGG, R., MEISSER, A., HAAS, N. & PERREN, S. 2001. Treating forearm fractures using an internal fixator: a prospective study. *Clinical orthopaedics and related research*, 196-205.
- FILAN, S. & HERBERT, T. 1996. Herbert screw fixation of scaphoid fractures. *The Journal of bone and joint surgery. British volume*, 78, 519-529.
- FINSEN, V., HOFSTAD, M. & HAUGAN, H. 2006. Most scaphoid non-unions heal with bone chip grafting and Kirschner-wire fixation. Thirty-nine patients reviewed 10 years after operation. *Injury*, 37, 854-9.
- FISHMAN, E. K., MAGID, D., NEY, D. R., CHANEY, E. L., PIZER, S. M., ROSENMAN, J. G., LEVIN, D. N., VANNIER, M. W., KUHLMAN, J. E. & ROBERTSON, D. D. 1991. Three-dimensional imaging. *Radiology*, 181, 321-337.
- FISK, G. R. 1970. Carpal instability and the fractured scaphoid. *Annals of the Royal College of Surgeons of England*, 46, 63.
- FOGG, Q. A. 2004. *Scaphoid variation and an anatomical basis for variable carpal mechanics*. Ph.D thesis Ph.D thesis, The University of Adelaide.
- FOWLER, J. R. & ILYAS, A. M. 2010. Headless compression screw fixation of scaphoid fractures. *Hand clinics*, 26, 351-361.
- FREEDMAN, D. M., BOTTE, M. J. & GELBERMAN, R. H. 2001. Vascularity of the Carpus. *Clinical Orthopaedics and Related Research (1976-2007)*, 383, 47-59.
- FUSETTI, C., POLETTI, P. A., PRADEL, P. H., GARAVAGLIA, G., PLATON, A., DELLA SANTA, D. R. & BIANCHI, S. 2005. Diagnosis of occult scaphoid fracture with high-spatial-resolution sonography: a prospective blind study. *J Trauma*, 59, 677-81.

- GALLEY, I., BAIN, G. I. & MCLEAN, J. M. 2007. Influence of lunate type on scaphoid kinematics. *The Journal of hand surgery*, 32, 842-847.
- GARALA, K. & DIAS, J. 2019. Scaphoid fracture geometrics: an assessment of location and orientation. *Journal of plastic surgery and hand surgery*, 1-8.
- GARALA, K., TAUB, N. A. & DIAS, J. J. 2016. The epidemiology of fractures of the scaphoid: impact of age, gender, deprivation and seasonality. *Bone Joint J*, 98-B, 654-9.
- GARCIA-ELIAS, M. & LLUCH, A. 2001. Partial excision of scaphoid: is it ever indicated? *Hand clinics*, 17, 687-95, x.
- GARCIA-ELIAS, M., RIBE, M., RODRIGUEZ, J., COTS, M. & CASAS, J. 1995. Influence of joint laxity on scaphoid kinematics. *Journal of hand surgery*, 20, 379-382.
- GARCIA, R. M., LEVERSEDGE, F. J., ALDRIDGE, J. M., RICHARD, M. J. & RUCH, D. S. 2014. Scaphoid nonunions treated with 2 headless compression screws and bone grafting. *J Hand Surg Am*, 39, 1301-7.
- GARG, B., GOYAL, T., KOTWAL, P. P., SANKINEANI, S. R. & TRIPATHY, S. K. 2013. Local distal radius bone graft versus iliac crest bone graft for scaphoid nonunion: a comparative study. *Musculoskeletal surgery*, 97, 109-114.
- GAUTIER, E., PERREN, S. & CORDEY, J. 2000. Effect of plate position relative to bending direction on the rigidity of a plate osteosynthesis. A theoretical analysis. *Injury*, 31, 14-92.
- GEISL, H. & PUHRINGER, A. 1986. [Chronic fractures and pseudarthroses of the scaphoid bone of the hand. Experiences with the Ender scaphoid bone plate]. *Aktuelle Traumatol*, 16, 149-52.
- GELBERMAN, R. H. & MENON, J. 1980. The vascularity of the scaphoid bone. *The Journal of hand surgery*, 5, 508-513.
- GELLMAN, H., CAPUTO, R., CARTER, V., ABOULAFIA, A. & MCKAY, M. 1989. Comparison of short and long thumb-spica casts for non-displaced fractures of the carpal scaphoid. *The Journal of bone and joint surgery. American volume*, 71, 354-357.
- GEOGHEGAN, J., WOODRUFF, M., BHATIA, R., DAWSON, J., KERSLAKE, R., DOWNING, N., ONI, J. & DAVIS, T. 2009. Undisplaced scaphoid waist fractures: is 4 weeks' immobilisation in a below-elbow cast sufficient if a week 4 CT scan suggests fracture union? *Journal of Hand Surgery (European Volume)*, 34, 631-637.
- GERBER, C., MAST, J. & GANZ, R. 1990. Biological internal fixation of fractures. *Archives of orthopaedic and trauma surgery*, 109, 295-303.
- GEURTS, G., VAN RIET, R., MEERMANS, G. & VERSTREKEN, F. 2011. Incidence of scaphotrapezial arthritis following volar percutaneous fixation of nondisplaced scaphoid waist fractures using a transtrapezial approach. *J Hand Surg Am*, 36, 1753-8.
- GHOLSON, J. J., BAE, D. S., ZURAKOWSKI, D. & WATERS, P. M. 2011. Scaphoid fractures in children and adolescents: contemporary injury patterns and factors influencing time to union. *JBJS*, 93, 1210-1219.
- GHONEIM, A. 2011. The unstable nonunited scaphoid waist fracture: results of treatment by open reduction, anterior wedge grafting, and internal fixation by volar buttress plate. *J Hand Surg Am*, 36, 17-24.
- GLICKEL, S. Z., KORNSTEIN, A. N. & EATON, R. G. 1992. Long-term follow-up of trapeziometacarpal arthroplasty with coexisting scaphotrapezial disease. *The Journal of hand surgery*, 17, 612-620.
- GREEN, D. P. & WOLFE, S. W. 2011. *Green's operative hand surgery*, Philadelphia, Saunders/Elsevier.
- GREEN, J. J. & RAYAN, G. 1997. Scaphoid fractures in soccer goalkeepers. *The Journal of the Oklahoma State Medical Association*, 90, 45-47.
- GREWAL, R., LUTZ, K., MACDERMID, J. C. & SUH, N. 2016. Proximal pole scaphoid fractures: a computed tomographic assessment of outcomes. *The Journal of hand surgery*, 41, 54-58.
- GREWAL, R., SUH, N. & MACDERMID, J. C. 2013. Use of computed tomography to predict union and time to union in acute scaphoid fractures treated nonoperatively. *The Journal of hand surgery*, 38, 872-877.

- GREWAL, R., SUH, N. & MACDERMID, J. C. 2015. The Missed Scaphoid Fracture—Outcomes of Delayed Cast Treatment. *Journal of wrist surgery*, 4, 278-283.
- GUO, Y., TIAN, G. L., CHEN, S. & TAPIA, C. 2014. Establishing a central zone in scaphoid surgery: a computational approach. *Int Orthop*, 38, 95-9.
- HAAK, D., PAGE, C.-E. & DESERNO, T. M. 2016. A survey of DICOM viewer software to integrate clinical research and medical imaging. *Journal of digital imaging*, 29, 206-215.
- HACKNEY, L. A. & DODDS, S. D. 2011. Assessment of scaphoid fracture healing. *Current reviews in musculoskeletal medicine*, 4, 16-22.
- HAIIDUKWYCH, G. J. & RICCI, W. 2008. Locked plating in orthopaedic trauma: a clinical update. *JAAOS—Journal of the American Academy of Orthopaedic Surgeons*, 16, 347-355.
- HANNEMANN, P., BROUWERS, L., VAN DER ZEE, D., STADLER, A., GOTTGENS, K., WEIJERS, R., POEZE, M. & BRINK, P. 2013. Multiplanar reconstruction computed tomography for diagnosis of scaphoid waist fracture union: a prospective cohort analysis of accuracy and precision. *Skeletal radiology*, 42, 1377-1382.
- HART, A., HARVEY, E. J., RABIEI, R., BARTHELAT, F. & MARTINEAU, P. A. 2016. Fixation strength of four headless compression screws. *Medical Engineering & Physics*, 38, 1037-1043.
- HASAN, A. P., PHADNIS, J., JAARSMA, R. L. & BAIN, G. I. 2017. Fracture line morphology of complex proximal humeral fractures. *Journal of shoulder and elbow surgery*, 26, e300-e308.
- HERAS-PALOU, C. 2009. Midcarpal instability. *Fractures and injuries of the distal radius and carpus. The cutting edge*. Philadelphia: Saunders.
- HERBERT, T. J. & FISHER, W. E. 1984. Management of the fractured scaphoid using a new bone screw. *The Journal of bone and joint surgery. British volume*, 66, 114-123.
- HINDMAN, B., KULIK, W., LEE, G. & AVOLIO, R. 1989. Occult fractures of the carpals and metacarpals: demonstration by CT. *American journal of roentgenology*, 153, 529-532.
- HODGKINSON, D. W., NICHOLSON, D. A., STEWART, G., SHERIDAN, M. & HUGHES, P. 1993. Scaphoid fracture: a new method of assessment. *Clin Radiol*, 48, 398-401.
- HORII, E., NAKAMURA, R., WATANABE, K. & TSUNODA, K. 1994. Scaphoid fracture as a "puncher's fracture". *Journal of orthopaedic trauma*, 8, 107-110.
- HOVE, L. M. 1999. Epidemiology of scaphoid fractures in Bergen, Norway. *Scand J Plast Reconstr Surg Hand Surg*, 33, 423-6.
- HU, Y.-L., YE, F.-G., JI, A.-Y., QIAO, G.-X. & LIU, H.-F. 2009. Three-dimensional computed tomography imaging increases the reliability of classification systems for tibial plateau fractures. *Injury*, 40, 1282-1285.
- HUENE, D. R. & HUENE, D. S. 1991. Treatment of nonunions of the scaphoid with the Ender compression blade plate system. *J Hand Surg Am*, 16, 913-22.
- HUNTER, J. C., ESCOBEDO, E. M., WILSON, A. J., HANEL, D. P., ZINK-BRODY, G. C. & MANN, F. A. 1997. MR imaging of clinically suspected scaphoid fractures. *AJR Am J Roentgenol*, 168, 1287-93.
- IMAEDA, T., NAKAMURA, R., MIURA, T. & MAKINO, N. 1992. Magnetic resonance imaging in scaphoid fractures. *Journal of Hand Surgery*, 17, 20-27.
- INGLIS, M., MCCLELLAND, B., SUTHERLAND, L. & CUNDY, P. 2013. Synthetic versus plaster of Paris casts in the treatment of fractures of the forearm in children: a randomised trial of clinical outcomes and patient satisfaction. *The bone & joint journal*, 95, 1285-1289.
- INOUE, G., SHIONOYA, K. & KUWAHATA, Y. 1997. Herbert screw fixation for scaphoid nonunions. An analysis of factors influencing outcome. *Clinical orthopaedics and related research*, 99-106.
- INTERNATIONAL WRIST INVESTIGATORS' WORKSHOP TERMINOLOGY, C. 2002. Wrist: terminology and definitions. *J Bone Joint Surg Am*, 84-A Suppl 1, 1-73.
- JENKINS, P. J., SLADE, K., HUNTLEY, J. S. & ROBINSON, C. M. 2008. A comparative analysis of the accuracy, diagnostic uncertainty and cost of imaging modalities in suspected scaphoid fractures. *Injury*, 39, 768-74.

- JIRANEK, W., RUBY, L., MILLENDER, L., BANKOFF, M. & NEWBERG, A. 1992. Long-term results after Russe bone-grafting: the effect of malunion of the scaphoid. *The Journal of bone and joint surgery. American volume*, 74, 1217-1228.
- JOHNSTON, H. M. 1907. Varying positions of the carpal bones in the different movements at the wrist: part I. *Journal of anatomy and physiology*, 41, 109.
- JURKOWITSCH, J., DALL'ARA, E., QUADLBAUER, S., PEZZEI, C., JUNG, I., PAHR, D. & LEIXNERING, M. 2016. Rotational stability in screw-fixed scaphoid fractures compared to plate-fixed scaphoid fractures. *Arch Orthop Trauma Surg*, 136, 1623-1628.
- KARL, J. W., SWART, E. & STRAUCH, R. J. 2015. Diagnosis of occult scaphoid fractures: a cost-effectiveness analysis. *JBJS*, 97, 1860-1868.
- KAUER, J. M. 1986. The mechanism of the carpal joint. *Clin Orthop Relat Res*, 16-26.
- KAWAMURA, K. & CHUNG, K. C. 2008. Treatment of scaphoid fractures and nonunions. *The Journal of hand surgery*, 33, 988-997.
- KAWANISHI, Y., OKA, K., TANAKA, H., SUGAMOTO, K. & MURASE, T. 2017. In vivo scaphoid motion during thumb and forearm motion in casts for scaphoid fractures. *The Journal of hand surgery*, 42, 475. e1-475. e7.
- KEHOE, N. J., HACKNEY, R. G. & BARTON, N. J. 2003. Incidence of osteoarthritis in the scapho-trapezial joint after Herbert screw fixation of the scaphoid. *J Hand Surg Br*, 28, 496-9.
- KELSON, T., DAVIDSON, R. & BAKER, T. 2016. Early MRI versus conventional management in the detection of occult scaphoid fractures: what does it really cost? A rural pilot study. *Journal of medical radiation sciences*, 63, 9-16.
- KIJIMA, Y. & VIEGAS, S. F. 2009. Wrist anatomy and biomechanics. *J Hand Surg Am*, 34, 1555-63.
- KILIC, A., SOKUCU, S., PARMAKSIZOGLU, A. S., GUL, M. & KABUKCUOGLU, Y. S. 2011. Comparative evaluation of radiographic and functional outcomes in the surgical treatment of scaphoid non-unions. *Acta Orthop Traumatol Turc*, 45, 399-405.
- KIRKHAM, S. G. & MILLAR, M. J. 2012. Cancellous bone graft and Kirschner wire fixation as a treatment for cavitory-type scaphoid nonunions exhibiting DISI. *Hand (N Y)*, 7, 86-93.
- KLIFTO, C. S., GANDI, S. D. & SAPIENZA, A. 2018. Bone graft options in upper-extremity surgery. *The Journal of hand surgery*, 43, 755-761. e2.
- KOJIMA, K. E. & PIRES, R. E. S. 2017. Absolute and relative stabilities for fracture fixation: the concept revisited. *Injury*, 48, S1.
- KORKALA, O. L., KUOKKANEN, H. O. & EEROLA, M. S. 1992. Compression-staple fixation for fractures, non-unions, and delayed unions of the carpal scaphoid. *J Bone Joint Surg Am*, 74, 423-6.
- KRAKAUER, J. D., BISHOP, A. T. & COONEY, W. P. 1994. Surgical treatment of scapholunate advanced collapse. *The Journal of hand surgery*, 19, 751-759.
- KUKLA, C., GAEBLER, C., BREITENSEHER, M. J., TRATTNIG, S. & VECSEI, V. 1997. Occult fractures of the scaphoid. The diagnostic usefulness and indirect economic repercussions of radiography versus magnetic resonance scanning. *J Hand Surg Br*, 22, 810-3.
- KULKARNI, R., WOLLSTEIN, R., TAYAR, R. & CITRON, N. 1999. Patterns of healing of scaphoid fractures: the importance of vascularity. *The Journal of bone and joint surgery. British volume*, 81, 85-90.
- LANE, W. A. 1895. Some remarks on the treatment of fractures. *British medical journal*, 1, 861.
- LANGHOFF, O. & ANDERSEN, J. L. 1988. Consequences of late immobilization of scaphoid fractures. *J Hand Surg Br*, 13, 77-9.
- LANZ, U. 2004. *Surgical Anatomy of the Hand*, Thieme.
- LARSEN, C. F., BRONDUM, V. & SKOV, O. 1992. Epidemiology of scaphoid fractures in Odense, Denmark. *Acta Orthop Scand*, 63, 216-8.
- LEIXNERING, M., PEZZEI, C., WENINGER, P., MAYER, M., BOGNER, R., LEDERER, S., SCHAUER, J. & FIGL, M. 2011. First experiences with a new adjustable plate for osteosynthesis of scaphoid nonunions. *J Trauma*, 71, 933-8.

- LESLIE, I. & DICKSON, R. 1981. The fractured carpal scaphoid. Natural history and factors influencing outcome. *The Journal of bone and joint surgery. British volume*, 63, 225-230.
- LIM, T. K., KIM, H. K., KOH, K. H., LEE, H. I., WOO, S. J. & PARK, M. J. 2013. Treatment of avascular proximal pole scaphoid nonunions with vascularized distal radius bone grafting. *The Journal of hand surgery*, 38, 1906-1912. e1.
- LITTLE, C., BURSTON, B., HOPKINSON-WOOLLEY, J. & BURGE, P. 2006. Failure of surgery for scaphoid non-union is associated with smoking. *Journal of Hand Surgery*, 31, 252-255.
- LOW, G. & RABY, N. 2005. Can follow-up radiography for acute scaphoid fracture still be considered a valid investigation? *Clin Radiol*, 60, 1106-10.
- LOZANO-CALDERÓN, S., BLAZAR, P., ZURAKOWSKI, D., LEE, S.-G. & RING, D. 2006. Diagnosis of scaphoid fracture displacement with radiography and computed tomography. *JBJS*, 88, 2695-2703.
- LURIA, S., HOCH, S., LIEBERGALL, M., MOSHEIFF, R. & PELEG, E. 2010. Optimal fixation of acute scaphoid fractures: finite element analysis. *J Hand Surg Am*, 35, 1246-50.
- LURIA, S., LENART, L., LENART, B., PELEG, E. & KASTELEC, M. 2012a. Optimal fixation of oblique scaphoid fractures: a cadaver model. *J Hand Surg Am*, 37, 1400-4.
- LURIA, S., LENART, L., LENART, B., PELEG, E. & KASTELEC, M. 2012b. Optimal fixation of oblique scaphoid fractures: a cadaver model. *The Journal of hand surgery*, 37, 1400-1404.
- LURIA, S., SCHWARCZ, Y., WOLLSTEIN, R., EMELIFE, P., ZINGER, G. & PELEG, E. 2015. 3-dimensional analysis of scaphoid fracture angle morphology. *J Hand Surg Am*, 40, 508-14.
- MACK, G., BOSSE, M., GELBERMAN, R. H. & YU, E. 1984. The natural history of scaphoid non-union. *J Bone Joint Surg Am*, 66, 504-9.
- MACK, G. R., WILCKENS, J. H. & MCPHERSON, S. A. 1998. Subacute scaphoid fractures. *The American journal of sports medicine*, 26, 56-58.
- MACK, M. G., KEIM, S., BALZER, J. O., SCHWARZ, W., HOCHMUTH, K., WINDOLF, J. & VOGL, T. J. 2003. Clinical impact of MRI in acute wrist fractures. *European radiology*, 13, 612-617.
- MALIZOS, K. N., ZACHOS, V., DAILIANA, Z. H., ZALAVRAS, C., VARITIMIDIS, S., HANTES, M. & KARANTANAS, A. 2007. Scaphoid nonunions: management with vascularized bone grafts from the distal radius: a clinical and functional outcome study. *Plastic and reconstructive surgery*, 119, 1513-1525.
- MALLEE, W. H., HENNY, E. P., VAN DIJK, C. N., KAMMINGA, S. P., VAN ENST, W. A. & KLOEN, P. 2014. Clinical diagnostic evaluation for scaphoid fractures: a systematic review and meta-analysis. *J Hand Surg Am*, 39, 1683-1691 e2.
- MALLEE, W. H., MELLEMA, J. J., GUITTON, T. G., GOSLINGS, J. C., RING, D., DOORNBURG, J. N. & SCIENCE OF VARIATION, G. 2016. 6-week radiographs unsuitable for diagnosis of suspected scaphoid fractures. *Arch Orthop Trauma Surg*, 136, 771-8.
- MARTINI, A. & SCHILTENWOLF, M. 1995. Changes in the wrist joint in spontaneous course of scaphoid pseudarthrosis. *Handchirurgie, Mikrochirurgie, plastische Chirurgie: Organ der Deutschsprachigen Arbeitsgemeinschaft für Handchirurgie: Organ der Deutschsprachigen Arbeitsgemeinschaft für Mikrochirurgie der Peripheren Nerven und Gefäße: Organ der V.* 27, 201-207.
- MATSON, A. P., GARCIA, R. M., RICHARD, M. J., LEVERSEDGE, F. J., ALDRIDGE, J. M. & RUCH, D. S. 2017. Percutaneous Treatment of Unstable Scaphoid Waist Fractures. *HAND*, 12, 362-368.
- MAZUR, K., STEVANOVIC, M., SCHNALL, S. B., HANNANI, K. & ZIONTS, L. E. 1997. Scaphocapitate syndrome in a child associated with a distal radius and ulna fracture. *Journal of orthopaedic trauma*, 11, 230-232.
- MCCALLISTER, W. V., KNIGHT, J., KALIAPPAN, R. & TRUMBLE, T. E. 2003. Central placement of the screw in simulated fractures of the scaphoid waist: a biomechanical study. *JBJS*, 85, 72-77.
- MCLAUGHLIN, H. & PARKES 2ND, J. 1969. Fracture of the carpal navicular (scaphoid) bone: gradations in therapy based upon pathology. *The Journal of trauma*, 9, 311.

- MCNALLY, E., GOODMAN, R. & BURGE, P. 2000. The role of MRI in the assessment of scaphoid fracture healing: a pilot study. *European radiology*, 10, 1926-1928.
- MCQUEEN, M., GELBKE, M., WAKEFIELD, A., WILL, E. & GAEBLER, C. 2008. Percutaneous screw fixation versus conservative treatment for fractures of the waist of the scaphoid: a prospective randomised study. *The Journal of bone and joint surgery. British volume*, 90, 66-71.
- MEERMANS, G. & VERSTREKEN, F. 2008. Percutaneous transtrapezial fixation of acute scaphoid fractures. *Journal of Hand Surgery (European Volume)*, 33, 791-796.
- MEERMANS, G. & VERSTREKEN, F. 2012. Influence of screw design, sex, and approach in scaphoid fracture fixation. *Clinical Orthopaedics and Related Research*®, 470, 1673-1681.
- MELLEMA, J. J., DOORNBERG, J. N., DYER, G. S. & RING, D. 2014. Distribution of coronoid fracture lines by specific patterns of traumatic elbow instability. *The Journal of hand surgery*, 39, 2041-2046.
- MELVILLE, D. M., TALJANOVIC, M. S., SCALCIONE, L. R., EBLE, J. M., GIMBER, L. H., DESILVA, G. L. & SHEPPARD, J. E. 2015. Imaging and management of thumb carpometacarpal joint osteoarthritis. *Skeletal Radiol*, 44, 165-77.
- MERRELL, G. A., WOLFE, S. W. & SLADE, J. F., 3RD 2002. Treatment of scaphoid nonunions: quantitative meta-analysis of the literature. *J Hand Surg Am*, 27, 685-91.
- MIRRER, J., YEUNG, J. & SAPIENZA, A. 2016. Anatomic Locking Plate Fixation for Scaphoid Nonunion. *Case Rep Orthop*, 2016, 7374101.
- MODY, B., BELLIAPPA, P., DIAS, J. & BARTON, N. 1993. Nonunion of fractures of the scaphoid tuberosity. *The Journal of bone and joint surgery. British volume*, 75, 423-425.
- MOOJEN, T. M., SNEL, J. G., RITT, M. J., VENEMA, H. W., KAUER, J. M. & BOS, K. E. 2002. Scaphoid kinematics in vivo. *The Journal of hand surgery*, 27, 1003-1010.
- MOON, E. S., DY, C. J., DERMAN, P., VANCE, M. C. & CARLSON, M. G. 2013. Management of nonunion following surgical management of scaphoid fractures: current concepts. *J Am Acad Orthop Surg*, 21, 548-57.
- MORITOMO, H., MURASE, T., OKA, K., TANAKA, H., YOSHIKAWA, H. & SUGAMOTO, K. 2008. Relationship between the fracture location and the kinematic pattern in scaphoid nonunion. *The Journal of hand surgery*, 33, 1459-1468.
- MORITOMO, H., VIEGAS, S. F., ELDER, K., NAKAMURA, K., DASILVA, M. F. & PATTERSON, R. M. 2000a. The scaphotrapezio-trapezoidal joint. Part 2: a kinematic study. *The Journal of hand surgery*, 25, 911-920.
- MORITOMO, H., VIEGAS, S. F., NAKAMURA, K., DASILVA, M. F. & PATTERSON, R. M. 2000b. The scaphotrapezio-trapezoidal joint. Part 1: An anatomic and radiographic study. *J Hand Surg Am*, 25, 899-910.
- MÜLLER, M. E., ALLGÖWER, M., SCHNEIDER, R., WILLENEGGER, H., ALLGÖWER, M. & SPRINGERLINK (ONLINE SERVICE) 1992. Manual of INTERNAL FIXATION Techniques Recommended by the AO-ASIF Group. Abridged AO-Manual, Limited 3rd Edition. ed. Berlin, Heidelberg: Springer Berlin Heidelberg,.
- MUNK, P. L., LEE, M. J., LOGAN, P. M., CONNELL, D. G., JANZEN, D. L., POON, P. Y., WORSLEY, D. F. & COUPLAND, D. 1997. Scaphoid bone waist fractures, acute and chronic: imaging with different techniques. *AJR Am J Roentgenol*, 168, 779-86.
- NAKAMURA, K., BEPPU, M., MATSUSHITA, K., ARAI, T. & IDE, T. 1997. Biomechanical analysis of the stress force on midcarpal joint in Kienböck's disease. *Hand Surgery*, 2, 101-115.
- NAKAMURA, R., IMAEDA, T., HORII, E., MIURA, T. & HAYAKAWA, N. 1991. Analysis of scaphoid fracture displacement by three-dimensional computed tomography. *The Journal of hand surgery*, 16, 485-492.
- NAVARRO, A. Luxaciones del carpo. *Anales de la Facultad de Medicina*, 1921. 113-141.
- NEWBERG, A., DALINKA, M. K., ALAZRAKI, N., BERQUIST, T. H., DAFFNER, R. H., DESMET, A. A., EL-KHOURY, G. Y., GOERGEN, T. G., KEATS, T. E., MANASTER, B. J., PAVLOV, H., SCHWEITZER, M.

- E., HARALSON, R. H., 3RD & MCCABE, J. B. 2000. Acute hand and wrist trauma. American College of Radiology. ACR Appropriateness Criteria. *Radiology*, 215 Suppl, 375-8.
- NEWPORT, M. L., WILLIAMS, C. D. & BRADLEY, W. D. 1996. Mechanical strength of scaphoid fixation. *J Hand Surg Br*, 21, 99-102.
- NGUYEN, Q., CHAUDHRY, S., SLOAN, R., BHOORA, I. & WILLARD, C. 2008. The clinical scaphoid fracture: early computed tomography as a practical approach. *The Annals of The Royal College of Surgeons of England*, 90, 488-491.
- NICHOLL, J. & BUCKLAND-WRIGHT, J. 2000. Degenerative changes at the scaphotrapezial joint following Herbert screw insertion: a radiographic study comparing patients with scaphoid fracture and primary hand arthritis. *Journal of Hand Surgery*, 25, 422-426.
- NORTH, E. R. & EATON, R. G. 1983. Degenerative joint disease of the trapezium: a comparative radiographic and anatomic study. *The Journal of hand surgery*, 8, 160-167.
- NUTTALL, D., TRAIL, I. A. & STANLEY, J. K. 1998. Movement of the scaphoid in the normal wrist. *J Hand Surg Br*, 23, 762-4.
- ODUWOLE, K. O., CICHY, B., DILLON, J. P., WILSON, J. & O'BEIRNE, J. 2012. Acutrak versus Herbert screw fixation for scaphoid non-union and delayed union. *J Orthop Surg (Hong Kong)*, 20, 61-5.
- OKA, K., MORITOMO, H., MURASE, T., GOTO, A., SUGAMOTO, K. & YOSHIKAWA, H. 2005a. Patterns of carpal deformity in scaphoid nonunion: a 3-dimensional and quantitative analysis. *The Journal of hand surgery*, 30, 1136-1144.
- OKA, K., MURASE, T., MORITOMO, H., GOTO, A., SUGAMOTO, K. & YOSHIKAWA, H. 2005b. Patterns of bone defect in scaphoid nonunion: a 3-dimensional and quantitative analysis. *J Hand Surg Am*, 30, 359-65.
- ORON, A., GUPTA, A. & THIRKANNAD, S. 2013. Nonunion of the scaphoid distal pole. *Hand Surgery*, 18, 35-39.
- PAPALOIZOS, M., FUSETTI, C., CHRISTEN, T., NAGY, L. & WASSERFALLEN, J. 2004. Minimally invasive fixation versus conservative treatment of undisplaced scaphoid fractures: a cost-effectiveness study. *Journal of Hand Surgery*, 29, 116-119.
- PARK, H. Y., YOON, J. O., JEON, I. H., CHUNG, H. W. & KIM, J. S. 2013. A comparison of the rates of union after cancellous iliac crest bone graft and Kirschner-wire fixation in the treatment of stable and unstable scaphoid nonunion. *Bone Joint J*, 95-B, 809-14.
- PARVIZI, J., WAYMAN, J., KELLY, P. & MORAN, C. G. 1998. Combining the clinical signs improves diagnosis of scaphoid fractures. A prospective study with follow-up. *J Hand Surg Br*, 23, 324-7.
- PATEL, S., TIEDEKEN, N., QVICK, L., DEBSKI, R. E., KAUFMANN, R. & FOWLER, J. R. 2019. Interfragmentary compression forces vary based on scaphoid bone screw type and fracture location. *HAND*, 14, 371-376.
- PATTERSON, R. M., MORITOMO, H., YAMAGUCHI, S., MITSUYASU, H., SHAH, M., BUFORD, W. L. & VIEGAS, S. F. 2003. Scaphoid anatomy and mechanics: update and review. *Operative Techniques in Orthopaedics*, 13, 2-10.
- PIALAT, J., BURGHARDT, A., SODE, M., LINK, T. & MAJUMDAR, S. 2012. Visual grading of motion induced image degradation in high resolution peripheral computed tomography: impact of image quality on measures of bone density and micro-architecture. *Bone*, 50, 111-118.
- PINDER, R. M., BRKLJAC, M., RIX, L., MUIR, L. & BREWSTER, M. 2015. Treatment of scaphoid nonunion: a systematic review of the existing evidence. *The Journal of hand surgery*, 40, 1797-1805. e3.
- PROSSER, A., BRENKEL, I. & IRVINE, G. 1988. Articular fractures of the distal scaphoid. *Journal of Hand Surgery*, 13, 87-91.
- PROSSER, G. H. & ISBISTER, E. S. 2003. The presentation of scaphoid non-union. *Injury*, 34, 65-7.
- PUOPOLO, S. M. & RETTIG, M. E. 2003. Management of acute scaphoid fractures. *BULLETIN-HOSPITAL FOR JOINT DISEASES NEW YORK*, 61, 160-163.

- RAMAMURTHY, C., CUTLER, L., NUTTALL, D., SIMISON, A. J., TRAIL, I. A. & STANLEY, J. K. 2007. The factors affecting outcome after non-vascular bone grafting and internal fixation for nonunion of the scaphoid. *J Bone Joint Surg Br*, 89, 627-32.
- RANCY, S. K., ZELKEN, J. A., LIPMAN, J. D. & WOLFE, S. W. 2016. Scaphoid proximal pole fracture following headless screw fixation. *Journal of wrist surgery*, 5, 071-076.
- RANKIN, G., KUSCHNER, S. H., ORLANDO, C., MCKELLOP, H., BRIEN, W. W. & SHERMAN, R. 1991. A biomechanical evaluation of a cannulated compressive screw for use in fractures of the scaphoid. *J Hand Surg Am*, 16, 1002-10.
- REIGSTAD, O., THORKILDSEN, R., GRIMSGAARD, C., REIGSTAD, A. & ROKKUM, M. 2009. Is revision bone grafting worthwhile after failed surgery for scaphoid nonunion? Minimum 8 year follow-up of 18 patients. *J Hand Surg Eur Vol*, 34, 772-7.
- RETTIG, M. E., KOZIN, S. H. & COONEY, W. P. 2001. Open reduction and internal fixation of acute displaced scaphoid waist fractures. *The Journal of hand surgery*, 26, 271-276.
- RETTIG, M. E. & RASKIN, K. B. 1999. Retrograde compression screw fixation of acute proximal pole scaphoid fractures. *The Journal of hand surgery*, 24, 1206-1210.
- RHEMREV, S. J., DE ZWART, A. D., KINGMA, L. M., MEYLAERTS, S. A., ARNDT, J. W., SCHIPPER, I. B. & BEERES, F. J. 2010. Early computed tomography compared with bone scintigraphy in suspected scaphoid fractures. *Clin Nucl Med*, 35, 931-4.
- RUBY, L. K., STINSON, J. & BELSKY, M. 1985. The natural history of scaphoid non-union. *J Bone Joint Surg*, 67, 428-432.
- RUSSE, O. 1960. Fracture of the carpal navicular: diagnosis, non-operative treatment, and operative treatment. *JBJS*, 42, 759-768.
- SAEDEN, B., TÖRNKVIST, H., PONZER, S. & HÖGLUND, M. 2001. Fracture of the carpal scaphoid: a prospective, randomised 12-year follow-up comparing operative and conservative treatment. *The Journal of bone and joint surgery. British volume*, 83, 230-234.
- SAFFAR, P. & SPRINGERLINK (ONLINE SERVICE) 1990. Carpal injuries Anatomy, radiology, current treatment. Paris: Springer Paris : Imprint: Springer,.
- SANDERS, W. E. 1988. Evaluation of the humpback scaphoid by computed tomography in the longitudinal axial plane of the scaphoid. *Journal of Hand Surgery*, 13, 182-187.
- SAUSER, D. D., BILLIMORIA, P. E., ROUSE, G. A. & MUDGE, K. 1980. CT evaluation of hip trauma. *American Journal of Roentgenology*, 135, 269-274.
- SAYEGH, E. T. & STRAUCH, R. J. 2014. Graft choice in the management of unstable scaphoid nonunion: a systematic review. *The Journal of hand surgery*, 39, 1500-1506. e7.
- SCHMIDT, H.-M. & LANZ, U. 2004. *Surgical anatomy of the hand*, Stuttgart ; New York, Thieme.
- SCHWARCZ, Y., SCHWARCZ, Y., PELEG, E., JOSKOWICZ, L., WOLLSTEIN, R. & LURIA, S. 2017. Three-dimensional analysis of acute scaphoid fracture displacement: proximal extension deformity of the scaphoid. *JBJS*, 99, 141-149.
- SCORDINO, L. E., BERNSTEIN, J., NAKASHIAN, M., MCINTOSH, M., COTE, M. P., RODNER, C. M. & WOLF, J. M. 2014. Radiographic prevalence of scaphotrapeziotrapezoid osteoarthritis. *J Hand Surg Am*, 39, 1677-82.
- SENNWALD, G., ZDRAVKOVIC, V. & OBERLIN, C. 1994. The anatomy of the palmar scaphotriquetral ligament. *The Journal of bone and joint surgery. British volume*, 76, 147-149.
- SHAH, C. M. & STERN, P. J. 2013. Scapholunate advanced collapse (SLAC) and scaphoid nonunion advanced collapse (SNAC) wrist arthritis. *Current reviews in musculoskeletal medicine*, 6, 9-17.
- SHAW, J. A. 1987. A biomechanical comparison of scaphoid screws. *J Hand Surg Am*, 12, 347-53.
- SHENOY, R., PILLAI, A. & HADIDI, M. 2007. Scaphoid fractures: variation in radiographic views - a survey of current practice in the West of Scotland region. *Eur J Emerg Med*, 14, 2-5.
- SHIRKHODA, A., BRASHEAR, H. & STAAB, E. 1980. Computed tomography of acetabular fractures. *Radiology*, 134, 683-688.

- SHORT, W. H., WERNER, F. W., FORTINO, M. D. & MANN, K. A. 1997. Analysis of the kinematics of the scaphoid and lunate in the intact wrist joint. *Hand clinics*, 13, 93-108.
- SHORT, W. H., WERNER, F. W., FORTINO, M. D., PALMER, A. K. & MANN, K. A. 1995. A dynamic biomechanical study of scapholunate ligament sectioning. *The Journal of hand surgery*, 20, 986-999.
- SINGH, H., FORWARD, D., DAVIS, T., DAWSON, J., ONI, J. & DOWNING, N. 2005. Partial union of acute scaphoid fractures. *Journal of Hand Surgery*, 30, 440-445.
- SINNATAMBY, C. S. & LAST, R. J. 2003. *Last's anatomy : regional and applied*, Edinburgh, Churchill Livingstone/Elsevier.
- SLADE, J. F., 3RD, GEISLER, W. B., GUTOW, A. P. & MERRELL, G. A. 2003. Percutaneous internal fixation of selected scaphoid nonunions with an arthroscopically assisted dorsal approach. *J Bone Joint Surg Am*, 85-A Suppl 4, 20-32.
- SLUTSKY, D. J. & SLADE, J. F. 2011. *The scaphoid*.
- SMITH, B. S. & COONEY, W. P. 1996. Revision of failed bone grafting for nonunion of the scaphoid. Treatment options and results. *Clin Orthop Relat Res*, 98-109.
- SMITH, D. 1993. Dorsal carpal ligaments of the wrist: normal appearance on multiplanar reconstructions of three-dimensional Fourier transform MR imaging. *AJR. American journal of roentgenology*, 161, 119-125.
- SOLGAARD, S. 1984. Angle of inclination of the articular surface of the distal radius. *Der Radiologe*, 24, 346-348.
- SONENBLUM, S. E., CRISCO, J. J., KANG, L. & AKELMAN, E. 2004. In vivo motion of the scaphotrapezio-trapezoidal (STT) joint. *J Biomech*, 37, 645-52.
- SOUBEYRAND, M., THOMSEN, L., DOURSOUNIAN, L., GAGEY, O. & NOURISSAT, G. 2010. Percutaneous retrograde screw fixation of non-displaced fractures of the scaphoid waist: an antirotation wire may not be necessary. *J Hand Surg Eur Vol*, 35, 209-13.
- SRINIVASAN, V. B. & MATTHEWS, J. P. 1996. Results of scaphotrapezotrapezoid fusion for isolated idiopathic arthritis. *J Hand Surg Br*, 21, 378-80.
- STANKOVIC, P. & BURCHHARDT, H. 1993. [Experience with the Ender hooked plate in the management of 42 scaphoid pseudarthroses]. *Handchir Mikrochir Plast Chir*, 25, 217-22.
- STARK, A., BROSTRÖM, L. & SVARTENGREN, G. 1987. Scaphoid nonunion treated with the Matti-Russe technique. Long-term results. *Clinical orthopaedics and related research*, 175-180.
- STARK, H. H., RICKARD, T. A., ZEMEL, N. P. & ASHWORTH, C. R. 1988. Treatment of ununited fractures of the scaphoid by iliac bone grafts and Kirschner-wire fixation. *J Bone Joint Surg Am*, 70, 982-91.
- STEIN, F. & SIEGEL, M. W. 1969. Naviculocapitate fracture syndrome: A case report: New thoughts on the mechanism of injury. *JBJS*, 51, 391-395.
- STEINMANN, S. P., BISHOP, A. T. & BERGER, R. A. 2002. Use of the 1, 2 intercompartmental supretinacular artery as a vascularized pedicle bone graft for difficult scaphoid nonunion. *The Journal of hand surgery*, 27, 391-401.
- STORDAHL, A., SCHJOTH, A., WOXHOLT, G. & FJERMEROS, H. 1984. Bone scanning of fractures of the scaphoid. *J Hand Surg Br*, 9, 189-90.
- SU-BUM, A. L., HYO-JIN, B. K., JAE-MYEUNG, C. C., CHOON-SUNG, D. L., SHIN-YOON, E. K., POONG-TAEK, F. K. & IN-HO, G. J. 2012. Osseous microarchitecture of the scaphoid: Cadaveric study of regional variations and clinical implications. *Clinical Anatomy*, 25, 203-211.
- SUH, N. & GREWAL, R. 2018. Controversies and best practices for acute scaphoid fracture management. *Journal of Hand Surgery (European Volume)*, 43, 4-12.
- SYMES, T. H. & STOTHARD, J. 2011. A systematic review of the treatment of acute fractures of the scaphoid. *J Hand Surg Eur Vol*, 36, 802-10.
- TAIT, M. A., BRACEY, J. W. & GASTON, R. G. 2016. Acute scaphoid fractures: a critical analysis review. *JBJS reviews*, 4.
- TALEISNIK, J. 1976. The ligaments of the wrist. *The Journal of hand surgery*, 1, 110-118.

- TALEISNIK, J. 1985. *The wrist*, New York, Churchill Livingstone.
- TALEISNIK, J. 1988. Current concepts review. Carpal instability. *J Bone Joint Surg Am*, 70, 1262-8.
- TAMBE, A., CUTLER, L., STILWELL, J., MURALI, S., TRAIL, I. & STANLEY, J. 2006. Scaphoid non-union: the role of vascularized grafting in recalcitrant non-unions of the scaphoid. *Journal of Hand Surgery*, 31, 185-190.
- TEMPLE, C. L., ROSS, D. C., BENNETT, J. D., GARVIN, G. J., KING, G. J. & FABER, K. J. 2005. Comparison of sagittal computed tomography and plain film radiography in a scaphoid fracture model. *The Journal of hand surgery*, 30, 534-542.
- TEN BERG, P. W., DRIJKONINGEN, T., STRACKEE, S. D. & BUIJZE, G. A. 2016. Classifications of Acute Scaphoid Fractures: A Systematic Literature Review. *J Wrist Surg*, 5, 152-9.
- TERRY, D. W., JR. & RAMIN, J. E. 1975. The navicular fat stripe: a useful roentgen feature for evaluating wrist trauma. *Am J Roentgenol Radium Ther Nucl Med*, 124, 25-8.
- THEUMANN, N. H., PFIRRMANN, C. W., ANTONIO, G. E., CHUNG, C. B., GILULA, L. A., TRUDELL, D. J. & RESNICK, D. 2003. Extrinsic carpal ligaments: normal MR arthrographic appearance in cadavers. *Radiology*, 226, 171-179.
- TIEL-VAN BUUL, M. M., VAN BEEK, E. J., BROEKHUIZEN, A. H., NOOITGEDACHT, E. A., DAVIDS, P. H. & BAKKER, A. J. 1992. Diagnosing scaphoid fractures: radiographs cannot be used as a gold standard! *Injury*, 23, 77-9.
- TOBY, E. B., BUTLER, T. E., MCCORMACK, T. J. & JAYARAMAN, G. 1997. A comparison of fixation screws for the scaphoid during application of cyclical bending loads. *J Bone Joint Surg Am*, 79, 1190-7.
- TRUMBLE, T. E., CLARKE, T. & KREDER, H. J. 1996. Non-union of the scaphoid. Treatment with cannulated screws compared with treatment with Herbert screws. *JBJS*, 78, 1829-37.
- TRUMBLE, T. E. & VO, D. 2001. Proximal pole scaphoid fractures and nonunion. *Journal of the American Society for Surgery of the Hand*, 1, 155-171.
- TSUYUGUCHI, Y., MURASE, T., HIDAKA, N., OHNO, H. & KAWAI, H. 1995. Anterior wedge-shaped bone graft for old scaphoid fractures or non-unions: An analysis of relevant carpal alignment. *Journal of Hand Surgery*, 20, 194-200.
- UHTHOFF, H. K., POITRAS, P. & BACKMAN, D. S. 2006. Internal plate fixation of fractures: short history and recent developments. *Journal of orthopaedic science*, 11, 118-126.
- VIEGAS, S. F., WAGNER, K., PATTERSON, R. & PETERSON, P. 1990. Medial (hamate) facet of the lunate. *The Journal of hand surgery*, 15, 564-571.
- VIEGAS, S. F., YAMAGUCHI, S., BOYD, N. L. & PATTERSON, R. M. 1999. The dorsal ligaments of the wrist: anatomy, mechanical properties, and function. *The Journal of hand surgery*, 24, 456-468.
- VINNARS, B., PIETREANU, M., BODESTEDT, Å., AF EKENSTAM, F. & GERDIN, B. 2008. Nonoperative compared with operative treatment of acute scaphoid fractures: a randomized clinical trial. *JBJS*, 90, 1176-1185.
- VRETTOS, B. C., ADAMS, B. K., KNOTTENBELT, J. D. & LEE, A. 1996. Is there a place for radionuclide bone scintigraphy in the management of radiograph-negative scaphoid trauma? *S Afr Med J*, 86, 540-2.
- WAITAYAWINYU, T., PFAEFFLE, H. J., MCCALLISTER, W. V., NEMECHEK, N. M. & TRUMBLE, T. E. 2007. Management of scaphoid nonunions. *Orthopedic Clinics of North America*, 38, 237-249.
- WAIZENEGGER, M., WASTIE, M., BARTON, N. & DAVIS, T. 1994. Scintigraphy in the evaluation of the "clinical" scaphoid fracture. *Journal of Hand Surgery*, 19, 750-753.
- WATSON, H. K. & BALLETT, F. L. 1984. The SLAC wrist: scapholunate advanced collapse pattern of degenerative arthritis. *The Journal of hand surgery*, 9, 358-365.
- WEBER, E. R. & CHAO, E. Y. 1978. An experimental approach to the mechanism of scaphoid waist fractures. *J Hand Surg Am*, 3, 142-8.
- WHEELER, D. L. & MCLOUGHLIN, S. W. 1998. Biomechanical assessment of compression screws. *Clin Orthop Relat Res*, 237-45.

- WHITLEY, A. S., SLOANE, C., HOADLEY, G., JEFFERSON, G., ANDERSON, C. & HOLMES, K. 2016. *Clark's positioning in radiography*, Boca Raton, Fla., CRC Press.
- WIJETUNGA, A. R., TSANG, V. H. & GIUFFRE, B. 2019. The utility of cross-sectional imaging in the management of suspected scaphoid fractures. *Journal of medical radiation sciences*, 66, 30-37.
- WOLF, J. M., DAWSON, L., MOUNTCASTLE, S. B. & OWENS, B. D. 2009. The incidence of scaphoid fracture in a military population. *Injury*, 40, 1316-9.
- WOLLSTEIN, R., WANDZY, N., MASTELLA, D. J., CARLSON, L. & WATSON, H. K. 2005. A radiographic view of the scaphotrapezium-trapezoid joint. *J Hand Surg Am*, 30, 1161-3.
- WOLLSTEIN, R. & WATSON, H. K. 2005. Scaphotrapeziotrapezoid arthrodesis for arthritis. *Hand Clin*, 21, 539-43, vi.
- WONG, K. & VON SCHROEDER, H. P. 2011. Delays and poor management of scaphoid fractures: factors contributing to nonunion. *The Journal of hand surgery*, 36, 1471-1474.
- XIE, X., ZHAN, Y., DONG, M., HE, Q., LUCAS, J. F., ZHANG, Y., WANG, Y. & LUO, C. 2017. Two and three-dimensional CT mapping of Hoffa fractures. *JBJS*, 99, 1866-1874.
- YANNI, D., LIEPPINS, P. & LAURENCE, M. 1991. Fractures of the carpal scaphoid. A critical study of the standard splint. *The Journal of bone and joint surgery. British volume*, 73, 600-602.
- YAZAKI, N., BURNS, S. T., MORRIS, R. P., ANDERSEN, C. R., PATTERSON, R. M. & VIEGAS, S. F. 2008. Variations of capitate morphology in the wrist. *The Journal of hand surgery*, 33, 660-666.
- YIN, Z.-G., ZHANG, J.-B. & GONG, K.-T. 2015. Cost-effectiveness of diagnostic strategies for suspected scaphoid fractures. *Journal of orthopaedic trauma*, 29, e245-e252.
- YIN, Z.-G., ZHANG, J.-B., KAN, S.-L. & WANG, X.-G. 2010. Diagnosing suspected scaphoid fractures: a systematic review and meta-analysis. *Clinical Orthopaedics and Related Research*®, 468, 723-734.
- ZAIDEMBERG, C., SIEBERT, J. W. & ANGRIGIANI, C. 1991. A new vascularized bone graft for scaphoid nonunion. *The Journal of hand surgery*, 16, 474-478.